

FUNDAMENTAL STUDIES OF TRIVALENT f -ELEMENT SEPARATIONS USING IONIC
LIQUIDS AND EXTRACTION CHROMATOGRAPHY: TOWARD AN IMPROVED
TALSPEAK PROCESS

by

Charles Donald Smith

A Dissertation Submitted in
Partial Fulfillment of the
Requirements for the Degree of

Doctor of Philosophy

in Chemistry

at

the University of Wisconsin-Milwaukee

May 2020

ABSTRACT

FUNDAMENTAL STUDIES OF TRIVALENT f -ELEMENT SEPARATIONS USING IONIC LIQUIDS AND EXTRACTION CHROMATOGRAPHY: TOWARD AN IMPROVED TALSPEAK PROCESS

by

Charles Donald Smith

The University of Wisconsin-Milwaukee, 2020
Under the supervision of Dr. Mark Dietz, Ph.D.

Nuclear power is one of many energy sources needed to meet current world demand. With certain radioisotopes in the waste generated requiring thousands of years to decay, limiting the amount of waste needing long-term storage is certainly in the interest of public health. By bombarding the long-lived radioisotopes (*e.g.* actinides) with neutrons, they can be converted (*i.e.*, transmutation) into radioisotopes with significantly shorter (several hundred years) half-lives, making storage a realistic solution for nuclear waste. Transmutation, however, can be negatively impacted by the presence of neutron poisons, particularly lanthanide ions, which have a high neutron capture cross section, preventing efficient bombardment.

The TALSPEAK (Trivalent Actinide Lanthanide Separations by Phosphorus-Reagent Extraction from Aqueous Komplexes) Process was devised to address this problem by providing a means to separate actinides and lanthanides. The process improved upon earlier single extractant systems that performed poorly by incorporating a complexant, diethylenetriaminepentaacetic acid (DTPA) in a buffered aqueous phase that prevents the partition of the actinides into a diisopropylbenzene (DIPB) organic phase containing *bis*(2-ethyl-

hexyl) phosphoric acid (HDEHP). While the separation factors were high (~100), the process used volatile solvents, exhibited modest distribution ratios (~10) and required strict pH control.

Ionic liquids (ILs) have been considered as a replacement for DIPB due to their low volatility, thermal stability and ability to solubilize a wide range of compounds. Initial studies were promising, as ILs exhibited significantly greater distribution ratios (~1000). Unexpectedly, however, ILs have shown limited ability to solubilize common metal ion extractants (*e.g.* HDEHP). In addition, many ILs are very viscous, complicating or precluding their use in conventional solvent extraction systems. While in principle this problem can be overcome by dispersing the IL into a porous support, this approach has not been systematically explored for the TALSPEAK system.

In conjunction with efforts to devise an improved IL-based analogue of the TALSPEAK Process for An(III)/Ln(III) separations, a simple thermogravimetric method for the determination of the solubility of extractants in an ionic liquid has been developed. Subsequent application of the method to the determination of the solubility of HDEHP in a variety of 1-alkyl-3-methylimidazolium ($C_n\text{mim}^+$) and *N*-alkyl-pyridinium ($N\text{-Pyr}^+$) ILs has unexpectedly revealed that solvent molar volume is the most important factor controlling HDEHP solubility in these solvents. Because ILs exhibiting a high molar volume are viscous, the utility of solid-supported IL phases was explored as an alternate to conventional liquid-liquid extraction. Measurements of the internal surface area of the porous polymer support employed as a function of support loading for various reagents revealed the presence of a complex network of pores of three distinct size ranges. Additional experiments using HDEHP as the loading reagent showed that the chromatographic performance (*e.g.*, column efficiency, peak tailing) of the material reached its optimum at intermediate levels of extractant loading, after the smallest of the interior pores

have been completely filled. This filling can also be accomplished by the use of inert “pore-blocking reagents”, atop which an extractant can be loaded. The performance of the materials too can be explained by consideration of the pore structure of the support. Finally, these pore-blocked supports have been employed in a comparison of HDEHP, both neat and as a solution in either a conventional solvent (*i.e.*, dodecane) or an ionic liquid, to a functionalized ionic liquid (FIL) incorporating the anion of HDEHP, $C_{10}mim^+DEHP^-$, as reagents for the separation of Am(III) and Eu(III). The results call into question the utility of the FIL and thus, the utility of ILs as the basis for an improved TALSPEAK Process.

TABLE OF CONTENTS

LIST OF FIGURES	x
LIST OF TABLES	xiv
ACKNOWLEDGEMENTS	xv
CHAPTER 1: INTRODUCTION	1
1.1 Overview and Scope.....	1
1.2 Liquid-Liquid Extraction.....	6
1.3 Ionic Liquids.....	8
1.4 Functionalized Ionic Liquids	10
1.5 Extraction Chromatography.....	11
1.6 Overview of Chapters.....	16
1.7 References	17
CHAPTER 2: DETERMINATION OF EXTRACTANT SOLUBILITY IN IONIC LIQUIDS BY THERMOGRAVIMETRIC ANALYSIS.....	25
2.1 Introduction.....	25
2.2 Experimental	27
2.2.1 Reagents.....	27
2.2.2 Equipment.....	28
2.2.3 Procedures.....	28
2.3 Results and Discussion.....	29

2.4 Conclusions	38
2.5 References	39
CHAPTER 3: SOLVENT STRUCTURAL EFFECTS ON THE SOLUBILITY OF <i>BIS</i>(2-ETHYLHEXYL)PHOSPHORIC ACID IN ROOM-TEMPERATURE IONIC LIQUIDS ..	44
3.1 Introduction	44
3.2 Experimental	46
3.2.1 Reagents.....	46
3.2.2 Equipment.....	47
3.2.3 Procedures.....	48
3.3 Results and Discussion	50
3.4 Conclusions	63
3.5 References	63
CHAPTER 4: EFFECT OF SUPPORT LOADING ON THE PERFORMANCE OF AN EXTRACTION CHROMATOGRAPHIC RESIN: IMPLICATIONS FOR THE DEVELOPMENT OF IMPROVED TRIVALENT <i>f</i>-ELEMENT SEPARATIONS	71
4.1 Introduction	71
4.2 Experimental	72
4.2.1 Reagents.....	72
4.2.2 Instrumentation	73
4.2.3 Methods.....	74
4.2.3.1 Resin Impregnation.....	74

4.2.3.2 Determination of weight distribution ratios.....	74
4.2.3.3 Determination of metal ion uptake kinetics	75
4.2.3.4 Determination of sorbent capacity	75
4.2.3.5 Column preparation and characterization	76
4.2.3.6 Elution behavior of europium-152/4.....	77
4.2.3.7 Elution behavior of neodymium, gadolinium, and inactive europium.	78
4.3 Results and Discussion.....	78
4.3.1 Effect of pore structure on support filling.....	78
4.3.2 Effect of support loading on column performance	80
4.3.3 Effect of reduced support loading on trivalent lanthanide separations.	84
4.4 Conclusions.....	90
4.5 References.....	90
CHAPTER 5: INCREASING COLUMN EFFICIENCY IN EXTRACTION CHROMATOGRAPHY MATERIALS THROUGH STAGNANT PORE PLUGGING....	95
5.1 Introduction.....	95
5.2 Experimental.....	97
5.2.1 Materials	97
5.2.2 Instrumentation	99
5.2.3 Methods.....	100
5.2.3.1 SPP Resin Preparation	100

5.2.3.2 Addition of HDEHP to impregnated resins	101
5.2.3.3 Determination of Weight Distribution Ratios.....	101
5.2.3.4 Capacity of the Resins	102
5.2.3.5 Column preparation and characterization	102
5.2.3.6 Elution curves of $^{152/4}\text{Eu}^{3+}$ for Resin Characterization	103
5.2.3.7 Elution curves of cold Eu^{3+} , Nd^{3+} , and Gd^{3+}	105
5.3 Results and Discussion.....	105
5.4 Applications in Intra-lanthanide Metal Ion Separations	120
5.4.1 $\text{Eu}^{3+}/\text{Nd}^{3+}$ Separation	120
5.4.2 $\text{Eu}^{3+}/\text{Gd}^{3+}$ Separation	122
5.5 Conclusions.....	125
5.6 References.....	126
CHAPTER 6: ASSESSMENT OF FUNCTIONALIZED IONIC LIQUIDS (FILs) IN THE EXTRACTION OF TRIVALENT EUROPIUM AND AMERICIUM.....	131
6.1 Introduction.....	131
6.2 Experimental.....	135
6.2.1 Materials	135
6.2.2 Methods.....	136
6.2.2.1 Filler-Impregnated Resin Preparation.....	136
6.2.2.2 Stagnantly-Pore Plugged (SPP) Resin Preparation.....	136

6.2.2.3 Determination of Weight Distribution Ratios.....	137
6.2.2.4 Metal Ion Uptake Kinetics	138
6.2.3 Equipment.....	138
6.3 Results and Discussion.....	138
6.4 Conclusions.....	149
6.5 References.....	150
CHAPTER 7: CONCLUSIONS AND RECOMMENDATIONS.....	155
7.1 Conclusions.....	155
7.2 Recommendations.....	158
7.2.1 Assessing extractant solubility in ILs	158
7.2.2 Effect of extractant loading on solid supports with high surface area.....	158
7.2.3 Filling a solid support with a thermally-polymerizable monomer	159
7.2.4 Applying a thin layer of extractant in controlled-porosity supports.....	159
7.3 References.....	160
CURRICULUM VITAE.....	162

LIST OF FIGURES

Figure 1.1: Radioactivity of spent nuclear fuel versus time	4
Figures 1.2: Crown (A) and HDEHP (B).....	7
Figure 1.3: Examples of water-miscible and immiscible ILs	9
Figure 1.4: calix[4]arene-bis(tert-octylbenzo-crown-6 (Bob-Calix).....	9
Figure 2.1: (A) TGA thermogram of $C_6mim^+Tf_2N^-$ (bottom; closed circles), $C_8mim^+Tf_2N^-$ (middle; open diamonds), and $C_{10}mim^+Tf_2N^-$ (top; open circles) (B) Isothermal heating of $C_6mim^+Tf_2N^-$ at 300 °C (top; open diamonds), 346°C (middle; closed circles), and 396 °C (bottom; open squares) for 60 min.....	31
Figure 2.2: Isothermal heating of $D7BuDCH18C6$ at 250 °C for 85 minutes.	32
Figure 2.3: (A) TGA thermogram of CMPO. (B) Isothermal heating of CMPO at 250 °C for 70 min.....	34
Figure 2.4: TGA thermogram of Bob-Calix.	35
Figure 2.5: TGA thermogram of BTP.....	35
Figure 2.6: (A) TGA thermogram of HDEHP. (B) Isothermal heating of HDEHP at 180°C (top; open diamonds), 190 °C(middle; open squares), 200°C (bottom; closed circles) for 75 min. ..	37
Figure 2.7: TGA thermogram of a saturated solution of HDEHP in $C_6mim^+Tf_2N^-$	38
Figure 3.1: Experimentally determined vs. calculated (according to Eqn. 10) solubility of HDEHP (as $\ln S_{HDEHP}$) in a series of hydrophobic room-temperature ionic liquids.....	60
Figure 3.2: HDEHP solubility (as $\ln S_{HDEHP}$) vs. molar volume (\tilde{V}) for a series of $C_8mim^+X^-$ ionic liquids.....	61
Figure 3.3. HDEHP solubility (as $\ln S_{HDEHP}$) vs. molar volume (\tilde{V}) for a series of $C_nmim^+Tf_2N^-$ ionic liquids.....	62
Figure 4.1: Effect of support loading on the surface area of Amberchrom CG-71m for two fillers. (●) PTHF 250; (□) HDEHP.	79

Figure 4.2A-E: Representation of the interior structure of Amberlite XAD-7 filled to increasing levels with the ionic liquid $P_{666,14}^+Cl^-$	80
Figure 4.3: Elution behavior of $^{152/4}Eu(III)$ on a column (0.90 mL bed volume) containing 5% (w/w) HDEHP-loaded Amberchrom CG-71m resin. (50-100 μm particle size; mobile phase = 0.026 M HNO_3 ; Note that the data is plotted in semi-log form to emphasize the extent of tailing.	82
Figure 4A-D: Elution behavior of $^{152/4}Eu(III)$ on a column (0.90 mL bed volume) containing HDEHP-loaded Amberchrom CG-71m resin. (A) 10% (w/w) loaded; (B) 15% (w/w) loaded; (C) 20% (w/w) loaded; (D) 30% (w/w) loaded. (50-100 μm particle size; mobile phase = 0.045, 0.080 0.13, 0.22 M HNO_3 , respectively.....	84
Figure 4.5: Separation of Nd(III) and Eu(III) on a column (0.90 mL bed volume) containing 20% (w/w) HDEHP-loaded Amberchrom CG-71m resin. (50-100 μm particle size; mobile phase = 0.13 M HNO_3 ; (o) Nd; (•) Eu.	86
Figure 4.6.A-B: (A) Separation of Eu(III) and Gd(III) on a column (0.90 mL bed volume) containing 20% (w/w) HDEHP-loaded Amberchrom CG-71m resin. (50-100 μm particle size; mobile phase = 0.13 M HNO_3 ; (•)Eu; (o) Gd. (B) Separation of Eu(III) and Gd(III) on a column (0.90 mL bed volume) containing Ln resin (40% (w/w) HDEHP-loaded Amberchrom CG-71m resin; (50-100 μm particle size; mobile phase = 0.30 M HNO_3 ; (•)Eu; (o) Gd.....	88
Figure 4.7: Separation of Eu(III) and Gd(III) on a column (0.90 mL bed volume) containing small particle size (20-50 μm) Ln resin (40% w/w HDEHP on Amberchrom CG-71m). (mobile phase = 0.30 M HNO_3 (•)Eu; (o) Gd.	89
Figure 4.7: Separation of Eu(III) and Gd(III) on a column (0.90 mL bed volume) containing small particle size (20-50 μm) 20% w/w HDEHP on Amberchrom CG-71m). (mobile phase = 0.13 M HNO_3 ; (•)Eu; (o) Gd.	89
Figure 4.8: Separation of Eu(III) and Gd(III) on a column (0.90 mL bed volume) containing small particle size (20-50 μm) 20% w/w HDEHP on Amberchrom CG-71m, mobile phase = 0.127 M HNO_3). (•)Eu (o) Gd.	89
Figure 5.1: Example graphite, trapezium-shaped pole	100
Figure 5.2: Phosphorus profile obtained using SEM-EDX for a PPG 400-loaded, 20% (%w/w) HDEHP resin.	106
Figure 5.3: Stripping of ionic liquid from a $C_{12}mimTf_2N$ -impregnated resin as a function of contact time with an ethanol (12 %v/v) solution in hexane.....	108

Figure 5.4: Phosphorus profile obtained using SEM-EDX [DHEA][HCOO] resin impregnated with 10% (%w/w) HDEHP	109
Figure 5.5: Surface area (m ² /g) of PTHF 250-impregnated resins	110
Figure 5.6: Surface Area (m ² /g) of PTHF 250-(□), C ₂ mim ⁺ Tf ₂ N ⁻ (⊞), P _{666,14} ⁺ Cl ⁻ (+)-, and Cetyl Alcohol (●)-impregnated resins.	112
Figure 5.7: C ₁₆ mim ⁺ Tf ₂ N ⁻ -impregnated, 10% (%w/w) HDEHP (□, cpm) (Eluent: 0.608 M HNO ₃ , Flow Rate = 1.38 ± 0.02 mL/min·cm ² , T = 23 ± 2°C, 0.9 mL bed volume) and commercial Ln (●, concentration (ng/mL)) resins (Eluent: 0.30 M HNO ₃ T = 23 ± 2°C, 0.9 mL bed volume) ^{152/4} Eu ³⁺ Elution Profile.	113
Figure 5.8: Pore distribution of C ₁₆ mim ⁺ Tf ₂ N ⁻ (a) and C ₂ mim ⁺ Tf ₂ N ⁻ (b) impregnated supports. 80% of the available resin volume is filled for both resins.....	114
Figure 5.9: The effect of support loading of (%w/w) HDEHP (□)-, PTHF 250 (●)-on the surface area of Amberchrom CG-71m resin	115
Figure 5.10A-E: 5%-30% (%w/w) HDEHP stagnantly-pore plugged (SPP) resins, 0.9 mL bed volume (Temperature: 23 ± 2°C, eluents: 0.026, 0.045, 0.086, 0.097, and 0.17 M HNO ₃ , respectively).....	118
Figure 5.11: 10% (%w/w) SPP HDEHP resin separation of Eu ³⁺ (Filled)/Nd ³⁺ (Open), 0.9 mL bed volume (Temperature: 23 ± 2°C, eluents: 0.045 M HNO ₃ followed by 1 M HNO ₃ at FCV = 17)	121
Figure 5.12: Ln Resin Separation of Eu ³⁺ (Filled)/Nd ³⁺ (Open), 0.9 mL bed volume (Temperature: 23 ± 2°C °C, eluents: 0.3 M HNO ₃)	121
Figure 5.13: 10% (%w/w) SPP HDEHP separation of Eu ³⁺ (●)/Gd ³⁺ (□), 0.9 mL bed volume (Temperature: 23 ± 2°C, eluent: 0.045 M HNO ₃).....	123
Figure 5.14: Ln resin separation of Eu ³⁺ (●)/Gd ³⁺ (□), 0.9 mL bed volume (Temperature: 23 ± 2°C, eluent: 0.3 M HNO ₃).....	123
Figure 5.15: Small particle 10% (%w/w) SPP HDEHP separation of Eu ³⁺ (●)/Gd ³⁺ (□), 1.8 mL bed (Temperature: 23 ± 2°C °C, eluent: 0.045 M HNO ₃)	125
Figure 5.16: Small particle Ln resin separation of Eu ³⁺ (●)/Gd ³⁺ (□), 1.8 mL bed (Temperature: 23 ± 2°C, eluents: 0.3 M HNO ₃)	125

Figure 6.1A-F: Effect of nitric acid concentration on metal ion uptake in (A) undiluted HDEHP and C₁₀mimDEHP w/ Eu³⁺ (B) undiluted HDEHP and C₁₀mimDEHP w/ Am³⁺ (C) 1 M HDEHP and C₁₀mimDEHP in n-dd w/ Eu³⁺ (D) 1 M HDEHP and C₁₀mimDEHP in n-dd w/ Am³⁺ (E) 1 M HDEHP and C₁₀mimDEHP in C₁₀mimTf₂N w/ Eu³⁺ (F) 1 M HDEHP and C₁₀mimDEHP in C₁₀mimTf₂N w/ Am³⁺. HDEHP (•); C₁₀mimDEHP (□); T = 23 ± 2°C. All extractants are supported on Amberchrom CG-71m resin whose deep pores have been blocked by 1-dodecanol (ref. text)140

Figure 6.2A-F: Effect of nitric acid concentration on Eu³⁺ (•) and Am³⁺ (□) uptake in undilute HDEHP (A), undilute C₁₀mimDEHP (B), 1 M HDEHP in n-dd (C), 1 M C₁₀mimDEHP in n-dd (D), 1 M HDEHP in C₁₀mimTf₂N (E) and 1 M C₁₀mimDEHP in C₁₀mimTf₂N (F);T = 23± 2°C 143

Figure 6.3A-F: Nitrate dependence on Am³⁺ uptake for undilute C₁₀mimDEHP (A), 1 M C₁₀mimDEHP in n-dd (B) and 1 M C₁₀mimDEHP in C₁₀mimTf₂N (C) and Eu³⁺ uptake for undilute C₁₀mimDEHP (D), 1 M C₁₀mimDEHP in n-dd (E) and 1 M C₁₀mimDEHP in C₁₀mimTf₂N (F). 145

Figure 6.4A-D: Extractant dependence on Am³⁺ and Eu³⁺ uptake for 1 M C₁₀mimDEHP in n-dd (A,B) and 1 M C₁₀mimDEHP in C₁₀mimTf₂N (C,D). 146

Figure 6.5: Effect of spiking aqueous phase with C₁₀mim⁺ cation on Eu³⁺ uptake for undiluted C₁₀mimDEHP SPP resin 148

Figure 6.6A-B: Kinetics of the uptake of europium ion from 0.05 M and 0.005 M HNO₃ by 10% (%w/w) HDEHP SPP and 9.69% (%w/w) C₁₀mimDEHP SPP resins, respectively 149

LIST OF TABLES

Table 1.1 Americium and curium ion separations using various supports and stationary phases	14
Table 3.1 Measured solubility of HDEHP in a series of <i>N,N</i> -dialkylimidazolium and <i>N</i> -alkylpyridinium ionic liquids ($T = 23 \pm 2 \text{ }^\circ\text{C}$)	53
Table 3.2 Kamlet-Taft solvent parameters and Hildebrand solubility parameters of a series of <i>N,N</i> -dialkylimidazolium and <i>N</i> -alkylpyridinium ionic liquids ($T = 23 \pm 2 \text{ }^\circ\text{C}$)	55
Table 3.3 Density and molar volume (\tilde{V}) values for a series of <i>N,N</i> -dialkylimidazolium and <i>N</i> -alkylpyridinium ionic liquids ($T = 23 \pm 2 \text{ }^\circ\text{C}$)	58
Table 4.1 Effect of support loading on the elution behavior of Eu(III) on Amberchrom CG-71m - supported HDEHP	83
Table 5.1 Characteristics of prepared and commercial Ln resins and packed columns.....	105
Table 5.2 Viscosity of Select Fillers at 25 $^\circ\text{C}$	112
Table 5.4 Theoretical plate height (H) and count (N), tailing factor (T_f), and peak asymmetry (A_s), and capacity for HDEHP-stagnantly-pore plugged resins.....	117
Table 6.1: Kinetics of the uptake of europium ion from 0.05 M and 0.005 M HNO_3 by 10% (w/w) HDEHP SPP and 9.69% (w/w) $\text{C}_{10}\text{mimDEHP}$ SPP resins, respectively.....	149

ACKNOWLEDGEMENTS

I have many to thank across this long, six-year journey. First and foremost, I need to thank my supportive and beautiful wife, Sara. Her unwavering support kept me going through the lowest of lows. I would not have gotten through the experience without her.

Next, of course, I must thank Dr. Mark Dietz. His “walk before we run” mentality has served me well in the laboratory. His vast knowledge of writing papers and making presentations will also serve me well in my professional life.

I want to thank my committee members as well. I knew that when I first met Dr. Altstadt in December 2013 that UWM was the right choice for me. I’m thankful for his advice in the classroom and laboratory. My thanks as well to Dr.’s Woehl, Arnold, and Indig for their guidance. I also want to thank Dr. F. Holger Foersterling, Shelley Harrington-Hagen, Elise Nicks, Kevin Blackburn, and Wendy Grober for the help they have given.

I want to thank Kevin Wolters, Michael Kaul, Christopher Harris and John Dudek as well. I appreciate being able to bounce thoughts and ideas off them, both in the laboratory and during group meetings. Their critical but constructive ideas will always be appreciated. Thank you to Dr.’s Md. Abdul Momen and James Wankowski for taking the time to train me in the radiation and sample preparation laboratories. It saved me a lot of time.

I have also been fortunate to work with researchers outside the Chemistry and Biochemistry Department at UWM. I am in debt to Dr. Heather Owen, a senior scientist and director of Electron Microscopy laboratory in the biological sciences department. She was always willing and able to help with work done on the scanning electron microscope. I’m also thankful for the help of Dr. Steven Hardcastle, manager of the Advanced Analysis Facility in the

Engineering Department. His insights on surface area analysis were immensely helpful. I also appreciate the guidance of Dr. Anna Benko, manager of the Shimadzu Laboratory. It was helpful to talk to someone who had worked in industry prior to joining UWM.

After moving here, I struggled to find that which I could enjoy outside the laboratory. I found that in Badger CrossFit of Wauwatosa, WI. I cannot thank the trainers enough, especially Tyler Sullivan, Tina Martin, and Joe Paul, for what they have given me. The morning classes were a great way to start my day.

I also want to acknowledge Dr. Joanne Graham and the other member of my dissertation support group in the UWM counseling department. They are an adult group of shoulders to lean on and I am thankful for them.

This financial support provided by the Single Investigator Small Group Research (SISGR) Program of the Office of Basic Energy Sciences of the United States Department of Energy through subcontract with Brookhaven National Laboratory and by the University of Wisconsin-Milwaukee Research Growth Initiative (RGI) Program is gratefully acknowledged.

CHAPTER 1:

INTRODUCTION

1.1 Overview and Scope

The rare earth elements (REEs) are named not for their scarcity (as some are much more common than gold), but rather from the fact that chemists in the 1800s had great difficulty isolating them in pure form. Rare earths are mainly found in mixed deposits, making the separation of these metals a necessity and concentrated deposits valuable. Known deposits typically consist of 80-99% lanthanum, praseodymium, cerium, and neodymium,¹ with lesser, varying amounts of the other rare earths.

The U.S. supply of REEs has come from a single mine, located in Mountain Pass, California (Mine Operations LLC). The mine has faced repeated environmental and regulatory obstacles due to its wastewater pipeline, which was used in the liquid-liquid extraction of REEs. In 2015, the operation went bankrupt, but re-opened in 2018. Currently the company ships its semi-processed output to China for purification, but it has announced plans to return to domestic processing in 2020.²

China is responsible for the bulk of world rare earth production today, and actually provides more than 80% of the U.S. supply and over 90% of global supplies. Due to decreasing domestic reserves, however, Chinese exports of these precious metals went from 50,145 tons in 2009 to 31,130 tons in 2012,³ and have continued to trend downward.

Unlike the rare earths/lanthanides, the other family of *f*-elements, the actinides, are not common in nature, with only uranium and thorium being found in appreciable quantities. In fact, of the known actinides, only the elements actinium through plutonium occur naturally. These

elements are, however, found in spent nuclear fuel (SNF) and other types of nuclear waste. Spent nuclear fuel exists in substantial quantities, a result of the “once-through” fuel cycle employed by American nuclear reactors.

As of December 2011, U.S. stores of spent fuel exceeded 67,000 tons, a quantity which is increasing at a rate of 2,000 tons per year.⁴ An additional 2500 tons is generated annually by European Union countries. Of this, americium, neptunium, and curium makeup 3.5 tons, which, while small relative to the total, still poses significant potential environmental health risks.⁵ Plutonium, while making up a mere 25 tons of the total waste generated, represents the greatest threat of radiotoxicity over the long-term (>10,000 years).⁶

The current amount of spent nuclear fuel in the U.S. exceeds the legal limit of the proposed nuclear waste site in Yucca Mountain, Nevada under the Nuclear Waste Policy Act. This site was designated in 1987 as the sole repository for nuclear waste generated in the U.S.⁷ Unfortunately, construction was stopped during the Obama administration in 2009 and was not included in the U.S. Congressional budgets from fiscal years 2011-2019. Funding to resume the licensing procedures was requested in the U.S. Federal budget for fiscal year 2020. Even so, if shipping to the waste site started in 2020, secondary storage would be required until 2056 to accommodate the ongoing waste generated by commercial sources and the shipment rate from source to storage.⁴

The composition of SNF designated for waste is as follows: 95.5% uranium, 0.9% plutonium, 3.1% stable fission products, 0.1% minor actinides, 0.2% short-lived fission products (Cs-137 and Sr-90), and 0.1% long-lived fission products (I-129, Tc-99, Zr-93, and Cs-135).⁸ Therefore, the separation of uranium is where most published reprocessing flow sheets start. In the PUREX Process (Plutonium and Uranium Extraction), first described in the 1940’s, the SNF

is dissolved in nitric acid, and Pu(IV) and U(VI) are extracted using a solution of 1.1 M tributylphosphate (TBP) in an aliphatic diluent such as n-dodecane or kerosene. Currently proliferation concerns necessitate that plutonium not be recovered in its pure form. Accordingly, the PUREX process is considered obsolete.⁹

In the UREX (Uranium Extraction) process, the same extractant-organic solvent system is used as in the PUREX Process, but Pu(IV) is reduced to the inextractable Pu(III) using acetohydroxamic acid, and thus remains in the aqueous phase.¹⁰

Once uranium extraction has been addressed, the remaining transuranic elements (TRUs) and lanthanides can be extracted using any of several available methods. In the TRUEX (TransUranium Extraction) Process, a solution of 0.2 M *n*-octyl(phenyl)-*N, N*-diisobutylcarbomoyl phosphine oxide (CMPO)-1.2 M TBP in n-dodecane is employed to extract both the lanthanides and actinides from a nitric acid solution.¹¹ In the DIAMEX (Diamide Extraction), a diamide, such as *N, N'*-dimethyl-*N, N'*-dioctyl hexylethoxymalonamide or dimethyldibutyltetradecylmalonamide, dissolved in a water-immiscible diluent such as hydrogenated tetrapropene is used to extract the actinides and lanthanides.¹² Lastly, the ALSEP (Actinide-Lanthanide Separation) Process uses both a neutral diglycolamide extractant (*N, N, N', N'*-tetra(2-ethylhexyl)diglycolamide or *N, N, N', N'*-tetraoctyldiglycolamide) and an acidic extractant, such as 2-ethylhexylphosphonic acid mono-2-ethylhexylester (HEH[EHP]) dissolved in an aliphatic diluent for extraction.¹³

Once the trivalent lanthanides and actinides have been extracted, separation of the actinides from the lanthanides is of vital interest, as the actinides can be transmuted to shorter-lived nuclides via neutron bombardment, but this process is disrupted by neutron poisons such as lanthanides. These metals have similar ionic radii and are almost always trivalent, however,

making their separation challenging. Nonetheless, it is critical if the transmutation of the long-lived actinides (especially Am-241, Pu-242, and Pu-239), which reduces the stress on the geologic depositories used for spent fuel storage, is to succeed.⁸

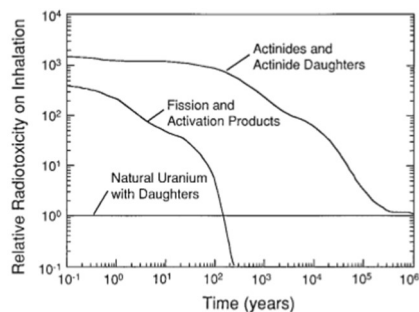


FIG. 1. Relative radiotoxicity on inhalation of spent nuclear fuel with a burnup of 38 megawatt days/kg U. The radiotoxicity values are relative to the radiotoxicity (horizontal line) of the quantity of uranium ore that was originally mined to produce the fuel (eight tons of natural uranium yields one ton of enriched uranium, 3.5% ²³⁵U) (11).

Figure 1.1: Radioactivity of spent nuclear fuel versus time

Although most An/Ln extraction processes rely on an organic phase extractant, the addition of water-soluble complexants to the aqueous phase can be used to enhance extraction selectivity. For example, adding a nitrogen-based complexant to the aqueous phase has been employed to hold the actinides in the aqueous phase while the lanthanides are brought into the organic phase by a suitable extractant. This approach provides the basis of the well-known TALSPEAK (Trivalent Actinide Lanthanide Separation with Phosphorus reagent Extraction from Aqueous Komplexes) Process. This process, first described in the 1960's, utilizes *bis*(2-ethylhexyl)phosphoric acid (HDEHP) dissolved in diisopropylbenzene (DIPB) to extract the lanthanides. The nitrogen-based complexant, diethylenetriaminepentaacetic acid (DTPA), which is dissolved in the aqueous phase (a pH 3.5 lactic acid buffer), preferentially complexes the actinides preventing their extraction by HDEHP. Modest distribution ratios of ~10 for the Ln's were achieved, but the Am(III)/Eu(III) separation factors (~100) were high.¹⁴

In an effort to improve the lanthanide distribution ratios obtained in the TALSPEAK process, ILs have been studied as replacements for the conventional organic solvents. These novel solvents frequently consist of a bulky organic cation paired with a charge diffuse anion to provide a water-miscible or immiscible solvent, depending on the application. Because ILs are known for their ability to solubilize a wide-range of solutes (bananas¹⁵, proteins¹⁶, and wood¹⁷ to name a few), it was thought that HDEHP would be readily miscible. HDEHP, however, has been shown to be only partially miscible with hydrophobic ionic liquids.¹⁸ Fortunately, in deprotonated form, it can be used as the ionic liquid anion (DEHP⁻) to produce a so-called “functionalized ionic liquid” (FIL). Unfortunately, these liquids are often too viscous to be used directly in liquid-liquid extractions.¹⁹ Impregnating solid supports with these solvents can represent a good alternative for the study of their extraction properties. Aside from the difficulties in working with viscous solvents, the drawbacks of liquid-liquid extraction (LLE) systems include the volume of waste generated and its cumbersome nature. Thus, studying extraction chromatographic analogs of LLE systems, TALSPEAK in particular, is attractive.

Among the objectives of the present studies are to assess whether or not FILs are superior to a simple solution of the corresponding extractant in an IL. First however, HDEHP solubility must be measured in different families of ILs to optimize the design of the FIL and to choose extractant-IL solutions for extraction experiments. Unfortunately, the viscosity of FILs makes biphasic, liquid-liquid extraction a cumbersome task. Therefore, the synthesized FIL will be dispersed in undiluted form as a thin layer in a porous, solid support. In addition, it will be dissolved in both IL and aliphatic diluents to extract $^{241}\text{Am}^{3+}$ and $^{152/4}\text{Eu}^{3+}$ from aqueous solutions. To lay down a thin layer of the prepared FIL on the support, the interior structure of the support (here, Amberchrom CG-71m) must be fully understood, as many are known to

exhibit complex interior pore structures encompassing pores of various diameter. The effect of various levels of pore filling of these solid supports will be explored, and once the optimal filling level of the support has been determined, mechanistic studies in solid-supported FIL systems will be conducted.

1.2 Liquid-Liquid Extraction (LLE)

Liquid-liquid extraction is a well-known separation technique dating back to the 1840's.²⁰ Briefly, it involves the partitioning of a solute in a biphasic system until equilibrium is reached. The distribution of a solute, S, between the organic and aqueous phases can be described thermodynamically by Nernst according to the following equation:

$$K_d = \frac{[S]_{org}}{[S]_{aq}} \quad (1.1)$$

The equilibrium constant, K_d , is independent of solute concentration at a constant temperature.²¹ When the solute is a charged species, such as a metal ion, the use of hydrophobic ligand is required to complex the metal, allowing for extraction of the complex into the organic phase from the aqueous. Often the introduction of complexing ligands can lead to the formation of multiple metal complexes in both the aqueous and organic phases. Thus, a volume distribution ratio (D_v) is used to express the total concentration of solute in all forms²²:

$$D_v = \frac{[S]_{org,total}}{[S]_{aq,total}} = \frac{[S_1]_{org} + [S_2]_{org} + \dots + [S_m]_{org,total}}{[S_1']_{aq} + [S_2']_{aq} + \dots + [S_m']_{aq,total}} \quad (1.2)$$

For extraction to be considered acceptable, the D-value should be greater than one.²³ If this is not the case, the metal favors the aqueous phase over the organic, and either a new separation system should be chosen, or the extraction conditions adjusted (*e.g.*, aqueous pH,

extractant concentration). Simply changing the solvent can drastically enhance the distribution ratio.^{24,25}

The complexes formed depend on the extractant chosen. Neutral extractants, for example, form charged complexes with the metal ion, which pair with charge-balancing counter-anions to form a neutral complex. $^{85}\text{Sr}^{2+}$, for instance, is efficiently extracted from long-chained alcohols using *bis*-4, 4', (5')-*tert*-butylcyclohexano-18-crown-6 (Crown) by the following reaction²⁶:

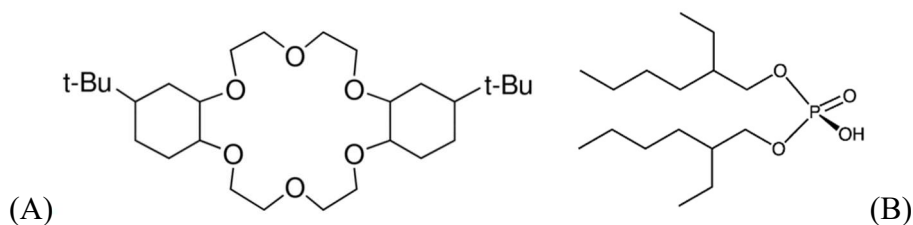
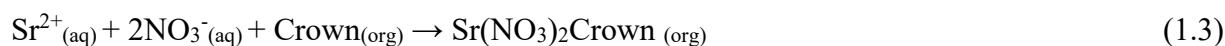


Figure 1.2: Crown (A) and HDEHP (B)

Acidic extractants, such as HDEHP, do not require the extraction of counteranions to yield a neutral (and therefore, extractable) complex. Instead, the metal ion is exchanged for a stoichiometric equivalent number of protons. For example, $^{241}\text{Am}^{3+}$ is extracted by the dimeric form of *bis*(2-ethylhexyl)phosphoric acid (HDEHP) into *n*-dodecane via the following mechanism²⁷:



Even if an efficient separation is achieved, the solvent and extractant chosen should be radiolytically, hydrolytically, and thermally stable, with few or no by-products generated during the separation process. Both should be relatively inexpensive, recyclable to reduce the waste generated, and readily stripped to allow for recovery of the metal of interest from the organic

solvent, ideally using only an using an acid solution.²⁸ Few LLE systems completely satisfy these criteria.

Ion-exchange (IX) resins address some of the issues observed in LLE. Unfortunately, IX resins require strict pH control so they are difficult to use with highly acidic media (the matrix of a typical nuclear waste solution).²⁹

Conventional solvents exhibit low flashpoints (e.g. alkanes) and high vapor pressures (e.g. chlorinated hydrocarbons). Thus, alternative, environmentally-friendly, solvent systems are sought.

1.3 Ionic Liquids (ILs)

The first ILs were reported in 1914,³⁰ but it was not until the late 1990's that their favorable characteristics - thermal stability, low volatility, wide electrochemical window, and tunability-^{31,32} would be widely appreciated. Not long after, their potential as media for separation processes attracted attention, and this interest has continued unabated until today.

The area of metal ion separations has generated particularly immense interest.³³⁻³⁷ Based on their ability to solubilize a wide-range of solutes, wide liquid range, and air and water stability, it was believed that metal ions would readily partition into ILs, several of which are shown below (Figure 1.3).³⁸ Since minimal extraction is usually observed with pure ILs alone, an extractant is often needed to complex the metal ion, making it more hydrophobic and allowing its partitioning from the aqueous to the organic phase. Increased distribution ratios are observed for metals in IL-based systems compared to that of conventional solvents under many conditions.

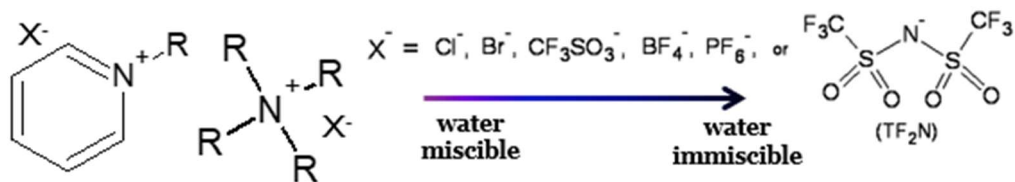


Figure 1.3: Examples of water-miscible and immiscible ILs

The specific class of extractant required is determined by the metal ion of interest. For example, crown ethers are used in the extraction of Sr^{2+} from acidic aqueous media,^{39,40} while calixarenes (Figure 1.4) are employed to extract Cs^+ under the same conditions.^{41,42} As already noted, HDEHP has long been studied for trivalent lanthanide/ actinide extraction and separations.^{43,44}

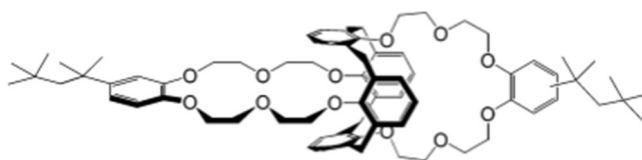
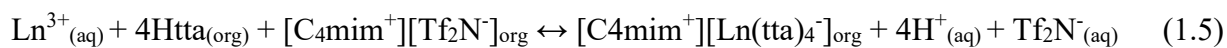


Figure 1.4: calix[4]arene-bis(tert-octylbenzo-crown-6 (Bob-Calix)

Once the use of ILs in LLE became popular, their shortcomings quickly became evident. First, the aforementioned extractants have limited solubility in several important IL families.^{41,45,46} Second, both IL cation and anion can be lost (as shown below) to the aqueous phase, becoming a costly factor given the price of ILs versus conventional solvents.⁴⁷ In Equation 1.5, trivalent lanthanides (Ln(III)) form anionic complexes with four 2-thenoyl-trifluoroacetone (Htta) ligands and exchange for the anionic component of the IL, *bis*(trifluoromethanesulfonyl) imide (Tf_2N^-) in a biphasic system:⁴⁸



Similarly, ion exchange of the cationic ($C_n\text{mim}^+$) component of an IL can occur during extraction with of strontium ion by a crown ether as shown in Equation 1.6:⁴⁹



To circumvent these problems, so-called “functionalized ionic liquids” (FILs) have been developed and investigated.

1.4 Functionalized Ionic Liquids (FILs)

FILs were created to address two significant problems encountered in IL-based LLE systems: exchange of the IL cation to the aqueous phase and poor extractant solubility in IL phases,⁵⁰ FILs can also simplify the chemistry found in single extractant LLE systems.⁵¹

While the earliest examples of IL modification involved tethering of the antifungal drug miconazole to an imidazolium cation, such “task-specific ionic liquids (TSILs)” have since found wide use in metal ion extraction. Visser *et al.*, for example, studied Cd^{2+} and Hg^{2+} extraction from water using urea and thiourea derivatives tethered to imidazolium cations.⁵² Similarly, Kogelnig *et al.* examined Cd^{2+} uptake from water, and paired the Aliquat 336 cation with a thiosalicylate anion.⁵³

In a TSIL, the extracting functional groups can be tethered to either the anion or cation. In the alternative, the IL anion can comprise the anionic portion of an acidic extractant. The latter type of IL is often referred to as a “FIL” to distinguish it from “conventional” TSILs. Among the published examples of a FIL are deprotonated forms of phthalic and alkyl phosphoric acids paired with quaternary ammonium cations for use in rare earth element extraction.^{54,55}

Applying *bis*(2-ethylhexyl)phosphate (DEHP) as a counteranion in a FIL is attractive as HDEHP has limited solubility in short-chained, imidazolium-based ILs. Sun *et al.* extracted rare earth elements using HDEHP in a series of $C_n\text{mim}^+\text{Tf}_2\text{N}^-$ and BETI^- ($n = 2-8$) ionic liquids but was limited to a concentration of 40 mM. In contrast, the conventional solvent used in the same study, diisopropylbenzene, was completely miscible with HDEHP. The authors then opted to pair the DEHP^- anion with quaternary ammonium and phosphonium cations to study the extraction of the same metals. Unfortunately, due to the viscosity of the resulting FIL, it was necessary to use $C_6\text{mimTf}_2\text{N}$ or DIPB as a diluent.⁵⁶ Thus, studying this family of FILs in pure form was not feasible in biphasic systems. FIL dilution was also employed by Rout *et al.* to study Nd^{3+} uptake from nitric acid solutions. Consistent with multiple, single-extractant, biphasic systems involving ionic liquids, ion exchange was observed during extraction when $C_6\text{mimDEHP}$ and $C_6\text{mpyrDEHP}$ were dissolved in $C_6\text{mim}^+\text{Tf}_2\text{N}^-$ and $C_6\text{mpyr}^+\text{Tf}_2\text{N}^-$, respectively. Interestingly, when extraction was performed using $\text{N}_{4,4,4,4}^+\text{DEHP}^-$ diluted in $\text{N}_{4,4,4,4}^+\text{Tf}_2\text{N}^-$ ion exchange was not observed. The factors responsible for the occurrence of an ion exchange process in certain FIL systems but not others remain unexplained.⁵⁷

While dilute FILs or TSILs makes LLE feasible, it obviously means that the FILs and TSILs are not being studied in pure form. Given the inconsistency of the reports of ion exchange, this gap in understanding requires study. These solvents will therefore be applied to solid supports in undiluted form for fundamental studies.

1.5 Extraction Chromatography

Extraction chromatography offers the selectivity of liquid-liquid extraction while avoiding large amounts of waste and inconvenience. The process involves the use of an inert solid support impregnated with pure extractant or a dilute extractant solution as the stationary

phase. The impregnated support is then contacted with an appropriate acid (often HCl or HNO₃) solution of the target analyte.⁵⁸

The earliest support materials, such as cellulose, diatomaceous earth, Kel-F, Hyflo Super Cel, Celite-45, and activated charcoal⁵⁹⁻⁶⁴, were impregnated with extractants still used today (*e.g.* tri-butyl-phosphate (TBP), and HDEHP). Unfortunately, the difficulties encountered with these materials, such as low theoretical plate counts and particle size inhomogeneity, quickly made these supports obsolete when better alternatives became available.⁶⁵

Older extractants such as trioctylamine (TOA), methylisobutyl ketone (MIBK), thenoyl trifluoroacetone (TTA) suffered from problems that are easily solved with today's extraction chromatography materials. TOA was impregnated onto a paper support for separation of thorium, uranium, and zirconium. Using 4 N HCl as the eluent, >90% recovery of each metal was achieved. Unfortunately, the resin capacity was three to four times lower than expected.⁶⁶ In another study, MIBK was impregnated onto Chromosorb-W for separation of Sn⁴⁺ from a series of divalent transition metals. While reported separation factors were adequate (>10), it was necessary to condition the prepared column with dilute extractant solution during the elution process to minimize column bleed.⁶⁷ Lastly, in work by Akaza,⁶⁸ an MIBK-TTA solution was impregnated onto Kel-F for alkaline earth metal extraction. The large amounts of TTA needed cause problems in achieving equilibration. Difficulty in attaining equilibrium during extraction is addressed by impregnating the solid support with a dilute extractant solution, especially when the extractant is viscous.

The phosphorus-based extractants, TBP and HDEHP, have been used since the 1950's and are found today in commercial resins. TBP paired with n-octyl(phenyl)-*N, N*-diisobutylcarbamoyl phosphine oxide (CMPO) on XAD-7, or TRU resin, was used to extract a

series of tetravalent actinides with TBP being added to prevent third-phase formation commonly seen in CMPO-based extractions.⁶⁹ For lanthanide separations, EiChrom Technologies markets the Ln resin, which is simply HDEHP impregnated onto an inert polymeric support.⁷⁰ While both are well known, each resin requires improvement in efficiency.

Separation of trivalent americium from trivalent lanthanides (*e.g.*, europium) and curium are among the most challenging of separations, due to identical oxidation state and similar ionic radii of these ions.⁷¹ Thus, this separation has long been of immense interest. Early reports of single-extractant systems displayed inadequate separation of Am³⁺ from Eu³⁺.⁷² In an attempt to develop a more selective extraction system, Yamaura *et al.*⁷³ devised a synergistic system combining CMPO with TBP on XAD-7. Poor separation was achieved, requiring the use of aqueous phase complexants to hold back Am³⁺. Saipriya *et al.*⁷⁴ tried a similar approach with CMPO and HDEHP impregnated onto Tulsion ADS 400, an acrylic polymer. Synergism was achieved below 0.5 M HNO₃, but not above. Even with the addition of citric and diethylenetriaminepentaacetic acids as aqueous complexing agents, the best separation factors were still less than five.

Regarding Am³⁺ and Cm³⁺ separation, a number of support-extractant combinations have been used as shown below (Table 1.1). Unfortunately, poor separation factors (<4) were obtained. Commercial extraction resins show only modest improvement. Kurosaki *et al.*⁷⁹ used CMPO-based TRU resin to achieve a resolution of 1.36 between the two, but this required a flow rate of 0.115 mL/minute leading to a 270-minute run time. Gharibyan *et al.*⁸⁰ looked at Am³⁺-Cm³⁺ separations using seven current commercial resins, including TRU resin, with no single column achieving separation between the two; rather a combination of DGA and TRU resins was needed.

Table 1.1: Americium and curium separations using various supports and stationary phases

Support	Stationary Phase	Reference
Kieselguhr	Aliquat 336	75
Dowex 1 x 8	Nitrate-Anion Exchange Resin	76
Silica	Tertiary pyridine	77
Polyacrylonitrile	N,N'-dimethyl-N,N'- dioctylhexylethoxymalonamide N,N,N',N'- tetraoctyl di-glycolamide	78

To prepare supported extractants, a pure support is slurried in a solution of extractant dissolved in a volatile solvent, followed by evaporation of the solvent. Alternatively, the support is contacted with excess extractant dissolved in an organic solvent. The excess extractant-solvent solution is filtered off, followed by evaporation of the excess solvent.⁸¹ Once prepared, the interactions between support and extractant are physical in nature, as opposed to the covalent bonds observed between the stationary phases and solid supports used in liquid and gas chromatography.⁸²

The ideal support-extractant (or extractant solution) combination should exhibit sufficient capacity, and be thermally and radiolytically stable, easily prepared, and reusable over multiple cycles. Also, the metal ion of interest should be strongly retained, but not so strongly that it cannot be eluted with a mineral acid solution of appropriate concentration. The system should also separate the target metal efficiently from interfering metals. Column efficiency is dependent on the support particle size, metal ion diffusion in the mobile and stationary phases, stationary phase thickness, and mobile phase velocity.⁸

Diffusion of the metal ion in the pores of the resin is impacted by the viscosity of the stationary phase. Accordingly, dilute extractant solutions have often been impregnated onto solid supports.⁸³ This is also helpful if the LLE system employs a viscous solvent, thus rendering LLE with undiluted extractant impractical. Often, extraction chromatographic behavior can be predicted at least semi-quantitatively using LLE results. Kimura observed similar behavior of Th⁴⁺ and U⁴⁺ extracted with tri-n-butyl phosphate (TBP) in both free form and impregnated onto an Amberlite XAD-4 support.⁸⁴ Likewise, Horwitz *et al.* observed similar distribution ratios for the lanthanide series extracted using HDEHP, 2-ethylhexyl 2-ethylhexylphosphonic acid, and *bis*(2,4,4-trimethylpentyl)phosphinic acid in free form and impregnated onto Amberchrom CG-71 resin.⁸⁵ For some systems, specifically that of crown in 1-octanol impregnated onto XAD-7 for Sr-85 extraction,⁵⁸ a loss in extraction efficiency is not observed. Thus, a cumbersome LLE system can be studied more quickly if impregnated onto a solid support.

Weight distribution ratios (D_w) are measured in extraction chromatography, akin to LLE, with the weight of the loaded resin included as shown by Equation 1.7:

$$D_w = \left(\frac{A_o - A_s}{w} \right) \left(\frac{A_s}{V} \right) \quad (1.7)$$

where A_o , A_s , w , and V are the aqueous phase concentration before equilibrium, aqueous phase concentration after equilibration, weight of the resin in grams, and volume of the aqueous phase in milliliters (Note that A_o and A_s can also be replaced with absorbance or counts per minute before and after equilibration).

To convert between the volume distribution ratios and weight distribution ratios, Equation 1.8 is used:

$$D_v = D_w \left(\frac{d_{extr}}{extr_{load}} \right) \quad (1.8)$$

where d_{extr} is the density of the extractant and $extr_{load}$ is the extractant loading onto the resin in grams of extractant per gram of resin. With a resin-packed column, the number of free column volumes to peak maximum, or k' , can be predicted from Equation⁸⁵ 1.9

$$k' = D_v \left(\frac{v_s}{v_m} \right) \quad (1.9)$$

While Equation 1.9 allows for the prediction of the peak maxima in an elution profile, it does not provide a measure of chromatographic efficiency in metal separation. The calculation of the number of theoretical plates (N) is used instead.

$$N = 5.54 \left(\frac{V_R}{w_{1/2}} \right)^2 \quad (1.10)$$

where V_R and $w_{1/2}$ are the free column volume at peak maximum and width of the elution peak at half the peak height.⁸⁶ The largest possible number of theoretical plates is desired as the eluted peaks are narrower allowing for better separation.

1.6 Overview of the chapters

Chapter 2 discusses a new method for measuring extractant solubility in ionic liquids. By taking advantage of the thermal stability of ILs relative to non-aromatic metal ion extractants, thermogravimetric analysis (TGA) was applied to degrade and/or evaporate the extractant from an extractant-IL solution, leaving behind the IL, and allowing for extractant quantification. The method provides the basis for the results reported in Chapter 3.

Chapter 3 discusses the solubility of HDEHP in several families of ILs and attempts to explain the solvent parameters that influence it. On the basis of the results, a set of guidelines is

proposed that allow for maximum solubility of HDEHP (and by analogy, other extractants) in ILs. The results also provide the basis for the experiments discussed in Chapter 6.

Chapter 4 discusses the advantages gained in extraction chromatography by incomplete loading. By coupling support surface area measurements with column efficiency data, an in-depth explanation of the interior pore structure of a commercial solid support, Amberchrom CG-71m is obtained. Once the pore structure is understood, these “lightly-loaded resins” are used to separate the adjacent lanthanides, $\text{Eu}^{3+}/\text{Nd}^{3+}$ and $\text{Eu}^{3+}/\text{Gd}^{3+}$.

Chapter 5 continues the improvement in the understanding of support pore structure gained in Chapter 4 by filling the least accessible pores of the support with an inert filler, 1-dodecanol. By then adding HDEHP at various amounts to these “stagnantly-pore plugged (SPP) resins,” improvements in column efficiency and capacity are achieved. As in Chapter 4, intra-lanthanide separations are used to highlight the advantages of these resins.

Chapter 6 further demonstrates the usefulness of the SPP supports by impregnating them with a thin layer of FIL, both in pure form and diluted in *n*-dodecane or 1-decyl-3-methylimidazolium *bis*(trifluoromethanesulfonyl)imide. These resins, along with sorbents incorporating pure or dilute HDEHP, are used for acid, extractant, and nitrate dependencies in order to elucidate the extraction mechanism of $^{152/4}\text{Eu}$ and ^{241}Am in these solvents.

1.7 References

1. Wall, F. (2014). *Rare earth elements*. (G. Gunn, Ed.) (First). Hoboken, NJ: John Wiley & Sons.
2. Orris, G.J.; Hedrick, J.B.; Haxel, G. B. (2002). *Rare earth elements — Critical resources for high technology*.
3. Binnemans, K., & Jones, P. T. (2015). Rare earths and the balance problem. *Journal of Sustainable Metallurgy*, 1, 29–38.

4. Werner, J. D. (2012). *U.S. spent nuclear fuel storage. Congressional Research Service.* Washington D.C.
5. Magill, J.; Berthou, V.; Haas, D.; Galy, J.; Schenkel, R.; Wiese, H.W.; Heusener, G.; Tommasi, J.; Youinou, G. (2003). Impact limits of partitioning and transmutation scenarios on the radiotoxicity of actinides in radioactive waste. *Nuclear Energy*, 42, 263–277.
6. Madic, C. (2007). *Partitioning : New solvent extraction processes for minor actinides.* Brussels, Belgium.
7. World Nuclear News (2019). US budget request supports Yucca mountain. Retrieved from <https://world-nuclear-news.org/Articles/US-budget-request-supports-Yucca-Mountain>
8. Salvatores, M., & Palmiotti, G. (2011). Radioactive waste partitioning and transmutation within advanced fuel cycles: achievements and challenges. *Progress in Particle and Nuclear Physics*, 66, 144–166.
9. Modolo, G., Wilden, A., Geist, A., Magnusson, D., & Malmbeck, R. (2012). A review of the demonstration of innovative solvent extraction processes for the recovery of trivalent minor actinides from PUREX raffinate. *Radiochimica Acta*, 100, 715–725.
10. Schroeder, N. C., Attrep, M., & Marrero, T. (2001). *Technetium and iodine separations in the urex process. Accelerator transmutation of waste program: Final report for WBS 1.24.01.01.* Los Alamos, NM.
11. Regalbuto, M. C. (2011). Alternative separation and extraction: UREX+ processes for actinide and targeted fission product recovery. *Advanced Separation Techniques for Nuclear Fuel Reprocessing and Radioactive Waste Treatment*, 176–200.
12. Baron, P., Heres, X., Lecomte, M., & Masson, M. (2001). Separation of the minor actinides: the DIAMEX-SANEX concept. Retrieved from <https://www.osti.gov/etdeweb/servlets/purl/20264249>.
13. Gelis, A. V., & Lumetta, G. J. (2014). Actinide lanthanide separation process – ALSEP. *Industrial and Engineering Chemistry Research*, 53, 1624–1631.
14. Weaver, B., & Kappelmann, F. A. (1964). *TALSPEAK: A new method of separating americium and curium from the lanthanides by extraction from an aqueous solution of an aminopolyacetic acid complex with a monoacidic organophosphate or phosphonate* (Vol. 32). ORNL-3559.
15. Fort, D.A.; Swatloski, R.P.; Moyna, P.; Rogers, R.D.; Moyna, G. (2006). Use of ionic liquids in the study of fruit ripening by high-resolution ¹³C-NMR spectroscopy: ‘Green’ solvents meet green bananas. *Chem. Comm.*, 7, 714-716.

16. Schröder, C. (2017). Proteins in ionic liquids: current status of experiments and simulations. *Topics Curr. Chem.* 375, 1-26.
17. Brandt, A., Hallett, J. P., Leak, D. J., Murphy, R. J., & Welton, T. (2010). The effect of the ionic liquid anion in the pretreatment of pine wood chips. *Green Chemistry*, 12, 672–679.
18. Sun, X., Luo, H., & Dai, S. (2012). Solvent extraction of rare-earth ions based on functionalized ionic liquids. *Talanta*, 90, 132–137.
19. Mohapatra, P. K., Kandwal, P., Iqbal, M., Huskens, J., Murali, M. S., & Verboom, W. (2013). A novel CMPO-functionalized task specific ionic liquid: synthesis, extraction and spectroscopic investigations of actinide and lanthanide complexes. *Dalton Transactions*, 42, 4343–4347.
20. Peligot ME. (1842). Analysis of green chloride. *Ann Chim Phys.* 5, 5-7.
21. Akaza, I. (1975). *Extraction chromatography*. (G. Braun, T.; Ghersini, Ed.) (2nd ed.). New York, New York: Elsevier.
22. Sekine, T., Hasegawa Y. *Solvent extraction chemistry*. New York: Marcel Dekker Inc.; 1977.
23. Hawkins C. *Fundamental and applied studies of metal ion extraction by crown ethers into imidazolium-based room temperature ionic liquids*. University of Wisconsin-Milwaukee, Milwaukee, WI; 2012.
24. Panja, S., Mohapatra, P.K., Tripathi, S.C., Gandhi, P.M., Janardan, P. (2012). A highly efficient solvent system containing TODGA in room temperature ionic liquids for actinide extraction. *Separation and Purification Technology*, 96, 289–295.
25. Sengupta, A., Mohapatra, P. K., Iqbal, M., Verboom, W., Huskens, J., & Godbole, S. V. (2012). Extraction of Am(III) using novel solvent systems containing a tripodal diglycolamide ligand in room temperature ionic liquids: A “green” approach for radioactive waste processing. *RSC Advances*, 2, 7492–7500.
26. Dietz, M. L., Horwitz, E. P., & Bond, A. H. (1999). Extraction chromatography: Progress and opportunities. *Metal Ion Separation and Preconcentration*, 234–250.
27. Cocalia VA, Jensen MP, Holbrey JD, Spear SK, Stepinski DC, Rogers RD. (2005). Identical extraction behavior and coordination of trivalent or hexavalent *f*-element cations using ionic liquid and molecular solvents. *Dalton Transactions*, 11, 1966-1971.
28. Dietz, M.L., Horwitz, E. P. (1993). Novel chromatographic materials based on nuclear waste processing chemistry. *LC-GC*, 11, 424–436.

29. C.R. Porter, B. Khan, M.W. Carter, G.L. Vehnberg, E. W. P., & Article. (1967). Determination of radiostrontium in food and other environmental samples. *Environmental Science and Technology*, 1, 745–750.
30. Walden, P. (1914). Molecular weights and electrical conductivity of several fused salts. *Bull. Acad. Imper. Sci. (St. Petersburg)*, 8, 405–422.
31. Wilkes, J. S. (2002). A short history of ionic liquids – From molten salts to neoteric solvents. *Green Chemistry*, 4, 73–80.
32. Janssen, C. H. C., Macías-Ruvalcaba, N. A., Aguilar-Martínez, M., & Kobrak, M. N. (2015). Metal extraction to ionic liquids: the relationship between structure, mechanism and application. *International Reviews in Physical Chemistry*, 34, 591–622.
33. Matsumiya, M., Kikuchi, Y., Yamada, T., & Kawakami, S. (2014). Extraction of rare earth ions by tri-n-butylphosphate/phosphonium ionic liquids and the feasibility of recovery by direct electrodeposition. *Separation and Purification Technology*, 130, 91–101.
34. Mohapatra, P. K., Sengupta, A., Iqbal, M., Huskens, J., & Verboom, W. (2013). Highly efficient diglycolamide-based task-specific ionic liquids: Synthesis, unusual extraction behavior, irradiation, and fluorescence studies. *Chemistry – A European Journal*, 19, 3230–3238.
35. Luo, H. M., Boll, R. A., Bell, J. R., & Dai, S. (2012). Facile solvent extraction separation of Th-227 and Ac-225 based on room-temperature ionic liquids. *Radiochimica Acta*, 100, 771–777.
36. Rout, A., Venkatesan, K. A., Srinivasan, T. G., & Vasudeva Rao, P. R. (2011). Room temperature ionic liquid diluent for the extraction of Eu(III) using TRUEX extractants. *Journal of Radioanalytical and Nuclear Chemistry*, 290, 215–219.
37. Panja, S., Mohapatra, P.K., Tripathi, S.C., Gandhi, P.M., Janardan, P. (2012). A highly efficient solvent system containing TODGA in room temperature ionic liquids for actinide extraction. *Separation and Purification Technology*, 96, 289–295.
38. Huddleston, J. G., Willauer, H. D., Swatloski, R. P., Visser, A. E., & Rogers, R. D. (1998). Room temperature ionic liquids as novel media for ‘clean’ liquid–liquid extraction. *Chemical Communications*, 1765–1766.
39. Garvey, S. L., Hawkins, C. A., & Dietz, M. L. (2012). Effect of aqueous phase anion on the mode of facilitated ion transfer into room-temperature ionic liquids. *Talanta*, 95, 25–30.
40. Hawkins, C. A., Momen, M. A., Garvey, S. L., Kestell, J., Kaminski, M. D., & Dietz, M. L. (2015). Evaluation of solid-supported room-temperature ionic liquids containing crown ethers as media for metal ion separation and preconcentration. *Talanta*, 135, 115–123.

41. Luo, H., Dai, S., Bonnesen, P.V., Buchanan III, A.C., Holbrey, J.D., Bridges, N.J., Rogers R.D. (2004). Extraction of cesium ions from aqueous solutions using calix[4]arene-bis(tert-octylbenzo-crown-6) in ionic liquids. *Anal. Chem.*, *76*, 3078–3083.
42. Tsuda, T., Hussey, C. L., Luo, H., & Dai, S. (2006). Recovery of cesium extracted from simulated tank waste with an ionic liquid: water and oxygen effects. *Journal of The Electrochemical Society*, *153*, D171.
43. Rout, A., Karmakar, S., Venkatesan, K. A., Srinivasan, T. G., & Vasudeva Rao, P. R. (2011). Room temperature ionic liquid diluent for the mutual separation of europium(III) from americium(III). *Separation and Purification Technology*, *81*, 109–115.
44. Lohithakshan, K. V., Patil, P., & Aggarwal, S. K. (2014). Solvent extraction studies of plutonium(IV) and americium(III) in room temperature ionic liquid (RTIL) by di-2-ethyl hexyl phosphoric acid (HDEHP) as extractant. *Journal of Radioanalytical and Nuclear Chemistry*, *301*, 153–157.
45. Sun, X., Bell, J. R., Luo, H., & Dai, S. (2011). Extraction separation of rare-earth ions via competitive ligand complexations between aqueous and ionic-liquid phases. *Dalton Transactions*, *40*, 8019–8023.
46. Zhao, L., Dong, Z., Ma, G., & Yuan, W. (2015). Solution extraction of several lanthanides from nitric acid with isohexyl-BTP in [C_nmim][NTf₂] ionic liquid. *Journal of Rare Earths*, *33*, 1182–1188.
47. George, A., Brandt, A., Tran, K., Zahari, S. M. S. N. S., Klein-Marcuschamer, D., Sun, N., Hallett, J. P. (2015). Design of low-cost ionic liquids for lignocellulosic biomass pretreatment. *Green Chemistry*, *17*, 1728–1734.
48. Jensen, M. P., Neuefeind, J., Beitz, J. V., Skanthakumar, S., & Soderholm, L. (2003). Mechanisms of metal ion transfer into room-temperature ionic liquids: the role of anion exchange. *Journal of the American Chemical Society*, *125*, 15466–15473.
49. Dietz, M. L., & Dzielawa, J. A. (2001). Ion-exchange as a mode of cation transfer into room-temperature ionic liquids containing crown ethers: Implications for the “greenness” of ionic liquids as diluents in liquid-liquid extraction. *Chemical Communications*, *20*, 2124–2125.
50. Dietz, M. L. Hawkins, C. (2020). Task-specific ionic liquids for metal ion extraction: progress, challenges, and prospects. Bruce A. Moyer (Ed.), In *Ion Exchange and Solvent Extraction* (23rd ed., pp. 83–113). Boca Raton, FL: CRC Press.
51. Visser, A. Swatloski, E. Reichert, P. Mayton, W.M., Sheff, R., Wierzbicki, S., Davis, Jr., A. Rogers, R.D. (2001). Task-specific ionic liquids for the extraction of metal ions from aqueous solutions. *Chemical Communications*. 135-136.

52. Visser, A., Swatloski, R. P., Reichert, W. M., Mayton, R., & Sheff, S. (2002). Task-specific ionic liquids incorporating novel cations for the coordination and extraction of Hg^{2+} and Cd^{2+} : Synthesis, characterization, and extraction studies. *Environ. Sci. Tech.*, 36, 2523–2529.
53. Kogelnig, D., Stojanovic, A., Galanski, M., Groessel, M., Jirsa, F., Krachler, R., & Keppler, B. K. (2008). Greener synthesis of new ammonium ionic liquids and their potential as extracting agents. *Tetrahedron Letters*, 49, 2782–2785.
54. Biswas, S., Rupawate, V. H., Roy, S. B., & Sahu, M. (2014). Task-specific ionic liquid tetraalkylammonium hydrogen phthalate as an extractant for U(VI) extraction from aqueous media. *Journal of Radioanalytical and Nuclear Chemistry*, 300, 853–858.
55. Sun, X., Ji, Y., Liu, Y., Chen, J., & Li, D. (2010). An engineering-purpose preparation strategy for ammonium-type ionic liquid with high purity, 56, 989–996.
56. Sun, X., Luo, H., & Dai, S. (2012). Solvent extraction of rare-earth ions based on functionalized ionic liquids. *Talanta*, 90, 132–137.
57. Rout, A., Kotlarska, J., Dehaen, W., & Binnemans, K. (2013). Liquid-liquid extraction of neodymium(III) by dialkylphosphate ionic liquids from acidic medium: The importance of the ionic liquid cation. *Physical Chemistry Chemical Physics*, 15, 16533–16541.
58. Dietz, M. L. (2003). *Recent progress in the development of extraction chromatographic methods for radionuclide separation and preconcentration*. (K. L. Nash & C. A. Laue, Eds.), *Radioanalytical methods in interdisciplinary research: Fundamentals in cutting-edge applications*. Washington D.C.: American Chemical Society.
59. Cerrai, E., Esla, C., Triulzi, C. (1962). Separation of rare earths by column chromatography with cellulose powder treated with di(2-ethylhexyl)orthophosphoric acid-Part 2. *Energia*, 9, 377–384.
60. E.P. Horwitz, C. A. A. B. (1967). The separation of milligram quantities of americium and curium by extraction chromatography. *Radiochimica Acta*, 8, 127–132.
61. Lieser, B. (1966). Separation of calcium and strontium by column chromatography. *Fresenius' Zeitschrift Fur Analytische Chemie*, 219, 401–408.
62. Eschrich, H. (1967). Separation of neptunium (IV), neptunium (V), neptunium(VI) by extraction chromatography. *Fresenius' Zeitschrift Fur Analytische Chemie*, 226, 100–114.
63. Horwitz, E. P., Bloomquist, C.A.A., Henderson, D. J. (1969). The extraction chromatography of californium, einsteinium, and fermium with di(2-ethylhexyl)orthophosphoric acid. *Journal of Inorganic and Nuclear Chemistry*, 31, 1149–1166.
64. McClaine, B. L. A., Noble, P., & Bullwinkel, E. P. (1958). The development and properties of an adsorbent for uranium. *The Journal of Physical Chemistry*, 62, 299–303.

65. Kirkland, J. J. (1971). Columns for modern analytical liquids. *Analytical Chemistry*, *43*, 36A–48A.
66. Cerria, E. (1961). The use of tri-n-octylamine-cellulose in chemical separations. *Journal of Chromatography*, *6*, 443–451.
67. Fritz, J.S., Latwesen, G. L. (1967). Separation of tin from other elements by partition chromatography. *Talanta*, *14*, 529–536.
68. Akaza, I. (1966). The separation of alkaline by reversed-phase earth metals as their tta-complexes partition chromatography by reversed-phase partition chromatography. *Bulletin of the Chemical Society of Japan*, *39*, 980–989.
69. Horwitz, E.P., Chiarizia, R., Dietz, M.L., Diamond, H. (1993). Separation and preconcentration of actinides from acidic media by extraction chromatography. *Analytica Chimica Acta*, *281*, 361–372.
70. Ln Resins – Eichrom Technologies Inc. (2020) Retrieved from <https://www.eichrom.com/eichrom/products/ln-resins/>.
71. Seaborg, G. T. (1993). Overview of the actinide and lanthanide (the f) elements. *Radiochimica Acta*, *61*, 115–122.
72. Weaver, B., & Kappelmann, F. A. (1964). *TALSPEAK: A new method of separating americium and curium from the lanthanides by extraction from an aqueous solution of an aminopolyacetic acid complex with a monoacidic organophosphate or phosphonate* (Vol. 32). ORNL-3559.
73. Yamaura, M., & Matsuda, H. T. (1999). Sequential separation of actinides and lanthanides by extraction chromatography using a CMPO-TBP/XAD-7 column. *Journal of Radioanalytical and Nuclear Chemistry*, *241*, 277–280.
74. Saipriya, G., Kumaresan, R., Nayak, P. K., Venkatesan, K. A., Kumar, T., & Antony, M. P. (2016). Extraction of Am(III) and Eu(III) from nitric acid medium in TEHDGA-HDEHP impregnated resins. *Radiochimica Acta*, *104*, 781–790.
75. E.P. Horwitz, C. A. A. Bloomquist. (1972). The preparation, performance and factors affecting band spreading of high efficiency extraction chromatography columns for actinide separation. *Journal of Inorganic and Nuclear Chemistry*, *34*, 3851–3871.
76. Kraak, W., Van Der Heijden, W. A. (1966). Anion exchange separation between americium and curium and between several lanthanide elements. *Journal of Inorganic and Nuclear Chemistry*, *28*, 221–234.

77. Suzuki, T., Otake, K., Sato, M., Ikeda, A., Aida, M., Fujii, Y., Ozawa, M. (2007). Separation of americium and curium by use of tertiary pyridine resin in nitric acid/methanol mixed solvent system. *Journal of Radioanalytical and Nuclear Chemistry*, 272, 257–262.
78. Šťastná, K., Distler, P., John, J., & Šebesta, F. (2017). Separation of curium from americium using composite sorbents and complexing agent solutions: part 2. *Journal of Radioanalytical and Nuclear Chemistry*, 312, 685–689.
79. Kurosaki, H., & Clark, S. B. (2011). Chromatographic separation of Am and Cm. *Radiochimica Acta*, 99, 65–69.
80. Gharibyan, N., Dailey, A., McLain, D. R., Bond, E. M., Moody, W. A., Happel, S., & Sudowe, R. (2014). Extraction behavior of americium and curium on selected extraction chromatography resins from pure acidic matrices. *Solvent Extraction and Ion Exchange*, 32, 391–407.
81. Markl, P., Schmid, E. R. (1975). *Extraction chromatography*. (M. Katykhin, G.S., Braun, T., Ghersini, Ed.) (First). New York: American Elsevier.
82. Bokobza, L. (1985). Spectroscopic investigation of adsorbed 7-(4-ethyl-1-methyloctyl)-9-quinolinol (Kelex 100) and of its gallium (III) complex: Comparison with the behaviours observed in solvent extraction systems. *Polyhedron*, 4, 1499–1505.
83. Hawkins, C. A., Momen, M. A., Garvey, S. L., Kestell, J., Kaminski, M. D., & Dietz, M. L. (2015). Evaluation of solid-supported room-temperature ionic liquids containing crown ethers as media for metal ion separation and preconcentration. *Talanta*, 135, 115–123.
84. Kimura, T. (1990). Extraction chromatography in the TBP-HNO₃ System. *Journal of Radioanalytical and Nuclear Chemistry*, 141, 295–306.
85. Horwitz, E.P., McAlister, D. R., Dietz, M.L. (2006). Extraction chromatography versus solvent extraction: How similar are they? *Separation Science and Technology*, 41, 2163–2182.
86. Shimadzu. (2017). Theoretical plate number and symmetry factor : SHIMADZU (Shimadzu Corporation). Retrieved from http://www.shimadzu.com/an/hplc/support/lib/lctalk/theoretical_plate.html.

CHAPTER 2:

DETERMINATION OF EXTRACTANT SOLUBILITY IN IONIC LIQUIDS BY THERMOGRAVIMETRIC ANALYSIS

2.1 Introduction

Of the characteristics of a metal ion extractant that determine its utility in liquid-liquid extraction, none is more important than its solubility in the organic solvent. While the strength of the metal complex(es) formed by the extractant, its selectivity over possible interferents, the organic phase solubility of the extracted complex, and the propensity of the extractant toward third-phase formation upon loading obviously play an important role in this determination as well, without adequate organic phase extractant solubility, other considerations are moot. For this reason, countless studies have sought to improve extractant solubility in various organic solvents by the addition of a phase modifier^{1,2} or co-solvents³ or by various structural modifications of the extractant.⁴

With the introduction of ionic liquids (ILs) as extraction solvents⁵ has come yet another possible means of improving the compatibility of an extractant with the organic phase, namely, structural modification of the solvent itself. Given the enormous variety of possible IL structures⁶ and the relative ease with which many ILs can be prepared⁷ this would appear to represent a very promising approach. In fact, ILs have been reported to dissolve a wide range of substances exhibiting poor solubility in conventional (*i.e.*, molecular) diluents, including cellulose,⁸ proteins,⁹ wood chips,¹⁰ polymers,¹¹ wool,¹² and even banana pulp.¹³ Despite this, reports have appeared indicating that certain common metal ion extractants are not particularly well solubilized by various ionic liquids.¹⁴⁻¹⁶ Recent work, for example, has shown that the unexpectedly poor performance of an extraction chromatographic resin incorporating a solution

of a crown ether in any of several 1,3-dialkylimidazolium-based ILs as strontium sorbents is likely the result, in part, of the limited solubility of the extractant in $C_n\text{mim}^+$ ILs.¹⁷ Similarly, the modest solubility of calixarenes in various ILs^{18,19} and the inability of short-chain 1,3-dialkylimidazolium *bis*[(trifluoromethyl)sulfonyl]imides ($C_n\text{mim}^+\text{Tf}_2\text{N}^-$) to dissolve *bis*(2-ethylhexyl)phosphoric acid (HDEHP) have been noted.^{20,21}

A number of methods for determining extractant solubility in molecular solvents have been described. Buschmann *et al.*,²² for example, measured the aqueous solubility of various aromatic crown ethers by UV-visible spectrophotometry, and this same approach was subsequently employed to determine the solubility of 2,4,6-tri(2-pyridyl)-1,3,5-triazine (TPTZ) in nitric acid²³ and of several alkyl-substituted calix[4]arene carboxylates in various organic solvents (*e.g.*, chloroform, toluene, and hexane).²⁴ UV-visible spectrophotometry was also employed by Engle *et al.*²⁵ as a means of detection for high-performance liquid chromatography, in the measurement of the solubility of several alkyl-substituted calixcrown compounds in Isopar L, a commercial blend of isoparaffinic hydrocarbons. Spectrophotometric methods are applicable only in cases in which the extractant incorporates a suitable chromophore, however, a characteristic clearly not shared by all extractants (*e.g.*, aliphatic crown ethers).

Principe and Demopoulos employed measurements of phosphorus emission obtained by inductively coupled plasma atomic emission spectroscopy (ICP-AES) to determine the solubility of selected organophosphorus extractants (*e.g.*, HDEHP) in various aqueous phases (*e.g.*, dilute sulfuric acid) following contact with a solution of the extractant in tridecanol-modified kerosene.²⁶ The approach appears not to have been applied to the determination of organic phase extractant solubility, however. Moreover, it is clearly applicable only to phosphorus-containing extractants. A more broadly applicable approach is suggested by the work of Nogawara *et al.*,²⁷

in which the water solubility of dioctyldiglycolamic acid (DODGAA), a prospective “green” extractant for lanthanides, was determined by measurements of the total organic carbon content (TOC) of the aqueous phase following equilibration with the extractant. Finally, Williams *et al.*²⁸ have measured the solubility of the anion receptor $\alpha,\alpha',\alpha'',\alpha'''$ -mesotetrahexyl- tetramethyl-calix[4]pyrrole in both water and a range of organic solvents using $^1\text{H-NMR}$. The measurements are neither rapid nor especially convenient, however.

In this work, we evaluate thermogravimetric analysis (TGA) as a method for the determination of the solubility of various extractants in room temperature ionic liquids. This method exploits the high thermal stability characteristic of many RTILs, which under appropriate conditions, allows for the decomposition or volatilization of the extractant from its solution with the ionic liquid without concomitant mass loss from the IL. As an illustration of the scope and limitations of the approach, its application to the determination of the solubility of several well-known extractants (*e.g.*, bis(2-ethylhexyl)phosphoric acid (HDEHP)) in a series of C_nmim^+ -based ILs is described.

2.2 Experimental

2.2.1 Reagents

All chemicals were of reagent grade and unless otherwise noted, were used as received. Lithium bis[(trifluoromethyl)sulfonyl]imide (LiTf_2N) was purchased from TCI America (Portland, OR), while 1-methylimidazole, lithium trifluoromethane sulfonate (*i.e.*, lithium triflate; LiTf), lithium perfluorobutane sulfonate (*i.e.*, lithium nonaflate; LiNfO), and all alkyl bromides were obtained from Sigma-Aldrich (St. Louis, MO). The ionic liquids were synthesized *via* a two-step procedure involving quaternization of the methylimidazole with an

appropriate alkyl bromide to yield the halide form of the IL, followed by anion metathesis to provide the desired (*e.g.*, Tf₂N⁻) product.^{29,30} The ILs were then dried for 24 hours *in vacuo* at 80°C^{31,32} and stored in a desiccator until use. HDEHP was purchased from Sigma-Aldrich and purified *via* copper salt precipitation.³³ The di-*tert*-butylcyclohexano-18-crown-6 (DtBuDCH18C6) was purchased from EiChrom Technologies (Lisle, IL) and purified by HClO₄ precipitation.³⁴ Its 4z,5'z *cis-syn-cis* isomer was isolated as described previously.¹⁷ Octyl(phenyl)-*N,N*-diisobutylcarbamoylmethylphosphine oxide (CMPO) was generously provided by Argonne National Laboratory. Its preparation and purification have been described in prior work.³⁵ The calix[4]arene-*bis*(*tert*-octylbenzo-crown-6 (“Bob-Calix”)) was a generous gift from Oak Ridge National Laboratory. The 2,6-*bis*(5,5,8,8-tetramethyl-5,6,7,8-tetrahydrobenzo[1,2,4]triazine-3-yl)pyridine (which is hereafter abbreviated as BTP) was synthesized according to published methods.³⁶

2.2.2 Equipment

A TA Instruments TGA Q50 equipped with a platinum pan was used for all thermal property measurements, and all mass loss data were processed using the TA Universal Analysis software.

2.2.3 Procedures

As a first step, the thermal stability of the IL was evaluated in the absence of added extractant. Following measurements using a temperature scan of 10 °C/ min under nitrogen to establish the temperature corresponding to the onset of mass loss (T_{onset}), a series of isothermal runs were carried out on the same IL to determine the rate and extent of mass loss at temperatures well removed from T_d (*e.g.*, $T_d - 50$ °C). The same process was then repeated for

the extractant of interest. On the basis of these results, conditions (*i.e.*, temperature, hold time) were identified whereby the extractant could be volatilized or decomposed without concomitant loss of the IL. Next, the IL was equilibrated with an excess of the extractant for at least six hours. A *ca.* 25 mg sample of extractant-saturated IL was then taken for thermal analysis. For blank determinations, the pure IL was subjected to an identical temperature program. The mass loss for each test sample and IL was measured three times. Finally, to verify the validity of the approach, measurements were made under conditions in which a solution of the extractant in the same (or a closely related) IL of known concentration (below saturation) could be prepared. Comparison of the results obtained to the expected (*i.e.*, as prepared) values of extractant concentration provided a measure of the accuracy of the method.

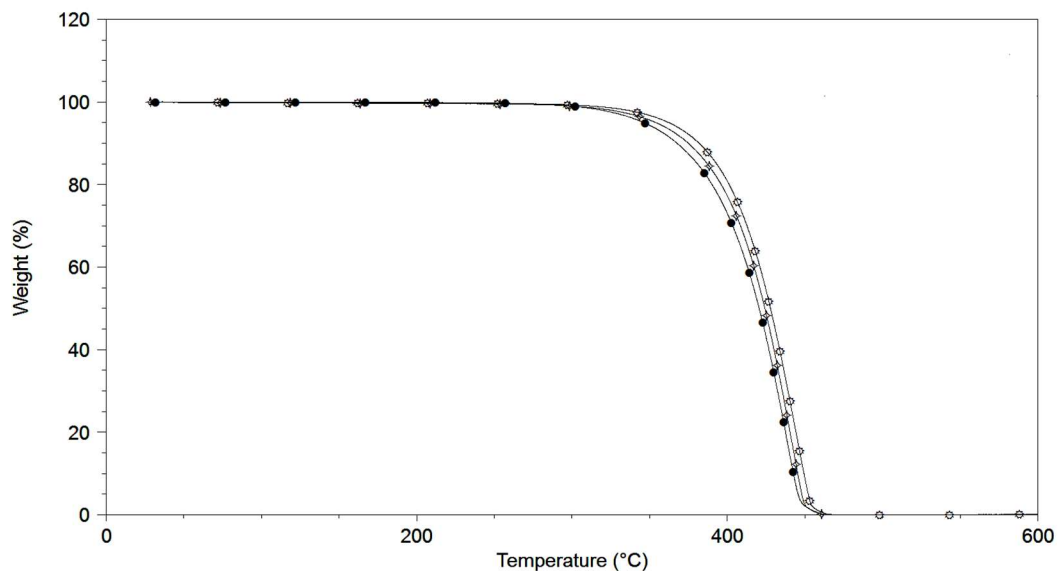
2.3 Results and Discussion

The exceptional thermal stability exhibited by many ionic liquids has long been recognized³⁷⁻³⁹ and it remains among the most often-cited advantages of ILs over conventional, molecular solvents. Early investigations suggested that this advantage was quite substantial, with a number of ILs exhibiting T_d values (the temperature corresponding to the onset of mass loss in a thermogravimetric analysis) exceeding 400 °C.³² Subsequent work, however, demonstrated that in part, this observation is a consequence of the method employed for assessing thermal stability. That is, in evaluating thermal stability, TGA measurements often employ a relatively rapid (10 °C/min) temperature ramp to determine the temperature dependence of mass loss, resulting in overestimation of the onset temperature.⁴⁰ It is now known that thermal stability is best assessed by isothermal experiments carried out at a series of temperatures. Such studies have revealed that over time, appreciable decomposition of ILs can occur even at temperatures well below the T_d established on the basis of temperature ramping.⁴¹

Our work therefore began with a systematic examination of the thermal stability of a series of 1,3-dialkylimidazolium ILs that included assessment of both the temperature dependence and time dependence (at fixed temperature) of the mass loss.

Figure 2.1 (panel A) shows the results obtained in temperature-ramping studies of three $C_n\text{mim}^+\text{Tf}_2\text{N}^-$ ILs ($n = 6, 8, \text{ and } 10$), while Figure 1B depicts the results of representative isothermal measurements carried out on the $C_6\text{mim}^+$ compound at both T_d and at temperatures 50 °C and nearly 100 °C below it. Conventional temperature ramping yields T_d values of 397 °C, 401 °C, and 404 °C, respectively, for the three ILs, values consistent with those reported previously.^{42,43} More importantly, all of these ILs (as exemplified by the $C_6\text{mim}^+$ compound) do exhibit measurable mass loss at temperatures well below T_d , a result in agreement with prior observations by several investigators for a variety of ILs.⁴⁴⁻⁴⁶ At 50 °C below the onset temperature, for example, a 29% loss in mass is observed for the C_6 -IL over a 60-minute period. Therefore, in developing a scheme by which the extractant can be volatilized or decomposed while the IL remains intact, it will clearly not suffice to simply select an arbitrary temperature below T_d . Rather, it is necessary to identify conditions under which no IL degradation occurs over the time frame required for removal of the extractant. For $C_6\text{mim}^+\text{Tf}_2\text{N}^-$, less than 1% mass loss occurs over a period of up to two hours when the temperature is maintained at 150 °C below T_d . For extractant solubility determinations then, the ideal situation is one in which the extractant is completely lost over this time period at the same (or lower) temperature.

(A)



(B)

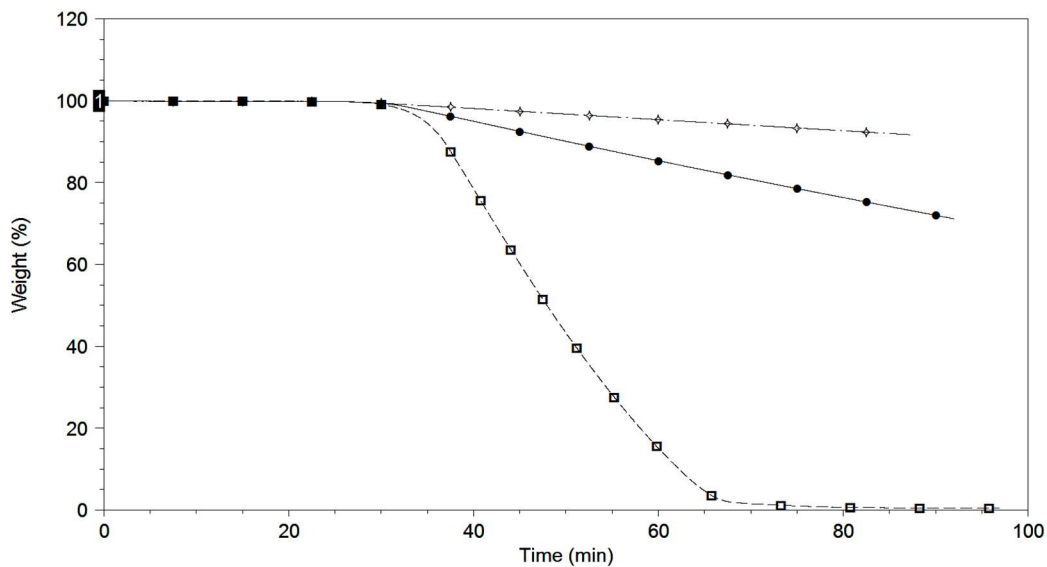


Figure 2.1: (A) TGA thermogram of C₆mim⁺Tf₂N⁻ (bottom; closed circles), C₈mim⁺Tf₂N⁻ (middle; open diamonds), and C₁₀mim⁺Tf₂N⁻ (top; open circles) (B) Isothermal heating of C₆mim⁺Tf₂N⁻ at 300 °C (top; open diamonds), 346°C (middle; closed circles), and 396 °C (bottom; open squares) for 60 min.

Prior work in this laboratory has shown that a number of aliphatic crown ethers can be completely volatilized at relatively low temperatures.⁴⁷ Several cyclohexano- and dicyclohexano-derivatives of 18-crown-6, for example, have been found to exhibit T_d values ranging from *ca.* 179-225 °C, well below the temperatures necessary to initiate mass loss in $C_n\text{mim}^+\text{Tf}_2\text{N}^-$ ILs. It should therefore be straightforward to remove these extractants from an IL solution and thus, to determine their solubility in the ILs. Indeed, as shown in Figure 2.2, which depicts the thermal behavior of 4*z*, 5'*z* *cis-syn-cis* isomer form of *DtBuCH18C6*, mass loss is complete for this extractant if the temperature is held at 250 °C for 60 minutes, conditions under which no mass loss is observed for the ILs of interest.

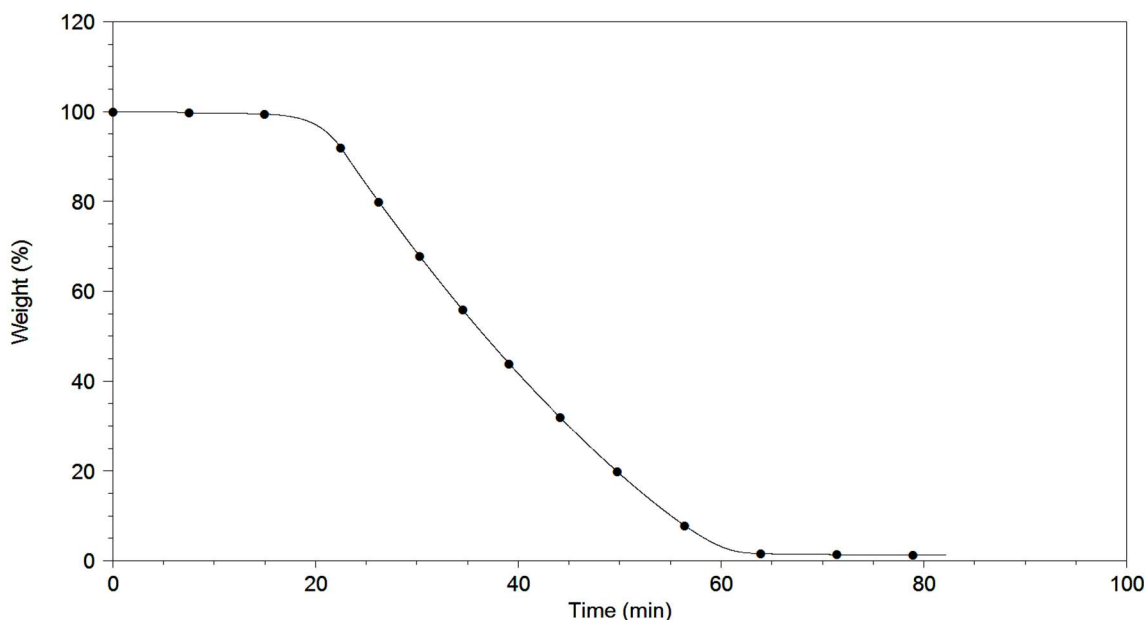


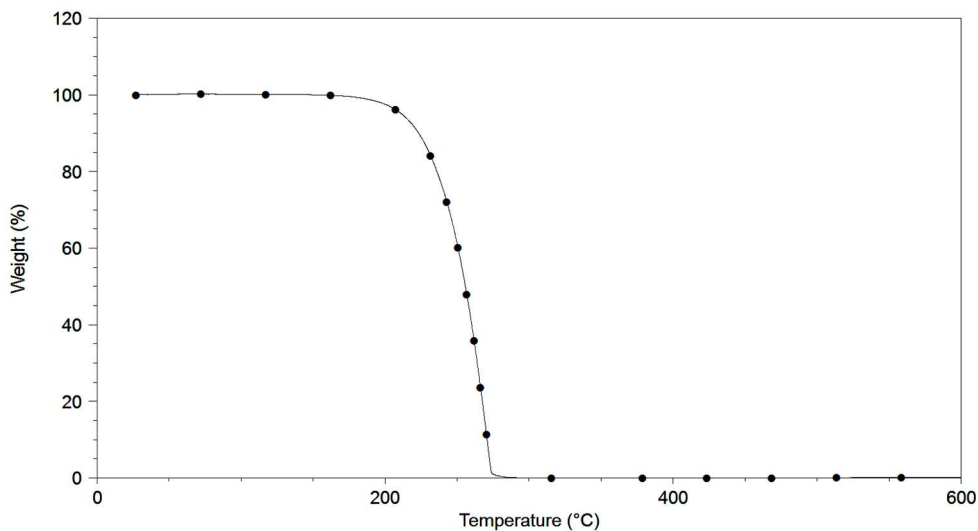
Figure 2.2: Isothermal heating of *DtBuDCH18C6* at 250 °C for 85 minutes.

As noted above, recent work in this laboratory demonstrating the inadequacy of solutions of *DtBuCH18C6* in various $C_n\text{mim}^+\text{Tf}_2\text{N}^-$ ILs as the basis of the stationary phase in an extraction chromatographic resin for strontium ion showed that problems with the sorbent could be partly attributed to limited extractant solubility in the ILs.¹⁷ In particular, metal ion uptake studies

suggested that the solubility of the 4z, 5'z *cis-syn-cis* form of DtBuCH18C6 was no more than 0.6 M, well under the 1 M required for satisfactory sorbent performance. Application of the temperature program described above (*i.e.*, 250 °C for 60 minutes) to a saturated solution of this isomer in C₁₀mim⁺Tf₂N⁻ yielded a solubility of 0.446 ± 0.009 M, a value consistent with our estimate. To confirm the validity of this result, a solution containing a lesser, known concentration (0.0986 M) of the same form of DtBuCH18C6 in C₁₀mim⁺Tf₂N⁻ was subjected to the same heating program, and the extractant molarity calculated on the basis of the observed mass loss. The value found, 0.0904 ± 0.0019 M, compares favorably with that expected.

The limited solubility of octyl(phenyl)-*N,N*-diisobutylcarbamoylmethylphosphine oxide (CMPO) in short-chain ILs, which necessitates the addition of tri-*n*-butyl phosphate (TBP) as a phase modifier in the liquid-liquid extraction of americium (III) from nitric acid using C₄mimTf₂N, has also been noted.¹ Like aliphatic crown ethers, CMPO exhibits a relatively low T_d (Figure 2.3A) and accordingly, can be readily decomposed by heating the sample to 250 °C, in this case for only 45 minutes (Figure 2.3B). Thus, as was the case for DtBuCH18C6, solubility determination for CMPO in the ILs of interest should be straightforward. As a test of the utility of TGA in this determination, a solution of CMPO of known concentration (0.199 M) in C₆mim⁺Tf₂N⁻ was subjected to the heating program, and the extractant concentration calculated on the basis of the observed mass loss. The molarity determined, $0.188 \text{ M} \pm 0.001 \text{ M}$, compares favorably with that expected.

(A)



(B)

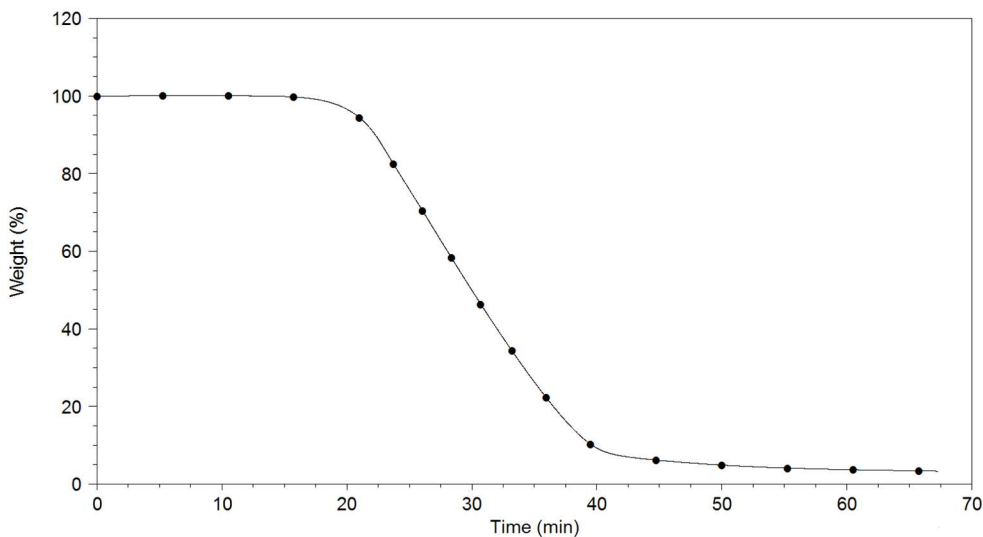


Figure 2.3: (A) TGA thermogram of CMPO. (B) Isothermal heating of CMPO at 250 °C for 70 min.

As noted by Pawlak⁴⁷ and others^{32,48,49} molecules incorporating aromatic functional groups are often considerably more thermally stable than those that do not. Accordingly, we anticipated that for such compounds, the decomposition of the extractant might actually occur at a temperature equaling or exceeding that of the IL. In fact, as shown in Figure 2.4, which depicts

the results of temperature ramping experiments for a representative calix-crown ether, Bob-Calix, this extractant exhibits thermal stability superior to that of the $C_n\text{mim}^+\text{Tf}_2\text{N}^-$ ILs (Figure 2.1). Clearly, under these circumstances, destruction or volatilization of the extractant without accompanying loss of the IL is not feasible, and for such extractants, solubility determination by this approach is not possible.

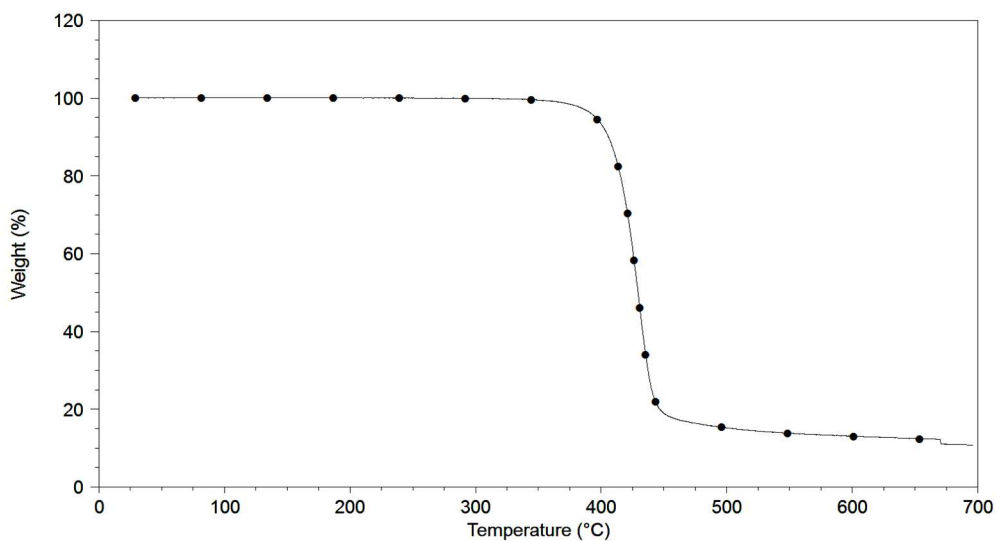


Figure 2.4: TGA thermogram of Bob-Calix.

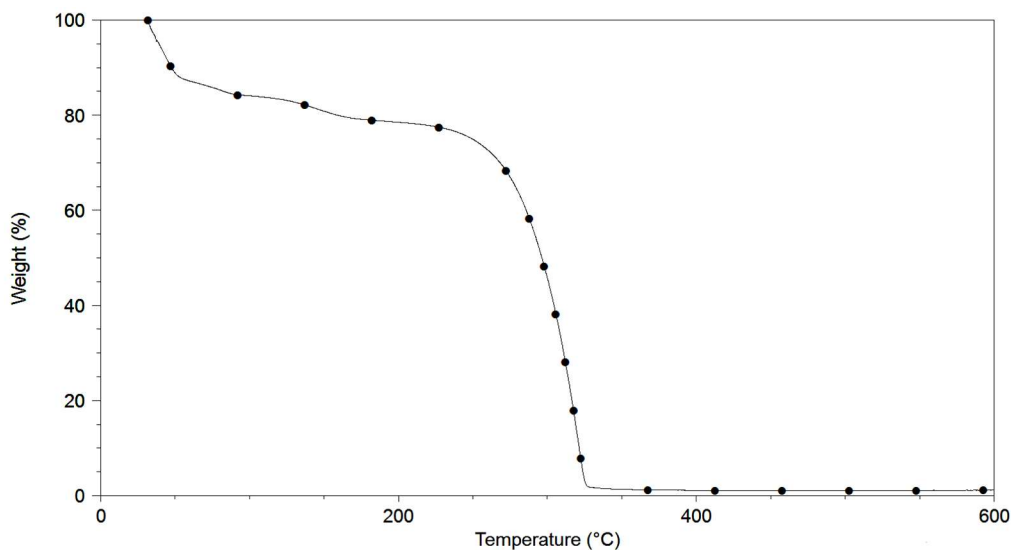
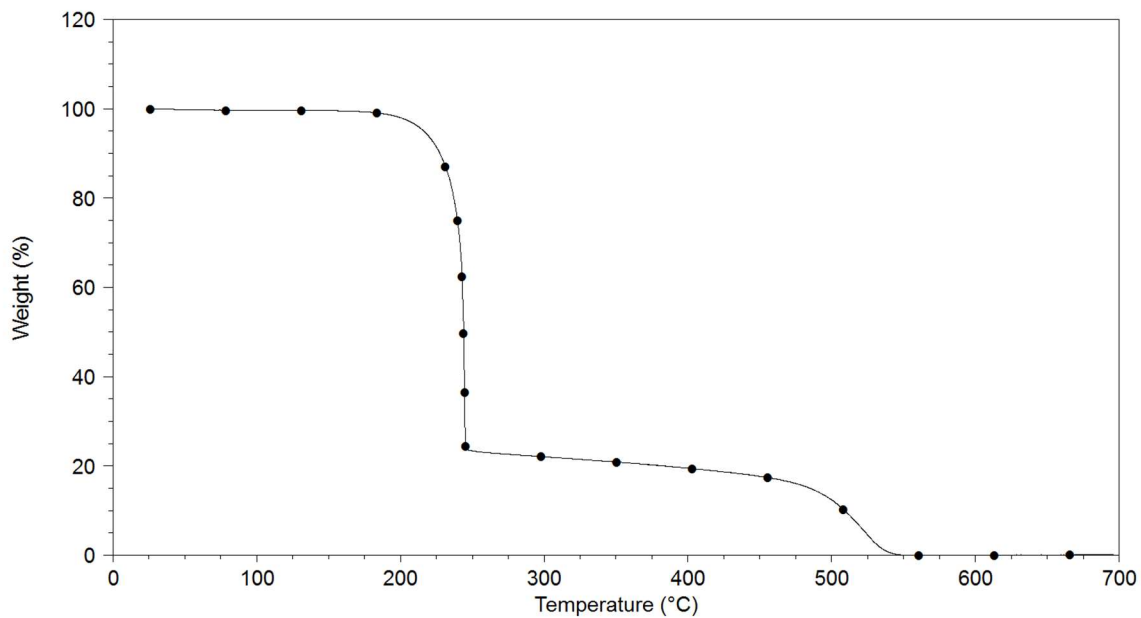


Figure 2.5: TGA thermogram of BTP.

Between the two extremes of extractant stability lie those compounds for which decomposition is measurable, yet incomplete, before the start of IL decomposition. In certain instances, as with the decomposition of BTP (Figure 2.5), the overlap with the behavior of the ILs is so extensive as to preclude measurement of the loss of extractant alone, regardless of conditions. In other cases, however, such as for *bis*(2-ethylhexyl)- phosphoric acid (HDEHP), whose thermal behavior in both a temperature-ramping experiment and at several fixed temperatures over an extended period is depicted in Figure 2.6 (panels A and B, respectively), the overlap does not preclude the determination. As shown in Figure 2.6A, HDEHP loses *ca.* 75% of its mass between 200-300 °C. The overall mass loss occurs in two steps, however, with the final stage occurring at a temperature at which it is obscured by the decomposition of the IL itself. By determining the fraction of the total mass loss represented by the peak(s) not obscured, however, one can calculate the total mass loss associated with the extractant decomposition. In the case of HDEHP in $C_6mim^+Tf_2N^-$ (Figure 2.7), it can be seen that the thermal behavior of the mixture exhibits features associated with both the extractant (Figure 2.6) and the ionic liquid (Figure 2.1). That is, the initial step corresponds to a weight loss event between 200-300 °C, while the bulk of the weight loss, corresponding to both HDEHP and $C_6mim^+Tf_2N^-$, occurs at approximately 400 °C. By calculating the ratio of the mass losses in the first and second steps and measuring the mass loss in the first step in a prepared solution, one can determine the total HDEHP mass in solution and, thus, its solubility. In this instance, the solubility of HDEHP in $C_6mim^+Tf_2N^-$ was found to be 0.0960 M.

(A)



(B)

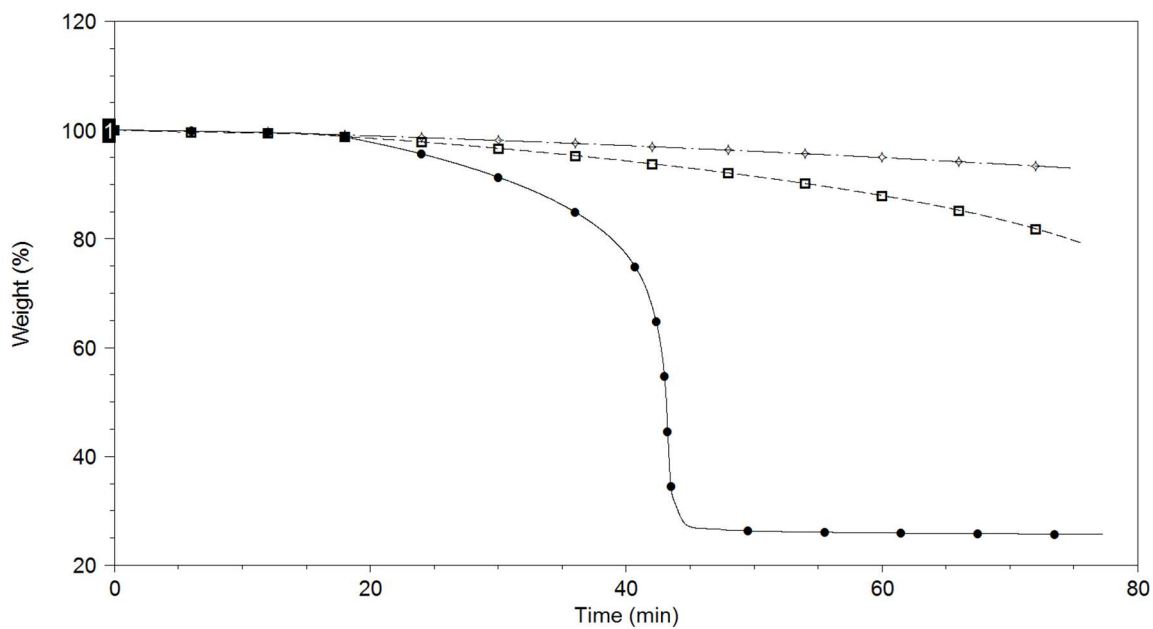


Figure 2.6: (A) TGA thermogram of HDEHP. (B) Isothermal heating of HDEHP at 180°C (top; open diamonds), 190 °C(middle; open squares), 200°C (bottom; closed circles) for 75 min.

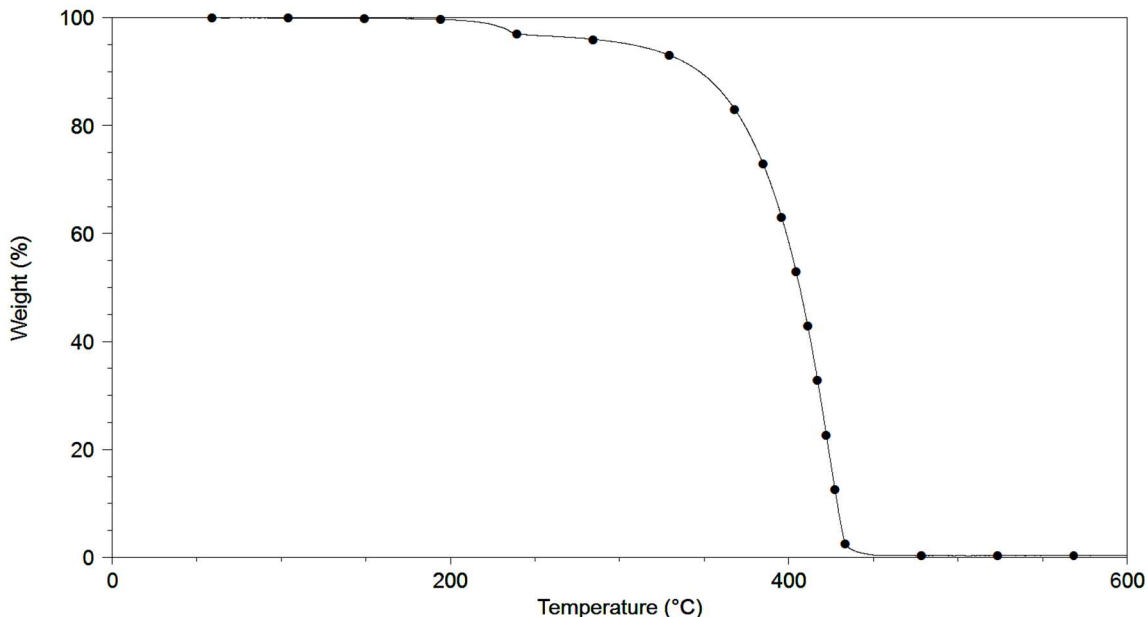


Figure 2.7: TGA thermogram of a saturated solution of HDEHP in $C_6mim^+Tf_2N^-$.

In preliminary experiments, it was observed that HDEHP is fully miscible with C_nmim^+ -based ILs incorporating a sufficiently long ($n \geq 10$) alkyl chain. This provides a means to assess the validity of the TGA approach to the measurement of its solubility in the short-chain ILs of interest to us. To this end, 0.113 and 0.123 M solutions of HDEHP in C_8mim^+Tf and $C_8mim^+NfO^-$, respectively, were prepared and subjected to the procedures described. The solutions were found to contain 0.122 ± 0.003 M and 0.115 ± 0.005 M, corresponding to errors of 7.96%, and 6.50%, respectively, thus confirming the utility of TGA in the determination of HDEHP solubility in these systems.

2.4 Conclusions

The results of this study demonstrate that for extractants readily volatilized or decomposed, TGA provides a straightforward method for the determination of their solubility in an IL. The approach is simple, requires little sample (<100 mg), and can be completed in as little

as a few hours. Although the method is not readily applicable to highly stable extractants, such as those incorporating multiple aromatic functional groups, this does not represent a significant drawback, as such extractants can often be determined by alternative means (e.g., UV-visible spectrophotometry). We anticipate that TGA will prove useful in efforts to establish the relationship between the structural characteristics of an IL and its suitability as a medium for dissolution of a variety of extractants. Work addressing this opportunity is now underway in this laboratory.

2.5 References

1. Rout, A.; Venkatesan, K.A.; Srinivasan, T.G.; Vasudeva Rao, P.R. (2009). Extraction of americium (III) from nitric acid medium by CMPO-TBP extractants in ionic liquid diluent. *Radiochim. Acta.*, *97*, 719-725.
2. Sengupta, A.; Murali, M.S. (2016). Effect of phase modifiers TBP and iso-decanol on the extraction and complexation of Eu^{3+} with CMPO. *Sep. Sci. Technol.*, *51*, 2153-2163.
3. Shimojo, K.; Aoyagi, N.; Saito, T.; Okamura, H.; Kubota, F.; Goto, M.; Naganawa, H. (2014). Highly efficient extraction separation of lanthanides using diglycolamic acid extractant. *Anal. Sci.* *30*, 263-269.
4. Laventine, D.M.; Afsar, A.; Hudson, M.J.; Harwood, L.M. (2012). Tuning the solubilities of bis-triazinylphenanthroline ligands (BTPhens) and their complexes. *Heterocycles.*, *86*, 1419-1429.
5. Huddleston, J.G.; Willauer, H.D.; Swatloski, R.P.; Visser, A.E.; Rogers, R.D. (1998). Room-temperature ionic liquids as novel media for 'clean' liquid-liquid extraction. *Chem. Comm.*, *16*, 1765-1766.
6. Rogers, R.D.; Seddon, K.R. (2003). Ionic liquids: solvents of the future. *Science* *302*, 792-793.
7. Luo, H.; Huang, J.; Dai, S. (2008). Studies on thermal properties of selected aprotic and protic ionic liquids. *Sep. Sci. Technol.*, *43*, 2473-2488.
8. Wang, H., Gurau, G., Rogers, R.D. (2012). Ionic liquid processing of cellulose. *Chem. Soc. Rev.*, *41*, 1519-1537.

9. Schröder, C. (2017). Proteins in ionic liquids: current status of experiments and simulations. *Topics Curr. Chem.*, 375, 1-26.
10. Viell, J.; Marquardt, W. (2011). Disintegration and dissolution kinetics of wood chips in ionic liquids. *Holzforschung.*, 65, 519-525.
11. Winterton, N. (2006). Solubilization of polymers in ionic liquids. *J. Mater. Chem.*, 16, 4281-4293.
12. Idris, A.; Vijayaraghavan, R.; Rana, U.A.; Patti, F.; MacFarlane, D.R. (2014). Dissolution and regeneration of wool keratin in ionic liquids. *Green Chem.*, 16, 2857-2864.
13. Fort, D.A.; Swatloski, R.P.; Moyna, P.; Rogers, R.D.; Moyna, G. (2006). Use of ionic liquids in the study of fruit ripening by high-resolution ¹³C-NMR spectroscopy: 'Green' solvents meet green bananas. *Chem. Comm.*, 7, 714-716.
14. Shimojo, K.; Goto, M. (2004). First application of calixarenes as extractants in room-temperature ionic liquids. *Chem. Lett.*, 33, 320-321.
15. Shimojo, K.; Goto, M. (2004). Solvent extraction and stripping of silver ions in room-temperature ionic liquids containing calixarenes. *Anal. Chem.*, 76, 5039-5044.
16. Kubota, F.; Goto, M. (2006). Application of ionic liquids to solvent extraction. *Solv. Extr. Res. Dev.*, 13, 23-36.
17. Hawkins, C.A.; Momen, M.A.; Garvey, S.; Kestell, J.; Kaminski, M.D.; Dietz, M.L. (2015). Evaluation of solid-supported room-temperature ionic liquids containing crown ethers as media for metal ion separation and preconcentration. *Talanta*, 135, 115-123.
18. Luo, H.; Dai, S.; Bonnesen, P.V.; Buchanan, A.C.; Holbrey, J.D.; Bridges, N.J.; Rogers, R.D. (2004). Extraction of cesium ions from aqueous solutions using calix[4]arene-bis(tert-octylbenzo-crown-6) in ionic liquids. *Anal. Chem.*, 76, 3078-3083.
19. Tsuda, T.; Hussey, C.L.; Luo, H.; Dai, S. (2006). Recovery of cesium extracted from simulated tank waste with an ionic liquid: Water and oxygen effects. *J. Electrochem. Soc.*, 153, D171-D176.
20. Sun, X.; Bell, J.R.; Luo, H.; Dai, S. (2011). Extraction separation of rare-earth ions via competitive ligand complexations between aqueous and ionic-liquid phases. *Dalton Trans.*, 40, 8019-8023.
21. Sun, X.; Luo, H.; Dai, S. (2012) Solvent extraction of rare-earth ions based on functionalized ionic liquids. *Talanta*, 90, 132-137.
22. Buschmann, H.; Cleve, E.; Denter, U.; Schollmeyer, E. (1997). Determination of complex stabilities with nearly insoluble host molecules. Part II. Complexation of alkali and alkaline

- earth metal cations with dibenzo crown ethers in aqueous solution. *J. Phys. Chem.*, *10*, 781-785.
23. Mesmin, C.; Liljenzin, J.-O. (2003). Determination of $H_2TPTZ_2^{2+}$ stability constant by TPTZ solubility in nitric acid. *Solv. Extr. Ion Exch.*, *21*, 783-795.
 24. Ohto, K.; Tanaka, H.; Ishibashi, H.; Inoue, K. (1999). Solubility in organic diluents and extraction behavior of calix[4]arene carboxylates with different alkyl chains. *Solv. Extr. Ion Exch.*, *17*, 1309-1325.
 25. Engle, N.L.; Bonnesen, P.V.; Tomkins, B.A.; Haverlock, T.J.; Moyer, B.A. (2004). Synthesis and properties of calix[4]arene-bis[4-(2-ethylhexyl)benzo-crown-6], a cesium extractant with improved stability. *Solv. Extr. Ion Exch.*, *22*, 611-636.
 26. Principe, F.; Demopoulos, G.P. (2003). The solubility and stability of organophosphoric acid extractants in H_2SO_4 and HCl media. *Hydrometallurgy*, *68*, 115-124.
 27. Naganawa, H.; Shimojo, K.; Mitamura, H.; Sugo, Y.; Noro, J.; Goto, M. (2007). A new "green" extractant of the diglycolamic acid type for lanthanides. *Solv. Extr. Res. Dev.*, *14*, 151-159.
 28. Williams, N.J.; Bryansev, V.S.; Custelcean, R.; Seipp, C.A. Moyer, B.A. (2016). $\alpha, \alpha', \alpha'', \alpha'''$ -meso-tetrahexyltetramethyl-calix[4]pyrrole: An easy-to-prepare isomerically pure anion extractant with enhanced solubility in organic solvents. *Supramol. Chem.*, *28*, 176-187.
 29. Deetlefs, M.; Seddon, K. (2003). Improved preparations of ionic liquids using microwave synthesis. *Green Chem.*, *5*, 181-186.
 30. Fredlake, C.P.; Crosthwaite, J.M.; Hert, D.G.; Aki, S.N.V.K.; Brennecke, J.F. (2004). Thermophysical properties of imidazolium-based ionic liquids. *J. Chem. Eng. Data*, *49*, 954-964.
 31. Kilaru, P.; Baker, G.A.; Scovazzo, P. (2007). Density and surface tension measurements of imidazolium-, quaternary phosphonium-, and ammonium-based room-temperature ionic liquids: Data and correlation. *J. Chem. Eng. Data*, *52*, 2306-2314.
 32. Awad, W.H.; Gilman, J.W.; Nyden, M.; Harris, R.H.; Sutto, T.E.; Callahan, J.; Trulove, P.C.; DeLong, H.C.; Fox, D.M. (2004). Thermal degradation studies of alkyl-imidazolium salts and their application in nanocomposites. *Thermochim. Acta*, *409*, 3-11.
 33. Partridge, J.A.; Jensen, R.C. (1969). Purification of di-(2-ethylhexyl)phosphoric acid by precipitation of copper (II) di-(2-ethylhexyl) phosphate. *J. Inorg. Nucl. Chem.*, *31*, 2587-2589.

34. Dietz, M.L.; Felinto, C.; Rhoads, S.; Clapper, M.; Finch, J.W.; Hay, B.P. (1999). Comparison of column chromatographic and precipitation methods for the purification of a macrocyclic polyether extractant. *Sep. Sci. Technol.*, *34*, 2943-2956.
35. Gatrone, R.C.; Kaplan, L.; Horwitz, E.P. (1987). The synthesis and purification of the carbamoylmethylphosphine oxides. *Solv. Extr. Ion Exch.*, *5*, 1075-1116.
36. Chin, A.; Carrick, J.D. (2016). Modular approaches to diversified soft Lewis basic complexants through Suzuki-Miyaura cross-coupling of bromoheteroarenes with organotrifluoroborates. *J. Org. Chem.*, *81*, 1106-1115.
37. Ngo, H.L.; LeCompte, K.; Hargens, L.; McEwen, A.B. (2000). Thermal properties of imidazolium ionic liquids. *Thermochim. Acta*, *357-358*, 97-102.
38. Aparicio, S.; Atilhan, M.; Karadas, F. (2010). Thermophysical properties of pure ionic liquids: Review of present situation. *Ind. Eng. Chem. Res.*, *49*, 9580-9595.
39. Baranyai, K.J.; Deacon, G.B.; MacFarlane, D.R.; Pringle, J.M.; Scott, J.L. (2004). Thermal degradation of ionic liquids at elevated temperatures. *Aust. Chem. J.*, *57*, 145-147.
40. Maton, C.; De Vos, N.; Stevens, C.V. (2013). Ionic liquid thermal stabilities: Decomposition mechanisms and analysis tools. *Chem. Soc. Rev.*, *42*, 5963-5977.
41. Van Valkenburg, M.E.; Vaughn, R.L.; Williams, M.; Wilkes, J.S. (2005). Thermochemistry of ionic liquid heat-transfer fluids. *Thermochim. Acta*, *425*, 181-188.
42. Tokuda, H.; Hayamizu, K.; Ishii, K.; Susan, M.A.B.H.; Watanabe, M. (2005). Physicochemical properties and structures of room-temperature ionic liquids. 2. Variation of alkyl chain length in imidazolium cation. *J. Phys. Chem. B.*, *109*, 6103-6110.
43. Chen, Y.; Chen, C.; Su, C.; Liaw, H. (2014). Auto-ignition characteristics of selected ionic liquids. *Procedia Eng.*, *84*, 285-292.
44. Fox, D.M.; Gilman, J.W.; De Long, H.C.; Trulove, P.C. (2005). TGA decomposition kinetics of 1-butyl-2,3-dimethylimidazolium tetrafluoroborate and the thermal effects of contaminants. *J. Chem. Thermo.*, *37*, 900-905.
45. Kamavaram, V.; Reddy, R.G. (2008). Thermal stabilities of di-alkylimidazolium chloride ionic liquids. *Int. J. Therm. Sci.*, *47*, 773-777.
46. Fox, E.B.; Visser, A.E.; Bridges, N.J.; Amoroso, J.W. (2013). Thermophysical properties of nanoparticle-enhanced ionic liquids (NEILs) heat-transfer fluids. *Energy Fuels*, *27*, 3385-3393.
47. Pawlak, A.J.; Dietz, M.L. (2014). Thermal properties of macrocyclic polyethers: Implications for the design of crown ether-based ionic liquids. *Sep. Sci. Technol.*, *49*, 2847-2855.

48. Chattopadhyay, D.K.; Webster, D.C. (2009). Thermal stability and flame retardancy of polyurethanes. *Prog. Polym. Sci.*, 34, 1068-1133.
49. Bhattacharya, S.; Subramanian, M.; Hiremath, U.S. (1995). Surfactant lipids containing aromatic units produce vesicular membranes with high thermal stability. *Chem. Phys. Lipids*, 78, 177-188.

CHAPTER 3:

SOLVENT STRUCTURAL EFFECTS ON THE SOLUBILITY OF *BIS*(2-ETHYLHEXYL)PHOSPHORIC ACID IN ROOM-TEMPERATURE IONIC LIQUIDS

3.1 Introduction

Organophosphorus reagents have long played an important role in the development of processes for the extraction and recovery of actinides and lanthanides.¹ Beginning with the synthesis of tri-butyl phosphate (TBP) and its subsequent application to nuclear fuel reprocessing in the 1940's,² this family of reagents has grown to encompass a wide variety of important extractants, among them other neutral organophosphates (*e.g.*, DAAP; diamyl amylphosphonate),³ dialkylphosphinic (*e.g.*, Cyanex 272),⁴ -phosphonic,⁵ and -phosphoric acids,⁶ and phosphine oxides (*e.g.*, TOPO; tri-octyl-phosphine oxide).⁷ Of these, bis(2-ethylhexyl)phosphoric acid (HDEHP) undoubtedly ranks as one of the most useful, a result of its ability to efficiently extract a number of metal ions, resistance to hydrolysis, and low water solubility.⁸ In the early 1960's, it was recognized that the selectivity of HDEHP for the extraction of trivalent lanthanides over actinides could be vastly improved by addition of an appropriate complexing agent (*i.e.*, an aminopolycarboxylic acid such as diethylenetriamine pentaacetic acid, DTPA) to the aqueous phase.^{9,10} In such systems, extraction selectivity arises not from the extractant alone, but also from competitive interactions of the aqueous complexing agent added with the various metal ions present. This approach ultimately provided the basis of the well-known TALSPEAK (Trivalent Actinide Lanthanide Separations by Phosphorus-Reagent Extraction from Aqueous Komplexes) Process, by which trivalent transplutonium actinides can be separated from fission product lanthanides.¹⁰ Since its first published description in 1968,¹¹ TALSPEAK has been the subject of extensive investigation to establish its capabilities and

limitations.¹²⁻¹⁵ As a result of such studies, it is now recognized that the process suffers from several significant drawbacks that limit its utility, among them the requirement for careful pH control, the need for multiple separation stages, and susceptibility to the effects of radiation damage.¹⁵ There has thus been considerable ongoing effort directed toward the development of alternatives to or modifications of the TALSPEAK Process.¹⁶⁻¹⁹

With the introduction of ionic liquids (ILs) as alternatives to conventional extraction solvents²⁰⁻²⁴ has come interest in the possibility of exploiting the unique properties of ILs to either completely “reinvent” the process or simply modify it by replacement of the molecular diluent ordinarily employed (i.e., n-dodecane or diisopropylbenzene). In pursuing reinvention, Shkrob et al.²⁵ have prepared DTPA-functionalized ILs, which are immiscible with organic solvents (e.g., cumene), as a replacement for the aqueous phase. Here competitive extraction involving this DTPA-IL conjugate and HDEHP in an organic solvent provides the basis for a group separation of actinides and lanthanides. While effective ($\alpha_{Eu/Am} > 250$ for certain incarnations), the unorthodox nature of the system has meant that interest in more “conventional” alternatives continues.²⁶⁻²⁹ For example, Sun et al.²⁹ have proposed simply replacing the organic diluent with an appropriate IL. Unfortunately, HDEHP was found to be poorly soluble in the short-chain (n = 2-6) 1-alkyl-3-imidazolium bis[(trifluoromethyl)sulfonyl] imides ($C_n\text{mim}^+\text{Tf}_2\text{N}^-$) examined, necessitating the use of longer-chain analogs (e.g., n = 10) that are substantially more viscous. That HDEHP would apparently be poorly miscible with an IL is somewhat unexpected, given the well-known ability of ionic liquids to dissolve a variety of solutes.

In conjunction with our ongoing studies of extractant solubility in ILs and its effects on the design of extraction chromatographic (EXC) sorbents employing these diluents,³⁴ we have

carried out a systematic examination of the effect of IL structure (i.e., the nature of the IL cation and anion) on the solubility of HDEHP in representative examples of two common IL families. As will be shown, HDEHP solubility can be related quantitatively to certain structural features of the ILs, most notably IL cation and anion molar volume. This observation, in addition to its relevance to the development of new EXC materials, has important implications in efforts to devise IL-based analogs of the TALSPEAK Process.

3.2 Experimental

3.2.1 Reagents

All chemicals were reagent grade and unless otherwise noted, were used as received. All water was obtained from a Milli-Q2 system and exhibited a specific resistance of at least 18 M Ω -cm. Lithium *bis*[(trifluoromethyl)sulfonyl]imide (LiTf₂N) and lithium *bis*(fluorosulfonyl)imide (Li(FSO₂)₂N) were purchased from TCI America (Portland, OR), while 1-methylimidazole, pyridine, lithium trifluoromethane sulfonate (*i.e.*, lithium triflate; LiTf), lithium tetrafluoroborate (LiBF₄) and all alkyl bromides were obtained from Sigma-Aldrich (St. Louis, MO). Lithium bis(pentafluoroethanesulfonyl)imide (LiBETI) was purchased from the 3M Corporation (Maplewood, MN). 1-octyl-3-methylimidazolium perfluorobutane sulfonate (*i.e.*, C₈mim⁺NfO⁻) was purchased from Iolitec (Heilbronn, Germany). With the exception of C₄mim⁺PF₆⁻, which was purchased from Acros Organics (Geel, Belgium), all ionic liquids were synthesized via a two-step procedure involving quaternization of either methylimidazole or pyridine with an appropriate alkyl bromide to yield the halide form of the IL (e.g. C_nmim⁺Br⁻, C_nPyr⁺Br⁻), followed by anion metathesis to provide the desired (e.g., Tf₂N⁻) product.^{35,36} To ensure that each was free of its halide precursor, the products were extensively washed with deionized water. Washing was continued until addition of silver nitrate to an aliquot of the wash solution yielded

no observable precipitate (AgBr) formation. As a further check of purity, the ILs were then dried for 24 hours in vacuo at 80°C^{37,38} and subjected to ¹H-NMR analysis. In no case was evidence of the presence of protons associated with the halide form of the ILs observed. Finally, all ILs were stored in a desiccator until used in the HDEHP solubility studies. HDEHP was purchased from Sigma-Aldrich and purified by copper salt precipitation.³⁹ Its purity was verified by ³¹P-NMR.

Deuterated methanol, chloroform and methylene chloride were purchased from Cambridge Isotope Laboratories (Tewksbury, MA). Trioctylphosphine oxide (TOPO) was purchased from the Eastman Kodak Company (Rochester, NY).

The 4-nitroaniline and N,N-diethyl-4-nitroaniline were purchased from Sigma-Aldrich and Oakwood Products Inc., respectively. Acetonitrile and non-deuterated methylene chloride were purchased from Honeywell Corporation (Muskegon, MI).

3.2.2 Equipment

A TA Instruments TGA-Q50 thermogravimetric analyzer equipped with a platinum pan was used for all thermal property measurements, and all mass loss data were processed using the TA Universal Analysis software. A Shimadzu UV-Vis Spectrophotometer 2450 with a 1-cm path length quartz cuvette was used to acquire all UV-Vis spectra. All spectra were processed with Shimadzu UV-Probe version 2.50 software.

All NMR experiments were performed at 25°C. ¹H-NMR spectra were obtained with a Bruker DPX-300 NMR spectrometer equipped with a broad-band optimized BBO probe operating a frequency of 300.13 MHz and were referenced against TMS. The ³¹P-NMR spectra were obtained on a Bruker Avance III HD 500-MHz spectrometer equipped with a 5-mm X-nuclei-optimized BBO Smart™ probe with z-gradients at a frequency of 202.4613964 MHz for

^{31}P using an inverse gated decoupling sequence to minimize NOE effects. Typical acquisition parameters for quantitative measurements were a 90° pulse length of 14 μs , a spectral width of 20,161 Hz and a data size of 65,536 points, resulting in an acquisition time of 1.6 s. Sixteen scans were accumulated with a relaxation delay of 10 s, which was chosen to be longer than five times the longest ^{31}P relaxation time measured for any of the samples (0.9 – 1.7 s). The ^{31}P relaxation times for the TOPO internal standard and HDEHP were measured for two representative samples using an inversion recovery sequence. All NMR spectra were recorded with Bruker Topspin version 3.5 pl7 software.

3.2.3 Procedures

Unless otherwise noted, the solubility of HDEHP in the various ILs was determined by thermogravimetric analysis (TGA) using the procedures described in Chapter 2.⁴⁰ Briefly, the IL was equilibrated with an excess of HDEHP for at least six hours. A ca. 25 mg sample of extractant-saturated IL was then taken for thermal analysis. For blank determinations, the pure IL was subjected to an identical temperature program. The mass loss for each test sample and IL was measured three times. For those ILs for which satisfactory results could not be obtained by TGA, the solubility of HDEHP was measured either by ^{31}P -NMR ($\text{C}_8\text{mim}^+(\text{FSO}_2)_2\text{N}^-$ and $\text{C}_4\text{Pyr}^+\text{Tf}_2\text{N}^-$) or via phosphorus determination in the extractant saturated IL using ICP-AES ($\text{C}_2\text{mim}^+\text{Tf}_2\text{N}^-$, $\text{C}_4\text{mim}^+\text{Tf}_2\text{N}^-$, $\text{C}_2\text{mim}^+\text{BETI}^-$, $\text{C}_4\text{mim}^+\text{BETI}^-$, and $\text{C}_8\text{mim}^+\text{BF}_4^-$), the latter performed at Galbraith Laboratories (Knoxville, TN). For the ^{31}P NMR measurements, the NMR spectra were processed using an exponential function with a line-broadening factor of one, and a baseline correction was applied. The signals of TOPO and HDEHP were integrated, the TOPO signal calibrated to one, and the HDEHP signal reported as a fraction of the standard signal.

Phosphorus chemical shifts were determined relative to 80% H₃PO₄ using the deuterium chemical shift of the deuterated chloroform signal as an indirect internal reference.

The hydrogen bond basicity (β) and dipolarity/ polarizability (π^*) of the ILs were measured following the procedures outlined by Fredlake et. al.⁴¹ Each ionic liquid was dried for 72 hours at 70 °C under vacuum and stored in a desiccator until use. A 3-mL aliquot of the dried IL was combined with a dye-dichloromethane solution such that the absorbance of the resulting mixture was approximately 1. The dichloromethane was then removed in vacuo at 60 °C over a period of 30 minutes. The dye-IL solution was then equilibrated for 30 minutes at 25 °C prior to analysis on the UV-Vis. Each sample solution was scanned three times, and from the average, π^* was calculated according to the following equation:^{41,42}

$$v_{max} = 27.52 - 3.182\pi^* \quad (3.1)$$

Here, $v_{max} = 10,000/\lambda_{max}$. v_{max} (in kiloKaisers, kK) is the wavenumber corresponding to the wavelength of the absorbance maxima, where λ_{max} was measured using N,N-diethyl-4-nitroaniline.

The solvent parameter β was calculated according to the following equation:⁴¹

$$\beta = [1.035v(2)_{max} - v(1)_{max} + 2.64 \text{ kK}]/2.80 \quad (3.2)$$

Here, $v(1)_{max}$ and $v(2)_{max}$ are the absorbance maxima for 4-nitroaniline and N,N-diethyl-4-nitroaniline, respectively, in kK.

The hydrogen bond acidity (α) was measured for each imidazolium-based IL according to the procedure outlined by Lungwitz et al.⁴³ Briefly, a 1.8 M solution of the IL of interest was prepared in deuterated methylene chloride. The shift of the C-2 proton of the imidazolium ring

was then measured by $^1\text{H-NMR}$, and the resulting shift used to calculate α from the following equation:

$$\delta \text{ (ppm)} = 12.686 - 7.770\alpha \quad (3.3)$$

The density of each IL was determined by filling a weighed 2-mL volumetric flask to volume with it and re-weighing. From the average of three trials, the molar volume (\tilde{V}) of each IL was then calculated from the IL molar mass and the measured density.

Regression analyses were performed on Microsoft Excel 2016 with the data analysis tool enabled.

3.3 Results and Discussion

The ability to solubilize a wide range of solutes is among the most often-cited advantages of ionic liquids over conventional (i.e., molecular) solvents.⁴⁴ Indeed, prior studies have demonstrated that such diverse materials as sugars,⁴⁵ cellulose,⁴⁶ wood,⁴⁷ and even bananas⁴⁸ can be dissolved in an appropriate IL. Unexpectedly, however, several studies have found that the solubility of various common extractants in certain ionic liquids is limited. As already noted, for example, the solubility of HDEHP in short-chain $\text{C}_n\text{mim}^+\text{Tf}_2\text{N}^-$ ILs is poor.²⁷⁻²⁹ Along these same lines, the adverse impact of the limited solubility of certain crown ethers in ILs upon the performance of IL-based EXC materials for strontium has previously been reported.³⁴ Although these studies do indicate that an extractant will be better solubilized by an IL whose cation incorporates a long alkyl chain than by an analogous short-chain solvent, to the best of our knowledge, no reports have appeared attempting to describe quantitatively the effect on extractant solubility brought about by changes in IL structure. Attempts have been made to quantify the effect of IL cation and anion structure on the solubility of other solutes, most

notably by use of Kamlet-Taft solvent parameters.⁴⁹⁻⁵² These parameters were developed to elucidate the role of various solvent properties in determining chemical reaction rates, or in influencing such processes as solute dissolution and chromatographic retention.⁵³⁻⁵⁶ By using a linear combination of parameters representing selected solvent characteristics (e.g., polarizability), the property of interest (designated as XYZ) within a given family of solvents can often be described by an equation of the general type:

$$XYZ = XYZ_0 + aA + bB + cC + \dots \quad (3.4)$$

where a, b, and c constitute measures of the relative susceptibility of property XYZ to solvent characteristics A, B, and C, respectively. As applied to the dissolution of a solute in a series of solvents, this equation will take the general form:⁵⁶

$$S = S_0 + s\pi^* + a\alpha + b\beta + h\delta_H \quad (3.5)$$

where S is the solubility of the solute of interest, π^* is the solvent dipolarity/ polarizability, α is the hydrogen bond acidity of the solvent (which describes its ability to donate a proton in a solvent-to-solute hydrogen bond), β is the hydrogen bond basicity of the solvent (which represents its ability to accept a proton in a solute-to-solvent hydrogen bond), and δ_H is the Hildebrand solubility parameter, a measure of the extent of disruption of solvent-solvent interactions resulting from the creation of a cavity in the solvent to accommodate the solute. (An additional term, $e\xi$, a measure of coordinate covalency, is sometimes incorporated for basic solvents.⁵⁶) While various reports have described correlations involving a single parameter, regression analyses including multiple Kamlet-Taft parameters are more common.^{50, 55, 57} For solute dissolution in conventional solvents, such analyses have often found statistically significant dependencies of solute solubility on the various K-T parameters, either alone or in

various combinations.⁵⁶ For solute dissolution in ionic liquids, the available data are more limited. Nonetheless, studies of alkane solubility in C_4mim^+ -systems have demonstrated an inverse relationship between solubility and the hydrogen bond basicity of the IL anion.⁴⁹ In contrast, the solubility of cellulose has been found to increase with increasing IL anion hydrogen bond basicity, as well as with increasing IL cation hydrogen bond acidity.^{50,51} Taken together, these observations indicate that the possible influence of all of the solvent parameters must be considered in efforts to understand the effect of IL structure on the solubility of HDEHP.

As a first step in the present study, prior qualitative observations on the solubility of HDEHP in $C_nmim^+Tf_2N^-$ ILs were examined quantitatively. In addition, the solubility of the extractant in a series of N-alkylpyridinium-based ILs was determined. Table 3.1 summarizes the results obtained. As can be seen, HDEHP solubility in both families of ILs decreases markedly as the alkyl chain length on the cation is reduced. For example, while HDEHP is completely miscible with $C_{10}mim^+Tf_2N^-$, its solubility falls to 0.0960 M for $n = 6$ and declines still further at $n = 2$. Analogous measurements on ILs pairing the same series of cations with other anions yield similar results.

Table 3.1. Measured solubility of HDEHP in a series of *N,N*-dialkylimidazolium and *N*-alkylpyridinium ionic liquids (T = 23 ± 2 °C).

Ionic Liquid	Solubility (M)±SD
<i>C</i> ₆ <i>PyrBETI</i>	0.107 ±0.010
<i>C</i> ₈ <i>PyrBETI</i>	0.522 ±0.026
<i>C</i> ₄ <i>PyrTf₂N</i>	0.0188 ±0.001
<i>C</i> ₆ <i>PyrTf₂N</i>	0.093 ±0.006
<i>C</i> ₈ <i>PyrTf₂N</i>	0.460 ±0.005
<i>C</i> ₈ <i>mimNfO</i>	0.664 ±0.019
<i>C</i> ₈ <i>mimTf</i>	0.341 ±0.007
<i>C</i> ₈ <i>mim(FSO₂)₂N</i>	0.205 ±0.010
<i>C</i> ₈ <i>mimBF₄</i>	0.108
<i>C</i> ₂ <i>mimTf₂N</i>	0.0046
<i>C</i> ₄ <i>mimTf₂N</i>	0.017
<i>C</i> ₅ <i>mimTf₂N</i>	0.042 ±0.003
<i>C</i> ₆ <i>mimTf₂N</i>	0.096 ±0.005
<i>C</i> ₇ <i>mimTf₂N</i>	0.238 ±0.006
<i>C</i> ₈ <i>mimTf₂N</i>	0.676 ±0.010
<i>C</i> ₂ <i>mimBETI</i>	0.0044
<i>C</i> ₄ <i>mimBETI</i>	0.019
<i>C</i> ₆ <i>mimBETI</i>	0.101 ±0.008
<i>C</i> ₈ <i>mimBETI</i>	0.793 ±0.007

Table 3.2 summarizes the available (experimentally determined or published) Kamlet-Taft parameters of these same ionic liquids. The values of α , β , and π^* measured here are in good agreement with literature values, where available.^{41,42,58,59} The measured values of α were found to be essentially constant regardless of the alkyl chain length, both for the BETI⁻ and the Tf₂N⁻ C_nmim⁺ ILs, making it difficult to employ this parameter in subsequent regression analyses. In fact, all regression analyses performed using α , either alone or in combination with other Kamlet-Taft parameters, indicate that it has no statistically significant effect on HDEHP solubility. Subsequent efforts to explain the observed trends in solubility therefore employed only β , π^* , and the Hildebrand solubility parameter, δ_H .^{60,61} Given that it is the free energy of dissolution of a solute, $\Delta G_{sol'n}$, that can be correlated with various solvent parameters, and given the known relationship between ΔG and $\ln K$, these efforts focused on the relationship between the natural logarithm of the HDEHP solubility, $\ln S_{HDEHP}$, and these three solvent properties:

$$\ln S_{HDEHP} = \ln S_{HDEHP,0} + b\beta + s\pi^* + h\delta_H \quad (3.6)$$

Table 3.2. Kamlet-Taft solvent parameters and Hildebrand solubility parameters of a series of *N,N*-dialkylimidazolium and *N*-alkylpyridinium ionic liquids (T = 23 ± 2 °C).

Ionic Liquid	α	B	π^*	$\delta_{H^{60.61}}$
<i>C</i> ₆ <i>PyrBETI</i>	—	0.24	0.98	—
<i>C</i> ₈ <i>PyrBETI</i>	—	0.36	0.93	—
<i>C</i> ₄ <i>PyrTf₂N</i>	—	0.12	0.82	22.58
<i>C</i> ₆ <i>PyrTf₂N</i>	—	0.26	1.01	21.40
<i>C</i> ₈ <i>PyrTf₂N</i>	—	0.21	1.04	20.39
<i>C</i> ₈ <i>mimnonaflate</i>	0.47	0.55	0.91	—
<i>C</i> ₈ <i>mimCF₃SO₃</i>	0.48 (0.51) ⁵⁸	0.58	0.96	22.73
<i>C</i> ₈ <i>mim (FSO₂)₂N</i>	0.53	0.45	1.03	22.39
<i>C</i> ₂ <i>mimTf₂N</i>	0.53	0.23	1.00	23.72
<i>C</i> ₄ <i>mimTf₂N</i>	0.56	0.24	0.98	22.41
<i>C</i> ₅ <i>mimTf₂N</i>	0.053	0.262 (0.26) ⁵⁹	0.984 (0.97) ⁵⁹	21.83
<i>C</i> ₆ <i>mimTf₂N</i>	0.52 (0.51) ⁵⁸	0.26	0.97	21.30
<i>C</i> ₇ <i>mimTf₂N</i>	0.52	0.30	0.97	20.80
<i>C</i> ₈ <i>mimTf₂N</i>	0.52	0.30	0.96	20.33
<i>C</i> ₂ <i>mimBETI</i>	0.53	0.19	0.95	—
<i>C</i> ₄ <i>mimBETI</i>	0.52	0.25	0.95	—
<i>C</i> ₆ <i>mimBETI</i>	0.52	0.29	0.93	—
<i>C</i> ₈ <i>mimBETI</i>	0.52	0.23	0.98	—
<i>C</i> ₈ <i>mimBF₄</i>	0.45 ⁵⁸	0.39 ⁴¹	0.96 ⁴¹	24.14
<i>Acetonitrile</i>	—	0.37 (0.37) ⁴¹	0.79 (0.78) ⁴¹	—
<i>C</i> ₄ <i>mimPF₆</i>	—	0.21 (0.21) ⁴¹	1.02 (1.05) ⁴¹	—

Plots of HDEHP solubility (as $\ln S_{HDEHP}$) versus either π^* or β alone failed to yield a well-defined trend. Although the plot of $\ln S_{HDEHP}$ against β did exhibit statistical significance ($p = 0.019$), an unacceptably low R^2 value (0.28) was obtained. A regression analysis incorporating both parameters was therefore performed, yielding the following equation:

$$\ln S_{HDEHP} = -0.090(0.94) + 0.83\beta(0.12) + 0.078\pi^*(0.95) \quad (3.7)$$

Shown in parentheses are the values of p associated with each fit parameter. Because statistical significance at the 95% level of confidence requires a p -value of less than 0.05 for a given Kamlet-Taft parameter, a combination of π^* and β clearly cannot be used to explain HDEHP solubility in ILs.

Attempts to correlate the observed solubility with δ_H , either alone or in combination with other parameters, proved problematic for several reasons. First, a variety of approaches to the determination of the Hildebrand solubility parameter (defined mathematically as per Equation 3.8, where ΔE is the interaction energy and \tilde{V} is the solvent molar volume) have been described.⁶⁰⁻⁶⁵ Unfortunately, published δ_H values for a given IL often exhibit significant dependence on the method of determination,⁶⁶ complicating attempts to apply the parameter to the interpretation of solubility data.

$$\delta_H = -\sqrt{\frac{\Delta E}{\tilde{V}}} \quad (3.8)$$

Next, although Equation 3.5 implies that the solubility of a given solute will vary monotonically with δ_H , it has been reported that solubility increases as the difference between the solubility parameters of the solute and solvent decreases; thus, a plot of solubility versus δ_H will exhibit a maximum at the solute δ_H .⁶⁷ (Lee et al., for example, observed that lignin solubility in a series of

C₄mim⁺-based ILs increased as the solvent δ_H value approached that of lignin (24.9).⁶⁸ Finally, in an extensive study involving more than two-dozen solutes and a comparable number of ILs, Marcus⁶⁹ reported difficulty in making solubility predictions on the basis of δ_H values. Even with the addition of an entropic correction term, in fact, acceptable solubility correlations were not observed. For the present data, the absence of an acceptable correlation is best illustrated by the results for C₄mim⁺Tf₂N⁻, C₄pyr⁺Tf₂N⁻, and C₈mim⁺CF₃SO₃⁻. That is, despite having essentially the same δ_H , the three ILs provide quite different HDEHP solubility (Table 3.1). All of this argues against a role for δ_H in correlating the HDEHP solubility data.

Despite this, prior work suggests that a related parameter, solvent molar volume (\tilde{V}), may be useful in rationalizing solute solubility. For example, in a 1993 study of the solubility of fullerenes in a number of conventional solvents, Ruoff et al.⁷⁰ noted that dissolution of C₆₀ increases with greater solvent molecular size (i.e., \tilde{V}). Along these same lines, several previous investigations have demonstrated that gas solubility in ionic liquids is directly related to solvent molar volume.^{71,72} Regression analysis using the IL molar volume (Table 3.3) alone was therefore carried out, yielding the following:

$$\ln S_{HDEHP} = -0.84(0.018) + 3.21\tilde{V}(0.0035) \quad (3.9)$$

Table 3.3. Density and molar volume (\tilde{V}) values for a series of *N,N*-dialkylimidazolium and *N*-alkylpyridinium ionic liquids ($T = 23 \pm 2$ °C).

Ionic Liquid	Density (g/mL)	Molar Volume (L/mol)
C ₂ mimTf ₂ N ⁷³	1.52	0.257
C ₄ mimTf ₂ N ⁷³	1.44	0.291
C ₅ mimTf ₂ N ⁷³	1.40	0.309
C ₆ mimTf ₂ N ⁷³	1.37	0.321
C ₇ mimTf ₂ N ⁷³	1.34	0.343
C ₈ mimTf ₂ N ⁷³	1.32	0.360
C ₂ mimBETI ⁷⁴	1.597±0.001	0.308
C ₄ mimBETI ⁷⁴	1.507±0.001	0.345
C ₆ mimBETI ⁷⁴	1.445±0.001	0.387
C ₈ mimBETI ⁷⁵	1.37±0.01	0.423
C ₆ PyrBETI	1.45±0.01	0.385
C ₈ PyrBETI	1.38±0.01	0.424
C ₄ PyrTf ₂ N ⁷⁶	1.50	0.287
C ₆ PyrTf ₂ N	1.38±0.01	0.332
C ₈ PyrTf ₂ N	1.29±0.02	0.376
C ₈ mimNfO	1.35±0.02	0.365
C ₈ mimTf ⁷⁷	1.19	0.368
C ₈ mim(FSO ₂) ₂ N	1.28±0.03	0.292
C ₈ mimBF ₄ ⁷⁸	1.12	0.252

While this regression did not provide an R^2 value high enough ($R^2 = 0.36$) to indicate that HDEHP solubility is fully and solely explained by solvent molar volume, the p-value (in parentheses) indicates that it does play a significant role in determining the solubility of HDEHP in the ionic liquids examined.

As noted above, statistical analysis of the relationship between $\ln S_{HDEHP}$ and β indicated that this parameter must be included in any treatment attempting to explain HDEHP dissolution. A regression analysis of $\ln S_{HDEHP}$ as a function of both \tilde{V} and β was thus performed, yielding the following relationship:

$$\ln S_{HDEHP} = -11.43(0.000) + 20.269\tilde{V}(0.000) + 7.798\beta(0.001) \quad (3.10)$$

The resulting (low) p-values, along with an R^2 of 0.684, show the improvement in solubility prediction (Figure 3.1). (Note that π^* , combined with either \tilde{V} alone or \tilde{V} and β together, did not yield statistically acceptable results.) While the p-values demonstrate the statistical significance of β and \tilde{V} , the modest value of R^2 indicates that the explanation of HDEHP solubility in the ILs studied remains incomplete.

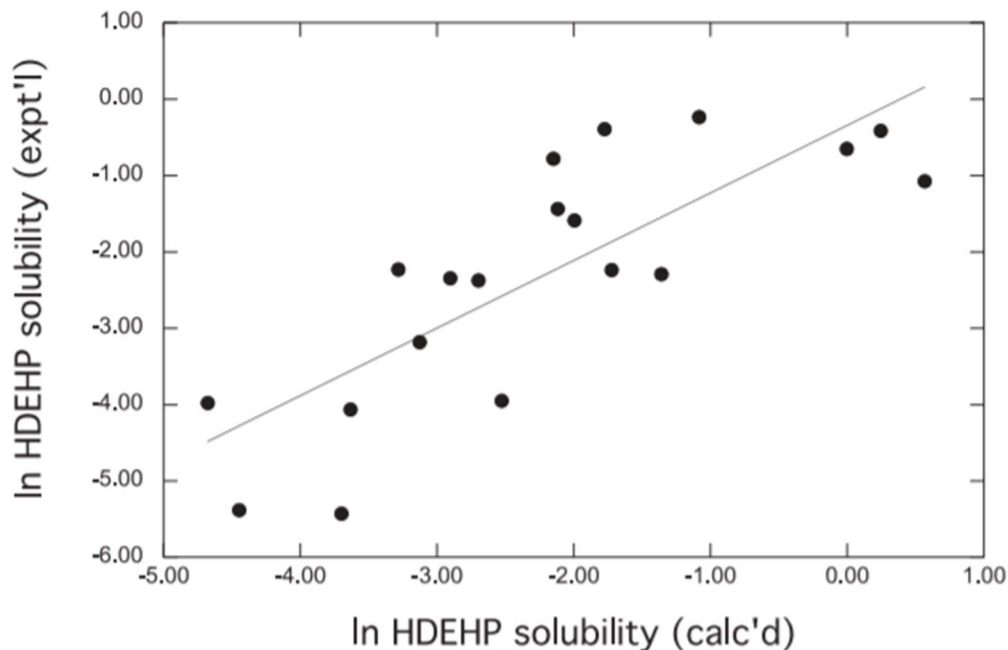


Figure 3.1. Experimentally determined vs. calculated (according to Eqn. 10) solubility of HDEHP (as $\ln S_{HDEHP}$) in a series of hydrophobic room-temperature ionic liquids.

In the course of a closer examination of the data relating HDEHP solubility to IL molar volume, it was noted that for certain subsets of the data, the relationship between the two variables was well defined. Indeed, when the HDEHP solubility was plotted for a set of ILs comprising a fixed cation in combination with various anions (*i.e.*, $C_8mim^+X^-$ ILs), a simple, straight-line relationship with a much-improved correlation coefficient ($R^2 = 0.934$) was observed (Figure 3.2):

$$\ln S_{HDEHP} = -0.967(0.007) + 4.332\tilde{V}(0.002) \quad (3.11)$$

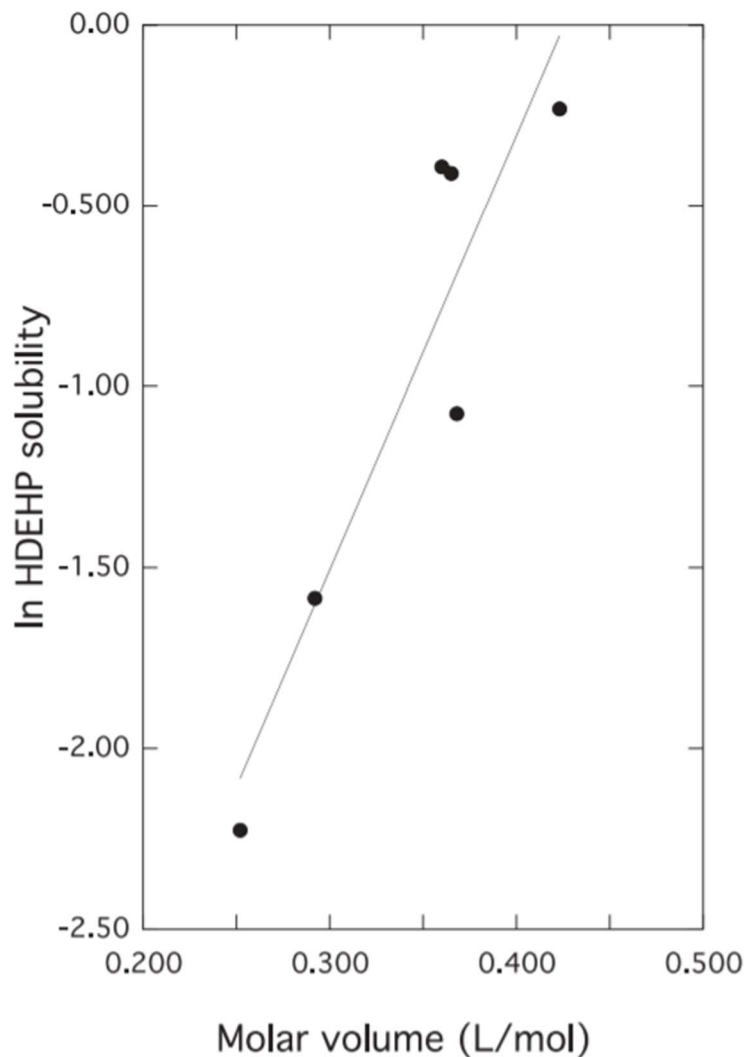


Figure 3.2. HDEHP solubility (as $\ln S_{HDEHP}$) vs. molar volume (\tilde{V}) for a series of $C_8mim^+X^-$ ionic liquids.

Similarly, when the IL anion was fixed (as Tf_2N^-) and the cation varied (C_nmim^+ , with $n = 2-8$), a linear relationship ($R^2 = 0.993$) between HDEHP solubility and IL molar volume was again obtained (Figure 3.3). Ultimately then, molar volume is seen to be most useful in predicting HDEHP solubility in ILs comprising fixed-cation-variable-anion or fixed-anion-variable-cation systems.

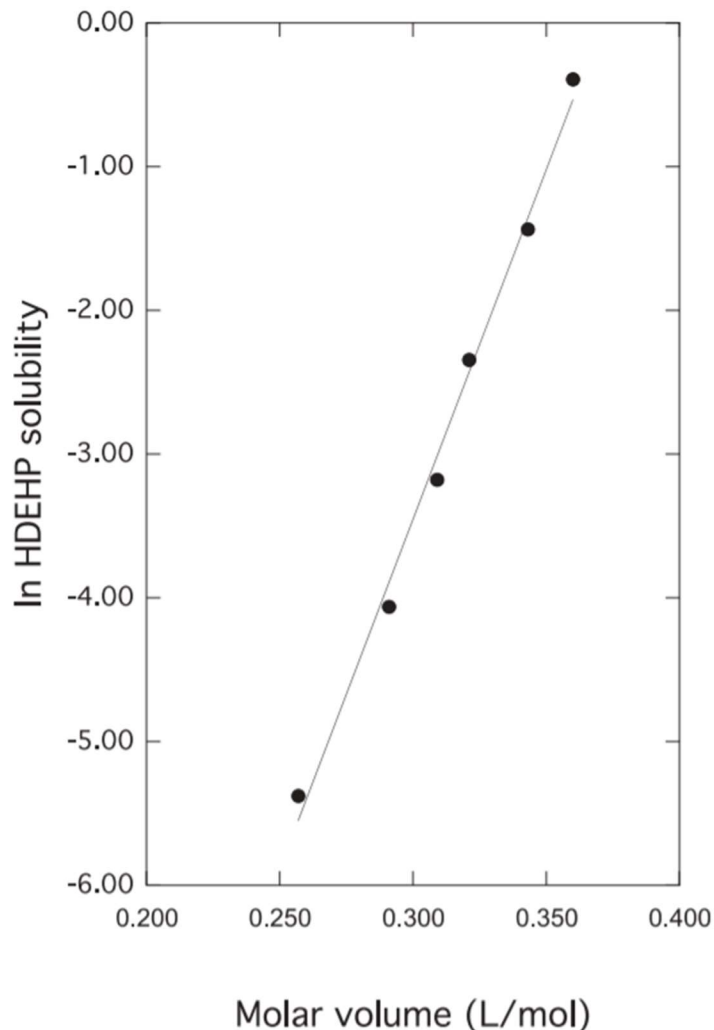


Figure 3.3. HDEHP solubility (as $\ln S_{HDEHP}$) vs. molar volume (\tilde{V}) for a series of $C_n\text{mim}^+\text{Tf}_2\text{N}^-$ ionic liquids.

Spear et al.⁷⁹ have previously noted that only limited conclusions can be drawn when multivariate analysis is applied to relatively small data sets, such as comprise the nearly twenty ILs examined here. Nonetheless, by demonstrating that both the IL cation and anion should be selected as to maximize the solvent molar volume and by quantifying the effect upon HDEHP solubility of changes in IL molar volume, our results provide useful guidance in efforts to identify ionic liquids providing a suitable medium for the dissolution of HDEHP and by extension, other extractants.

3.4 Conclusions

The results of this study represent the first systematic quantitative determination of the solubility of HDEHP in ionic liquids. Previously used to describe gas solubility in ILs, solvent molar volume has proven useful as a predictor of HDEHP solubility and thus, as a guide to the selection of an IL system that will dissolve concentrations of this extractant of practical significance. While larger (*i.e.*, higher molar volume) ILs dissolve substantially more HDEHP than their lower \tilde{V} analogs, they are also significantly more viscous.⁸⁰ Efforts to replace conventional molecular diluents with ILs in the TALSPEAK Process will thus need to confront the increase in process solvent viscosity certain to accompany this replacement. Although raising the temperature will reduce the viscosity of the IL, perhaps substantially,⁸¹ this reduction may be accompanied by a decrease in metal ion extraction efficiency and/or selectivity,⁸² a clearly undesirable result.

Of course, highly viscous solvent systems can be employed on solid-supports for metal ion extraction,^{83,84} and this may ultimately prove to be the preferred approach to employing HDEHP-IL mixtures (and solutions of extractants in ILs in general) in metal ion separations. Work to address this opportunity, as well as to determine the relevance of our results to other extractant families, is now underway in our laboratory.

3.5 References

1. Peppard, D.F.; Moline, S.W.; Mason, G.W. (1957) Isolation of berkelium by solvent extraction of the tetravalent species. *J. Inorg. Nucl. Chem.* 4, 344-348.
2. Warf, J. C. (1949). Extraction of cerium(IV) nitrate by butyl phosphate. *J. Am. Chem. Soc.* 71, 3257–3258.
3. McCann, K., Brigham, D. M., Morrison, S., & Braley, J. C. (2016). Hexavalent americium recovery using copper(III) periodate. *Inorg. Chem.* 55, 11971–11978.

4. Banda, R., Jeon, H., & Lee, M. (2012). Solvent extraction separation of Pr and Nd from chloride solution containing Ia using Cyanex 272 and its mixture with other extractants. *Sep. Purif. Technol.* 98, 481–487.
5. Lumetta, G.J., Sinkov, S.I., Krause, J.A., Sweet, L.E. (2016) Neodymium (III) complexes of dialkylphosphoric and dialkylphosphonic acids relevant to liquid-liquid extraction systems. *Inorg. Chem.* 55, 1633-41.6.
6. Lumetta, G. J., Levitskaia, T. G., Latesky, S. L., Henderson, R. V., Edwards, E. A., Braley, J. C., & Sinkov, S. I. (2012). Lipophilic ternary complexes in liquid-liquid extraction of trivalent lanthanides. *J. Coord. Chem.* 65, 741–753.
7. Tsurubou, S., Mizutani, M., Kadota, Y., Yamamoto, T., Umetani, S., Sasaki, T., Matsui, M. (1995). Improved extraction-separation of alkaline earths and lanthanides using crown ethers as ion size selective masking reagents: A novel macrocycle application. *Anal. Chem.* 67, 1465–1469.
8. Peppard, D.F.; Mason, G.W.; Maier, J.L.; Driscoll, W.J. (1957) Fractional extraction of the lanthanides as their dialkyl-orthophosphates. *J. Inorg. Nucl. Chem.* 4, 334-343.
9. Weaver, B.; Kappelmann, F.A. (1964). TALSPEAK: A new method of separating americium and curium from the lanthanides by extraction from an aqueous solution of an aminopolyacetic acid complex with a monoacidic organophosphate or phosphonate (Vol. 32). ORNL-3559.
10. Baybarz, R.D. (1965) Dissociation constants of the transplutonium element chelates of diethylenetriaminepentaacetic acid (DTPA) and the application of DTPA chelates to solvent extraction separations of transplutonium elements from the lanthanide elements. *J. Inorg. Nucl. Chem.* 27, 1831-1839.
11. Weaver, B.; Kappelmann, F.A. (1968). Preferential extraction of lanthanides over trivalent actinides by monoacidic organophosphates from carboxylic acids and from mixtures of carboxylic and aminopolyacetic Acids. *J. Inorg. Nucl. Chem.* 30, 263-272.
12. Braley, J.C., Grimes, T.S., Nash, K.L. (2012) Alternatives to HDEHP and DTPA for simplified TALSPEAK separations. *Ind. Eng. Chem. Res.* 51, 629-638.
13. Nilsson, M., Nash, K.L. (2007) Review article: A review of the development and operational characteristics of the TALSPEAK process. *Solv. Extr. Ion Exch.* 25, 665-701.
14. Mincher, B. J., Modolo, G., Mezyk, S. P. (2010) Review: The effects of radiation chemistry on solvent extraction: Separation of the trivalent actinides and considerations for radiation-resistant solvent systems. *Solv. Extr. Ion Exch.* 28, 415- 436.
15. Nash, K. L. (2015). The chemistry of TALSPEAK: A review of the science. *Solv. Extr. Ion Exchange*, 33, 1-55.

16. Del Cul, G.D., Toth, L.M., Bond, W.D., Davis, G.D., Dai, S. (1997). Citrate-based TALSPEAK actinide-lanthanide separation process. *Sep. Sci. Technol.* *32*, 431–446.
17. Taylor, P., Braley, J.C., Carter, J.C., Sinkov, S.I., Nash, K. L. (2012) The role of carboxylic acids in TALSQuEAK separations, *J. Coord. Chem.* *65*, 37–41.
18. Persson, G., Svantesson, I., Liljenzin, J. O., Wingefors, S. (1984) Hot test of a TALSPEAK procedure for separation of actinides and lanthanides using recirculating DTPA-lactic acid solution. *Solv. Extr. Ion Exchange*, *2*, 89–113.
19. Liljenzin, J.O., Persson, G., Svantesson, I., Wingefors, S. (1984) The CTH-Process for HLLW Treatment. *Radiochim. Acta*, *35*, 155–162.
20. Dietz, M.L. (2006) Ionic liquids as extraction solvents: Where do we stand? *Sep. Sci. Technol.*, *41*, 2047-2063.
21. Dietz, M.L. (2009) Neoteric solvents as the basis of alternative approaches to the separation of actinides and fission products. Moyer, B.A. (Ed.). In *Ion Exchange and Solvent Extraction: A Series of Advances*, Vol. 19, Taylor and Francis, New York, pp. 617-639.
22. Han, D., Row, K.H. (2010) Recent applications of ionic liquids in separation technology. *Molecules*, *15*, 2405-2426.
23. Zgola-Grzeskowiak, A., Grzeskowiak, T. (2011) Dispersive liquid-liquid microextraction. *TRAC*, *30*, 1382-1399.
24. Sun, X., Luo, H., Dai, S. (2012) Ionic liquid-based extraction: A promising strategy for the advanced nuclear fuel cycle. *Chem. Rev.*, *112*, 2100-2128.
25. Shkrob, I.A., Marin, T.W., & Jensen, M.P. (2014). Ionic liquid-based separations of trivalent lanthanide and actinide ions. *Ind. Eng. Chem. Res.*, *53*, 3641–3653.
26. Rout, A., Karmakar, S., Venkatesan, K.A., Srinivasan, T.G., Vasudeva Rao, P.R. (2011) Room temperature ionic liquid diluent for the mutual separation of europium(III) from americium(III). *Sep. Purif. Technol.* *81*, 109–115.
27. Sun, X., Luo, H., Dai, S. (2012) Solvent extraction of rare-earth ions based on functionalized ionic liquids. *Talanta*, *90*, 132–137.
28. Sun, X., Do-Thanh, C. L., Luo, H., Dai, S. (2014) The optimization of an ionic liquid based TALSPEAK-like process for rare earth ions separation. *Chem. Eng. J.*, *239*, 392–398.
29. Sun, X., Bell, J. R., Luo, H., Dai, S. (2011) Extraction separation of rare-earth ions via competitive ligand complexations between aqueous and ionic-liquid phases. *Dalton Trans.*, *40*, 8019–8023.

30. Winterton, N. (2006) Solubilization of polymers by ionic liquids. *J. Mater. Chem.*, *16*, 4281–4293.
31. Viell, J., Marquardt, W. (2011) Disintegration and dissolution kinetics of wood chips in ionic liquids. *Holzforschung*, *65*, 519–525.
32. Schröder, C. (2017) Proteins in ionic liquids: Current status of experiments and simulations. *Topics in Current Chemistry*, *375*, 25.
33. Ueno, K., Fukai, T., Nagatsuka, T., Yasuda, T., Watanabe, M. (2014) Solubility of poly(methyl methacrylate) in ionic liquids in relation to solvent parameters. *Langmuir*, *30*, 3228–3235.
34. Hawkins, C.A., Momen, M.A., Garvey, S.L., Kestell, J., Kaminski, M.D., Dietz, M.L. (2015) Evaluation of solid-supported room-temperature ionic liquids containing crown ethers as media for metal ion separation and preconcentration. *Talanta*, *135*, 115–123
35. Deetlefs, M., Seddon, K.R. (2003) Improved preparation of ionic liquids using microwave irradiation. *Green Chem.*, *5*, 181–186.
36. Fredlake, C.P., Crosthwaite, J.M., Hert, D.G., Aki, S.N.V.K., Brennecke, J.F. (2004) Thermophysical properties of imidazolium-based ionic liquids. *J. Chem. Eng. Data*, *49*, 954–964.
37. Kilaru, P., Baker, G.A., Scovazzo, P. (2007) Density and surface tension measurements of imidazolium-, quaternary phosphonium-, and ammonium-based room-temperature ionic liquids: Data and correlation. *J. Chem. Eng. Data*, *52*, 2306–2314.
38. Awad, W.H., Gilman, J.W., Nyden, M., Harris, R.H., Sutto, T.E., Callahan, J., Trulove, P.C., DeLong, H.C., Fox, D.M. (2004) Thermal degradation studies of alkyylimidazolium salts and their application in nanocomposites. *Thermochim. Acta*, *409*, 3–11.
39. Partridge, J.A.; Jensen, R.C. (1969) Purification of di-(2-ethylhexyl)phosphoric acid by precipitation of copper (II) di-(2-ethylhexyl) phosphate. *J. Inorg. Nucl. Chem.*, *31*, 2587–2589.
40. Smith, C.D., Downs, R.P., Carrick, J.D., Dietz, M.L. (2018) Determination of extractant solubility in ionic liquids by thermogravimetric analysis. *Solv. Extr. Ion Exch.*, *36*, 304–314.
41. Fredlake, C.P., Muldoon, M.J., Aki, S.N. V.K. (2004) Solvent strength of ionic liquid/CO₂ mixtures. *Phys. Chem. Chem. Phys.*, *6*, 3280–3285.
42. Padró, J.M., Reta, M. (2016) Solvatochromic parameters of imidazolium-, hydroxyammonium-, pyridinium- and phosphonium-based room temperature ionic liquids. *J. Mol. Liq.*, *213*, 107–114.

43. Lungwitz, R., Friedrich, M., Linert, W., Spange, S. (2008) New aspects on the hydrogen bond donor (HBD) strength of 1-butyl-3-methylimidazolium room temperature ionic liquids. *New J. Chem.*, *32*, 1493–1499.
44. Cláudio, A.F.M., Neves, M.C., Shimizu, K., Canongia Lopes, J.N., Freire, M.G., Coutinho, J.A.P. (2015) The magic of aqueous solutions of ionic liquids: Ionic liquids as a powerful class of catanionic hydrotropes. *Green Chem.* *17*, 3948–3963.
45. Carneiro, A.P., Held, C., Rodríguez, O., Sadowski, G., Macedo, E.A. (2013) Solubility of sugars and sugar alcohols in ionic liquids: Measurement and PC-SAFT modeling. *J. Phys. Chem. B*, *117*, 9980–9995.
46. Wang, H., Gurau, G., Rogers, R.D. (2012) Ionic liquid processing of cellulose. *Chem. Soc. Rev.*, *41*, 1519–1537.
47. Brandt, A., Hallett, J.P., Leak, D.J., Murphy, R.J., Welton, T. (2010) The effect of the ionic liquid anion in the pretreatment of pine wood chips. *Green Chem.*, *12*, 672–679.
48. Fort, D.A., Swatloski, R.P., Moyna, P., Rogers, R.D., Moyna, G. (2006) Use of ionic liquids in the study of fruit ripening by high-resolution ¹³C-NMR spectroscopy: “Green” solvents meet green bananas. *Chem. Commun.*, *7*, 714–716.
49. Ferreira, A.R., Freire, M.G., Ribeiro, J.C., Lopes, F.M., Crespo, J.G., Coutinho, J.A.P. (2011) An overview of the liquid-liquid equilibria of (ionic liquid + hydrocarbon) binary systems and their modeling by the conductor-like screening model for real solvents. *Ind. Eng. Chem. Res.*, *50*, 5279–5294.
50. Lu, B., Xu, A., Wang, J. (2014) Cation does matter: How cationic structure affects the dissolution of cellulose in ionic liquids. *Green Chem.*, *16*, 1326–1335.
51. Xu, A., Wang, J., Wang, H. (2010) Effects of anionic structure and lithium salts addition on the dissolution of cellulose in 1-butyl-3-methylimidazolium-based ionic liquid solvent systems. *Green Chem.*, *12*, 268–275.
52. Chen, Q., Xu, A., Li, Z., Wang, J., Zhang, S. (2011) Influence of anionic structure on the dissolution of chitosan in 1-butyl-3-methylimidazolium-based ionic liquids. *Green Chem.*, *13*, 3446–3452.
53. Crowhurst, L., Falcone, R., Lancaster, N. L., Llopis-Mestre, V., & Welton, T. (2006) Using Kamlet-Taft solvent descriptors to explain the reactivity of anionic nucleophiles in ionic liquids. *J. Org. Chem.*, *71*, 8847–8853.
54. Cheong, W.J.; Choi, J. D. (1997) Linear solvation energy relationships in normal phase chromatography based on retention data on silica in 2-propanol/hexane eluents. *Anal. Chim. Acta*, *342*, 51–57.

55. Yazdanshenas, R., Gharib, F. (2017) Solubility and thermodynamic functions measurement of morin hydrate in different alcohols. *J. Mol. Liq.*, 233, 9–14.
56. Kamlet, M.J., Abboud, J.L.M., Abraham, M.H., Taft, R.W. (1983) Linear solvation energy relationships, 23. A comprehensive collection of the solvatochromic parameters, π^* , α , and β , and some methods for simplifying the generalized solvatochromic equation. *J. Org. Chem.*, 48, 2877-2887.
57. Gharib, F., Shamel, A., Jaber, F., & Farajtabar, A. (2013) Spectral investigations of preferential solvation and solute-solvent interactions of free base and protonated 5, 10, 15, 20-tetrakis(4-trimethyl-ammonio-phenyl)-porphine tetratosylate in aqueous organic mixed solvents. *J. Sol. Chem.*, 42, 1083–1095.
58. Spange, S., Lungwitz, R., Schade, A. (2014) Correlation of molecular structure and polarity of ionic liquids. *J. Mol. Liq.*, 192, 137–143.
59. Ab Rani, M. A., Brant, A., Crowhurst, L., Dolan, A., Lui, M., Hassan, N. H., Hallett, J.P., Hunt, P.A., Niedermeyer, H., Perez-Arlandis, J.M., Schrems, M., Welton, T., Wilding, R. (2011) Understanding the polarity of ionic liquids. *Phys. Chem. Chem. Phys.*, 13, 16831-16840.
60. Marcus, Y. (2017) Room temperature ionic liquids: Their cohesive energies, solubility parameters and solubilities in them. *J. Sol. Chem.*, 46, 1778–1791.
61. Marcus, Y. (2015) Ionic and molar volumes of room temperature ionic liquids. *J. Mol. Liq.*, 209, 289-293.
62. Veldhorst, A. A., Faria, L. F. O., & Ribeiro, M. C. C. (2016) Local solvent properties of imidazolium-based ionic liquids. *J. Mol. Liq.*, 223, 283–288.
63. Luo, H., Baker, G.A., Dai, S. (2008) Isothermogravimetric determination of the enthalpies of vaporization of 1-alkyl-3-methylimidazolium ionic liquids. *J. Phys. Chem. B*, 112, 10077–10081.
64. Lee, S.H., Lee, S.B. (2005) The Hildebrand solubility parameters, cohesive energy densities and internal energies of 1-alkyl-3-methylimidazolium-based room temperature ionic liquids. *Chem. Comm.*, 27, 3469–3471.
65. Alavianmehr, M.M., Hosseini, S.M., Mohsenipour, A.A., Moghadasi, J. (2016). Further property of ionic liquids: Hildebrand solubility parameter from new molecular thermodynamic model. *J. Mol. Liq.*, 218, 332–341.
66. Marciniak, A. (2010) The solubility parameters of ionic liquids. *Int. J. Mol. Sci.*, 11, 1973-1990.

67. Mäki-Arvela, P., Anugwom, I., Virtanen, P., Sjöholm, R., Mikkola, J.P. (2010) Dissolution of lignocellulosic materials and its constituents using ionic liquids – A review. *Ind. Crop. Prod.*, 32, 175–201.
68. Lee, S.H., Doherty, T.V., Linhardt, R.J., Dordick, J.S. (2008) Ionic liquid-mediated selective extraction of lignin from wood leading to enhanced enzymatic cellulose hydrolysis. *Biotechnol. Bioeng.*, 102, 1368–1376.
69. Marcus, Y. (2016) Are solubility parameters relevant for the solubility of liquid organic solutes in room temperature ionic liquids? *J. Mol. Liq.*, 214, 32–36.
70. Ruoff, R.S., Tse, D.S., Malhotra, R., Lorents, D.C. (1993) Solubility of C₆₀ in a variety of solvents. *J. Phys. Chem.*, 97, 3379–3383.
71. Anthony, J. L., Anderson, J. L., Maginn, E. J., & Brennecke, J. F. (2005) Anion effects on gas solubility in ionic liquids. *J. Phys. Chem. B*, 109, 6366–6374.
72. Camper, D., Bara, J., Koval, C., & Noble, R. (2006) Bulk-fluid solubility and membrane feasibility of rmim-based room-temperature ionic liquids. *Ind. Eng. Chem. Res.*, 45, 6279–6283.
73. Dzyuba, S.V, Bartsch, R.A. (2002) Influence of structural variations in 1-alkyl(aralkyl)-3-methylimidazolium hexafluorophosphates and bis(trifluoromethyl-sulfonyl)imides on physical properties of the ionic liquids. *Chem. Phys. Phys. Chem.*, 3, 161–166.
74. Decerbo, J.N. (2008) 1-Alkyl-3-methylimidazolium bis(pentafluoroethylsulfonyl)imide based ionic liquids: A study of their physical and electrochemical properties. M.S. Thesis, Wright State University, Dayton, OH.
75. Fitchett, B.D., Knepp, T.N., Conboy, J.C. (2004) 1-Alkyl-3-methylimidazolium bis(perfluoroalkylsulfonyl)imide water-immiscible ionic liquids: The effect of water on electrochemical and physical properties. *J. Electrochem. Soc.*, 151, E219–E225.
76. 1-butylpyridinium bis(trifluoromethanesulfonyl)imide. Retrieved Oct. 4, 2018. https://iolitec.de/en/products/ionic_liquids/catalog/pyridinium-based/il-0213-hp.
77. 1-octyl-3-methylimidazolium trifluoromethanesulfonate. Retrieved Oct. 1, 2018. <https://www.sigmaaldrich.com/catalog/product/aldrich/68902?lang=en®ion=US>.
78. 1-methyl-3-octylimidazolium tetrafluoroborate (2018) Retrieved Sept. 30, 2018. <https://iolitec.de/en/node/140>.
79. Spear, S.K., Griffin, S.T., Granger, K.S., Huddleston, J.G., Rogers, R.D. (2007) Renewable plant-based soybean oil methyl esters as alternatives to organic solvents. *Green Chem.*, 9, 1008–1015.

80. Seddon, K.R., Stark, A., Torres, M.-J. (2002) Viscosity and density of 1-alkyl-3-methylimidazolium ionic liquids. In *Clean Solvents* (ACS Symposium Series, Vol. 819), American Chemical Society, Washington, DC, pp. 34–49.
81. Dietz, M.L., Rickert, P.G., Antonio, M.R., Firestone, M.A., Wishart, J.F., Szreder, T. (2008) Tetraalkylphosphonium polyoxometalates as novel ionic liquids in solvent extraction: fundamentals to industrial applications (Proceedings of ISEC 2008, Vol. 2), Moyer B.A. (Ed.), Canadian Institute of Mining, Metallurgy and Petroleum, Montreal, pp. 799-804.
82. Nilsson, M., Nash, K.L. (2009) Trans-lanthanide extraction studies in the TALSPEAK system: Investigating the effect of acidity and temperature. *Solv. Extr. Ion Exch.*, 27, 354-377.
83. Horwitz, E.P., Dietz, M.L., Chiarizia, R., Diamond, H., Maxwell, S.L. III, Nelson, M.R. (1995) Separation and preconcentration of actinides by extraction chromatography using a supported liquid anion exchanger: Application to the characterization of high-level nuclear waste solutions. *Anal. Chim. Acta*, 310, 63-78.
84. Hawkins, C.A., Momen, M.A., Dietz, M.L. (2018) Application of ionic liquids in the preparation of extraction chromatographic materials for metal ion separations: Progress and prospects. *Sep. Sci. Technol.*, 53, 1820-1833.

CHAPTER 4

SUPPORT LOADING EFFECTS ON THE PERFORMANCE OF AN EXTRACTION CHROMATOGRAPHIC RESIN: TOWARD IMPROVED SEPARATIONS OF TRIVALENT LANTHANIDES

4.1 Introduction

Since the introduction of the first commercial extraction chromatographic materials more than two decades ago,¹⁻⁶ extraction chromatography (EXC) has become the most widely employed technique for the separation and preconcentration of radionuclides for subsequent determination,⁷ largely supplanting classical methods based upon solvent extraction, precipitation, and ion exchange.⁸⁻¹⁰ Extraction chromatography has also attracted increasing interest as a possible complement to or replacement for solvent extraction in the large-scale separation of various metal ions in nuclear fuel reprocessing and hydrometallurgy.¹¹⁻¹⁵ Unlike conventional liquid chromatography, in EXC, the stationary phase comprises a metal ion extractant or a solution of an extractant in a water-immiscible diluent, supported on an inert, porous, (typically) polymeric support. By appropriate choice of mobile (aqueous) phase, the retention of the metal ion of interest and ideally, its separation from matrix constituents and interfering species, can be effected.

Despite its widespread application, EXC is not without limitations.¹⁶ For example, because the extractant molecules are not covalently tethered to the support, physical stability can be problematic, despite efforts at improvement.¹⁷⁻¹⁸ Along these same lines, because the ability of the support to contain extractant is limited, so too is the capacity of an extraction chromatographic resin to sorb metal ions.¹⁹ While recent results suggest that extractant encapsulation in an appropriate polymer may offer a means of increasing the maximum metal ion uptake of an EXC sorbent,¹⁹ these efforts are still in their early stages. Lastly, the comparatively

large particle size supports typically employed in EXC (often 50-100 μm or larger) means that column efficiency is generally poor. Recent work by the author, for example, has shown that for columns of a size (*e.g.*, 200 μL) suitable for high-throughput radiochemical separations (*i.e.*, lab-on-a-valve format), plate numbers only in the single digits may be observed.²⁰

With this observation in mind, we have undertaken efforts to improve the column efficiency associated with extraction chromatographic materials. Despite a substantial body of literature concerning EXC, systematic investigations of the factors governing column efficiency are comparatively few.²¹⁻²⁸ Moreover these studies have generally focused on materials prepared using such supports as porous silica^{21,24} or diatomaceous earth,^{25,26} not the macroporous polymers employed in contemporary extraction chromatography.¹⁻⁶ As a first step in our investigations, we have examined the effect of the level of extractant impregnation of a support upon column efficiency, as exemplified by HDEHP-loaded Amberchrom CG-71m, macroporous beads of poly(methyl methacrylate) (PMMA) that provide the basis of most commercial EXC sorbents. The results demonstrate that reduced support loading can lead to a measurable increase in column efficiency, in addition to reduced peak tailing. As will be shown, these improvements can have practical significance, as illustrated by their effect on the separation of selected trivalent lanthanides.

4.2 Experimental

4.2.1 Reagents

Unless otherwise noted, all chemicals were ACS reagent grade and were used without further purification. All water was obtained from a Milli-Q2 system and exhibited a specific resistance of at least 18 $\text{M}\Omega\text{-cm}$. Methanol and nitric acid (Optima grade) were purchased from

Fisher Scientific. Polytetrahydrofuran (PTHF) 250, along with trace metal grade (99.9% pure) europium (III) nitrate pentahydrate, neodymium (III) nitrate hexahydrate, gadolinium (III) nitrate hexahydrate, and cesium nitrate were obtained from Sigma-Aldrich (St. Louis, MO). The *bis*(2-ethylhexyl)phosphoric acid was purchased from Sigma-Aldrich and purified by copper salt precipitation prior to use.²⁹ Its purity was verified by ³¹P-NMR.

The ^{152/154}Eu and ¹³⁷Cs radiotracers were obtained from Eckert and Ziegler Isotope Products (Valencia, CA). The Ln resin (50-100 μm particle size) was purchased from EiChrom Technologies (Lisle, IL). Amberchrom CG-71m (50-100 μm diameter beads of porous poly(methylmethacrylate)) was obtained from Rohm and Haas (Philadelphia, PA) and preconditioned before use as described previously.³⁰ Briefly, a weighed portion of the crude resin was contacted with deionized water for 30 minutes with occasional swirling. The resulting slurry was then transferred to a coarse-fritted glass funnel and the water removed by vacuum filtration. Methanol was then poured over the wet resin and allowed to percolate through the bed under gravity. The last traces of methanol were removed under vacuum. This process was repeated twice more, and the washed resin transferred to a round-bottomed flask using a small volume of methanol. The methanol was removed under vacuum at 50 °C using a rotary evaporator, yielding the dried, purified resin.

4.2.2 Instrumentation

The radiotracers were assayed using a Perkin-Elmer Model 2480 Automatic Gamma Counter. Inactive (*i.e.*, non-radioactive) metal ions were quantified using a Shimadzu Inductively Coupled Plasma-Mass Spectrometer (ICP-MS) 2030. Surface area analyses were conducted using a Micromeritics ASAP 2020 Plus. Chromatographic elution profiles were

determined on Bio-Rad (Hercules, CA) Econo-Pac[®] chromatography columns (diameter = 0.5 cm; height = 5 cm).

4.2.3 Methods

4.2.3.1 Resin impregnation

A weighed portion of purified Amberchrom CG-71m was slurried with methanol, then combined with a solution containing an appropriate quantity of PTHF 250 or HDEHP, also in methanol. The mixture was equilibrated for 24 hours, after which loaded support particles were recovered by rotary evaporation of the methanol *in vacuo* at 50°C.

4.2.3.2 Determination of weight distribution ratios

Solid-liquid (weight) distribution ratios (D_w) for europium were measured radiometrically using a $^{152/154}\text{Eu}$ radiotracer. For neodymium and gadolinium, D_w values were determined by ICP-MS using solutions of inactive $\text{Nd}(\text{NO}_3)_3 \cdot 6 \text{H}_2\text{O}$ and $\text{Gd}(\text{NO}_3)_3 \cdot 6 \text{H}_2\text{O}$, respectively. Specifically, the uptake of each metal ion solution from a series of nitric acid solutions by the resins was measured by contacting a known volume (typically 1 mL) of $^{152/154}\text{Eu}(\text{III})$ -, $\text{Gd}(\text{III})$ -, or $\text{Nd}(\text{III})$ -spiked acid solution of appropriate concentration with a known quantity of resin (*ca.* 20-25 mg). The ratio of the aqueous phase volume (mL) to the weight of the chromatographic material (in grams) typically ranged from 40-50. Such a ratio was found to provide a readily measured decrease in the aqueous phase metal ion content upon contact with the resin. A two-hour contact time was used for equilibration. Following equilibration, an aliquot of aqueous phase was withdrawn from each culture tube and the gamma activity or concentration measured. From the difference in the activity or concentration of the aqueous phase before and after contact

with the resins, the weight distribution ratio (D_w) of europium, neodymium, or gadolinium was calculated according to Equation 4.1:

$$D_w = [(A_0 - A_f) / A_f] (V/w) \quad (4.1)$$

where A_0 and A_f are the aqueous phase activity (cpm) or concentration before and after equilibration, respectively, w is the mass (g) of the resin, and V is the volume of the aqueous phase (mL).

4.2.3.3 Determination of metal ion uptake kinetics.

Into a series of screw-cap test tubes, each containing the same amount (20-25 mg) of the sorbent of interest, was introduced a known volume (generally 1 mL) of an appropriate nitric acid solution containing a $^{152/154}\text{Eu}$ radiotracer. At various time intervals following the introduction of the tracer solution, during which the samples were periodically mixed to ensure equilibration, the aqueous phase was withdrawn from one of the test tubes and filtered through a 0.45 μm PVDF filter. From the initial and final activity of the aqueous phases, D_w values were calculated as described above (Eqn. 1) and a plot of the time dependence of D_w prepared.

4.2.3.4 Determination of sorbent capacity

For capacity determinations, a concentrated solution of inactive europium nitrate (each 1-mL aliquot containing five times the stoichiometric amount of extractant present) in dilute nitric acid (0.025 M, 0.05 M, 0.1 M, and 0.15 M HNO_3 for the 10%, 15%, 20%, and 30% (%w/w) HDEHP resins, respectively, chosen so as to correspond to $\gg 99\%$ extraction) was prepared and spiked with a $^{152/154}\text{Eu}$ radiotracer. A weighed quantity (20-25 mg) of the sorbent of interest was then placed in a test tube and contacted with 1 mL of the radiotracer-spiked europium solution. After vortex mixing, samples were allowed to stand undisturbed for 24 hours, well beyond the 20

minutes found in kinetics studies to be required for establishment of equilibrium. The aqueous phase was then withdrawn and filtered through a plastic frit. From the initial and final activity of the aqueous phase, the capacity of the sorbent (mg Eu/g of sorbent) was then calculated based on the assumption that the fraction of inactive europium taken up corresponds to the fraction of Eu-152/154 sorbed.

4.2.3.5 Column preparation and characterization

To pack a column, a small quantity of the resin of interest was slurried in Milli-Q2 water, and aliquots of the slurry transferred to an Econo-Pac[®] column. Because the resins settled readily, packing was carried out without applied pressure. When the resin bed reached the desired height, a small plug of glass wool was placed atop the bed so that it would not be disturbed by the introduction of a sample. The bed was then preconditioned with 10 free column volumes (FCVs) of the desired nitric acid solution. Unless otherwise noted, all column runs utilizing the 50-100 μm particles were carried out as part of studies of the effects of support loading were performed without applied pressure, corresponding to a flow rate of 1.57 ± 0.12 $\text{mL}/\text{cm}^2 \cdot \text{min}$. No systematic changes in gravity flow rates were noted upon changes in the level of support loading. All column runs utilizing 20-50 μm particles were carried out at a flow rate of 1.50 ± 0.05 $\text{mL}/\text{cm}^2 \cdot \text{min}$.

The resin density and column parameters such as the bed density, stationary phase volume (v_s , the volume of liquid extractant contained in the pores of the support), and mobile phase volume (v_m , the free column volume) were measured using established methods.³¹ Specifically, the resin density was determined by adding a small amount of resin to a series of nitric acid solutions of increasing concentration until a concentration was found at which the resin remained suspended upon mixing. At this point, the resin density matches that of the

solution, which in turn, can be determined by weighing a known volume of the solution. The bed density was determined by measuring the mass of resin required to prepare a bed of known (0.90 mL) volume. The volume of stationary phase, V_s , was determined from the weight of EXC material in the column, the resin loading (*i.e.*, the weight percent of extractant present in the resin), and the density of the extractant. The mobile phase volume, V_m , was determined by first equilibrating the resin bed with a nitric acid solution of known concentration (*ca.* 1 M). A small volume ($\sim 5 \mu\text{L}$) of ^{137}Cs (or inactive cesium nitrate solution) was then added to the top of the bed and eluted with the acid solution. Because HDEHP extracts monovalent cations poorly under the experimental conditions,³² cesium will be essentially un-retained. Therefore, the mobile phase volume can be calculated from the average drop volume and the number of the drop in which cesium first appears in the column effluent. All runs were carried out at ambient temperature ($23 \pm 2 \text{ }^\circ\text{C}$).

4.2.3.6 Elution behavior of europium-152/54.

The elution profiles of $^{152/154}\text{Eu(III)}$ on packed beds (0.90 mL bed volume) of 5%, 10%, 15%, 20%, and 30% (w/w) HDEHP on Amberchrom CG-71m and on commercial Ln resin were determined using Bio-Rad Econo-Pac® chromatography columns (0.5 x 5 cm) with dilute HNO_3 as the eluent. Specifically, 0.026 M, 0.045 M, 0.080 M, 0.13 M, 0.22 M and 0.30 M HNO_3 were employed as the eluent for the 5%, 10%, 15%, 20%, and 30% (w/w) resins and the Ln resin, respectively. Samples of the eluent were collected at intervals necessary to fully define the elution curve (typically 1-2 FCVs) and gamma counted.

4.2.3.7 Elution behavior of neodymium, gadolinium and (inactive) europium.

After column preconditioning with 10 FCV of an appropriate nitric acid solution, a ~10- μ L aliquot of a stock solution combining Eu(III) (2.5 mM), Nd(III) (2.3 mM), and/or Gd(III) (2.5 mM) (the precise combination depending on the separation of interest) was introduced atop the resin bed and eluted using the same acid solution. The eluent was collected in 1-2 FCV fractions and assayed using the ICP-MS. All runs were carried out at ambient temperature (23-25°C).

4.3 Results and Discussion

4.3.1 Effect of pore structure on support filling

Any discussion of the effect of support loading on the column efficiency observed for an EXC resin must begin with consideration of the internal structure of the support employed, in particular, the nature, size, and arrangement of the pores present. Prior work by Arias *et al.*,³³ in which the impregnation of Amberlite XAD-7 with a tetraalkylphosphonium ionic liquid (*i.e.*, trihexyl(tetradecyl)phosphonium chloride, abbreviated hereafter as $[P_{666,14}^+][Cl^-]$) was systematically examined, concluded that the interior of the resin comprises interconnected pores of three distinct size ranges: micropores 50 Å or less in diameter, mesopores 50-200 Å in diameter, and macropores greater than 200 Å in diameter. Figure 4.1, which depicts the effect of loading various quantities of either a low molecular weight polymer (PTHF 250) or an organophosphorus extractant (*bis*(2-ethylhexyl)-phosphoric acid) into a smaller-particle analog of the same support (*i.e.*, Amberchrom CG-71m) on its total surface area, supports this view. That is, as can be seen, the surface area vs. loading plots exhibit two discontinuities (*i.e.*, slope changes), the first at a loading level (expressed as the volume fraction filled) of 0.18 and the second at 0.30.

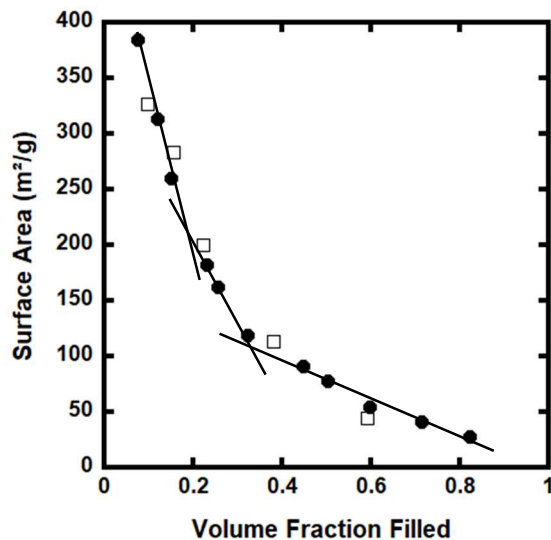


Figure 4.1: Effect of support loading on the surface area of Amberchrom CG-71m for two fillers. (●) PTHF 250; (□) HDEHP.

Because the decline in surface area is steepest at low loading levels, the first of these must correspond to the transition from the filling of the smallest pores to the filling of intermediate-size pores. Similarly, the second must represent the start of the filling of the largest pores. From the perspective of optimizing the level of extractant impregnation, it is instructive to consider a pictorial representation of the support (Figure 4.2), first suggested by Arias *et al.*³³ on the basis of surface area vs. loading data for $[P_{666,14}^+][Cl^-]$ on XAD-7. From this, it is clear that low levels of loading, which will serve to confine the extractant primarily to the smallest and least accessible pores (Figure 4.2C), are not desirable. Of course, as has already been noted, high loading levels that result in filling of the entirety of the support (Figure 4.2E), such as are employed in commercial EXC resins, do not yield acceptable column efficiencies. (Moreover they are known to reduce the physical stability of the sorbent.^{17,19}) This suggests that an intermediate level of loading, in particular one that leaves a significant portion of the extractant

deposited as a thin film on the walls of the mesopores (Figure 4.2D), should yield the highest column efficiency.

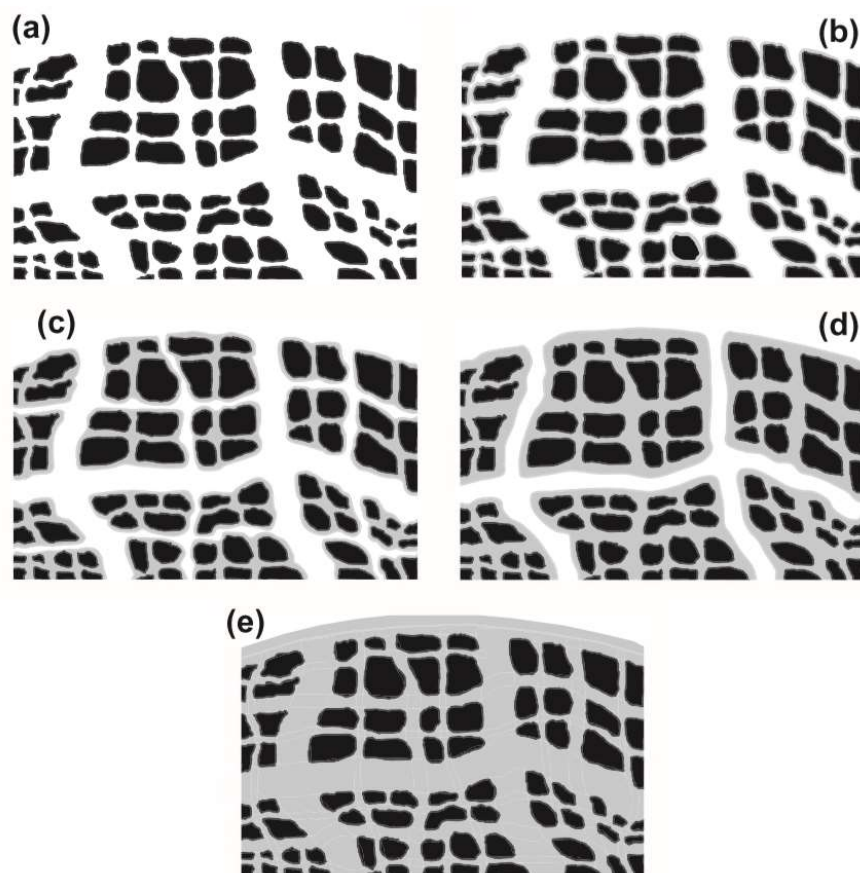


Figure 4.2A-E: Representation of the interior structure of Amberlite XAD-7 filled to increasing levels with the ionic liquid $P_{666,14}^+Cl^-$.³³

4.3.2 Effect of support loading on column performance

Prior studies concerning loading effects on column efficiency for various extractants on other supports, it should be noted, have yielded inconsistent results. In an examination of tri-*n*-butyl phosphate (TBP) supported on a macroporous styrene-divinylbenzene copolymer (*i.e.*, Amberlite XAD-4), for example, Louis *et al.*²⁷ observed a decrease in plate height (*i.e.*, an increase in the number of theoretical plates, *N*) as the support loading was increased. Horwitz *et al.*,²⁶ however, observed an increase in plate height (decreased *N*) as HDEHP loading on a

hydrophobic Celite support was increased, while Sochaka *et al.*²² observed analogous behavior for the same extractant on kieselguhr. Finally, an examination of the effect of impregnation level on the behavior of HDEHP-loaded Amberlite XAD-4 (macroporous PS-DVB) in the extraction of uranium showed no such monotonic variation.²⁸ Instead the relationship between the column efficiency and loading exhibited a minimum in plate height (maximum N) at intermediate (*ca.* 43% w/w) loading, with significantly decreased efficiency (lower N) at higher or lower loading levels. Similar behavior was reported by Horwitz *et al.*²⁵ in an examination of Cf(III) elution on hydrophobic Celite loaded to various levels with HDEHP. In the absence of detailed information on support structure (such as has been described for the Amberchrom CG-71 resin used here), however, it is difficult to fully rationalize these observations.

Figure 4.3 depicts the elution behavior of Eu(III) on a column of an extraction chromatographic material comprising 5% (w/w) HDEHP on the Amberchrom support. As might be expected from the fact that the extractant is present largely in the least accessible pores of the support, the elution is protracted, and is in fact incomplete even after more than 100 free column volumes (FCVs) of eluent have passed, far beyond the peak maximum at *ca.* 8 FCVs. Increasing the support loading to 10% (w/w) provides an obvious improvement in the chromatographic behavior (Figure 4.4A) and makes feasible the determination of the plate number associated with the elution. Calculation of the number of theoretical plates according to Equation 4.2 yields a value of 20 (*i.e.*, H = 0.24 cm).

$$N = 5.54 * \left(\frac{t_R}{W_{0.5h}} \right)^2 \quad (4.2)$$

As has been noted elsewhere, the number of theoretical plates is not the sole factor governing the effectiveness of a particular sorbent as a medium for chromatographic separation;

rather, the extent of peak tailing is also an important consideration.³⁴ Two parameters are commonly employed to quantify tailing,³⁵ the peak asymmetry factor (A_s), defined as per Equation 4.3:

$$A_s = \frac{b}{a} \quad (4.3)$$

and the peak tailing factor (T_f), defined by Equation 4.4:

$$T_f = \frac{ac}{2ab} \quad (4.4)$$

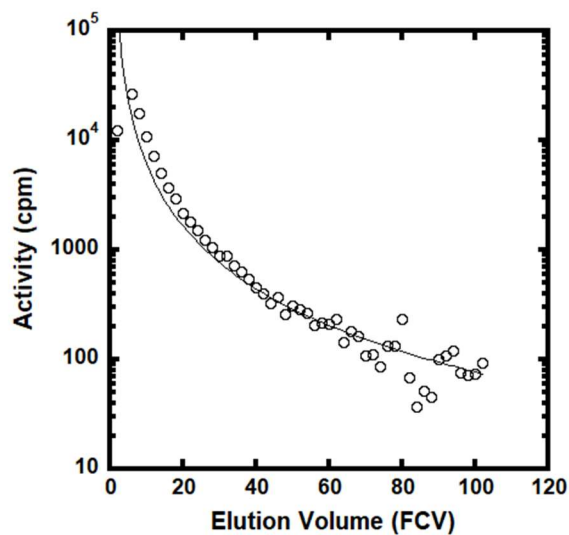


Figure 4.3: Elution behavior of $^{152/4}\text{Eu(III)}$ on a column (0.90 mL bed volume) containing 5% (w/w) HDEHP-loaded Amberchrom CG-71m resin. (50-100 μm particle size; mobile phase = 0.026 M HNO_3 .) Note that the data is plotted in semi-log form to emphasize the extent of tailing.

Table 4.1: Effect of support loading on the elution behavior of Eu(III) on Amberchrom CG-71m - supported HDEHP

Support loading (% w/w)	T _f	A _s	H (cm)	N	Capacity (mg Eu/mL bed)
10	1.67	2.21	0.239	20	1.25
15	1.36	1.47	0.239	20	1.94
20	1.11	1.14	0.140	33	3.81
30	1.24	1.40	0.191	25	10.28
40	1.36	1.74	0.199	24	11.04

Experimental conditions: V_{column} = 0.90 mL; L_{column} = 4.77 cm; Flow rate: 1.57 ± 0.12 mL/cm²·min.

Application of these equations to the chromatogram shown in Figure 4.4A yields values of 2.21 and 1.67, respectively, for A_s and T_f. The remaining panels of Figure 4.4 (panels B-D) depict the effect of increasing support loading with HDEHP on the elution behavior of Eu³⁺, and the corresponding values of N, H, A_s, and T_f are summarized in Table 4.1. Also included in this table are values for the sorbent capacity for metal ion (*i.e.*, Eu³⁺) retention. Several important conclusions can be drawn from these data. First, as anticipated from consideration of the pore structure of the support (Figure 4.2), the number of theoretical plates passes through a maximum (*i.e.*, H reaches a minimum) at intermediate levels of support loading. That is, at a loading level of 20% (w/w), N=33, nearly a factor of two improvement over the poorest of the values seen. In addition, peak tailing is at its minimum at the same level of support loading. Lastly, and unfortunately, the improvements in column efficiency and peak tailing come at the expense of column capacity. That is, at a support loading of 20% (w/w), the capacity of the sorbent is less than half of that observed for a 40% loaded (commercial) resin. Taken together, these results suggest that in applications for which high metal ion uptake capacity is not the primary consideration, peak capacity (*i.e.*, the number of peaks that can successfully be resolved in any

given chromatographic run) can be enhanced simply by employing an intermediate level of support loading.

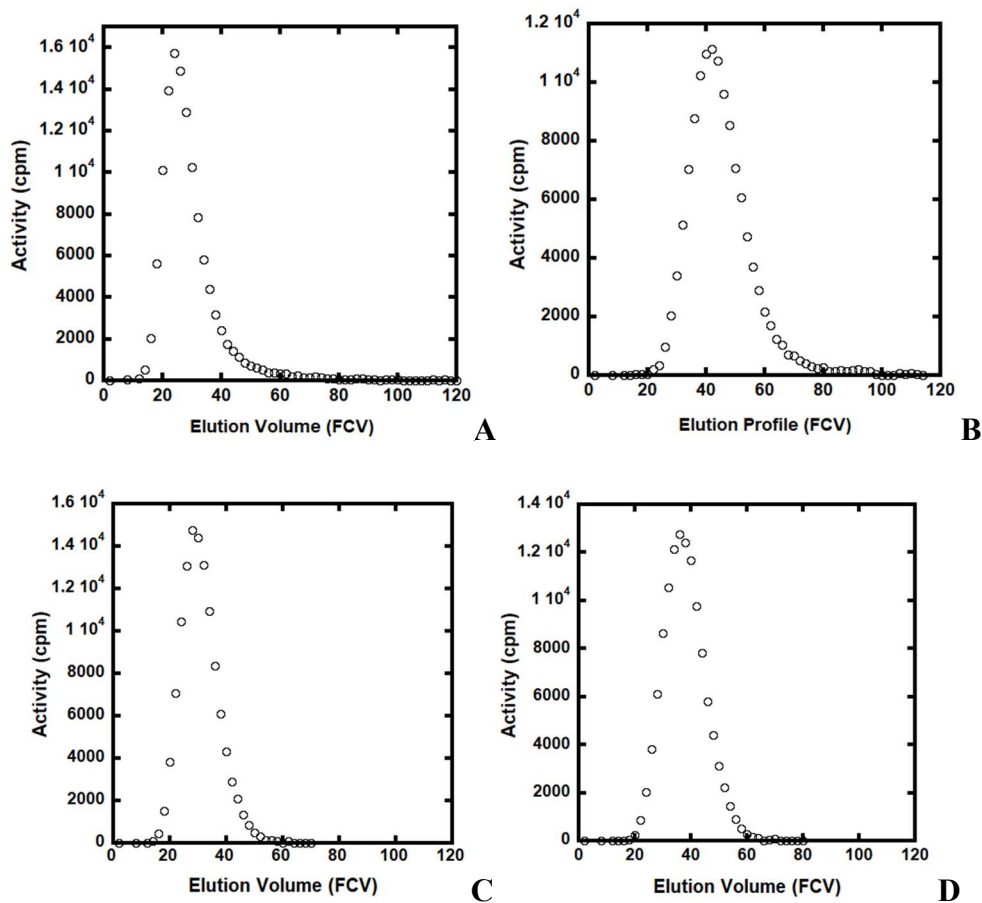


Figure 4.4A-D: Elution behavior of $^{152/4}\text{Eu(III)}$ on a column (0.90 mL bed volume) containing HDEHP-loaded Amberchrom CG-71m resin. (A) 10% (w/w) loaded; (B) 15% (w/w) loaded; (C) 20% (w/w) loaded; (D) 30% (w/w) loaded. (50-100 μm particle size; mobile phase = 0.045, 0.080 0.13, 0.22 M HNO_3 , respectively.

4.3.3 Effect of reduced support loading on trivalent lanthanide separations

Although metal ion sorbents comprising HDEHP supported on a porous substrate have been known since the early 1960's,^{36,37} it was not until more than three decades later that the first such material ("Ln resin", EiChrom Technologies) was commercialized and systematic characterization data reported for it.^{38,39} Of particular significance in the present context are data

describing the acid dependency of the retention of the trivalent lanthanides on the resin, which provide an indication of the feasibility of their separation under various solution conditions. Such separations, in particular analytical-scale trivalent actinide/ lanthanide (An/Ln) and intra-lanthanide separations, are important in radiochemical analysis, in areas ranging from personnel monitoring⁴⁰ and nuclear forensics^{41,42} to environmental monitoring⁴² and nuclear fuel and waste characterization.⁴³ These separations remain a significant challenge, however.⁴⁴⁻⁴⁶ It is therefore of interest then to determine if they can be facilitated by the increased column efficiency and diminished tailing associated with reduced extractant loading.

To this end, we have examined two representative separations – Nd(III)/Eu(III) and Eu(III)/Gd(III) – to determine the extent of improvement of their resolution made possible using a “lightly loaded” support. Certain prior work indicates that these separations are not entirely satisfactory on the Ln resin. In a recent study by Bertelsen *et al.*,⁴⁷ for example, in which the separation of Nd(III) and Eu(III) in nitric acid media using HDEHP-impregnated mesoporous silica nanoparticles was compared to that obtained using the commercial resin, nearly complete overlap of the elution bands was observed for the two metal ions on the latter sorbent. While the columns employed in the study were small (200 μ L), and thus the number of theoretical plates (while not specified) was undoubtedly low, unsatisfactory results were also noted in a study by Payne *et al.*⁴⁸ in which a much larger (2-mL) pre-packed column of the Ln resin was employed. In this instance, incomplete separation of Nd(III) and Eu(III) was again noted, even when a nitric acid step-gradient was employed for elution.

As a starting point in our investigations of Nd(III)/Eu(III) separation, batch studies were performed in which weight distribution ratios for the two ions were measured for Amberchrom CG-71m containing 20%(w/w) HDEHP. The observed Eu/Nd separation factors ($\alpha_{Eu/Nd}$),

defined as the ratio of the respective D_w values, suggest that their separation should be feasible (e.g., $\alpha_{Eu/Nd} = 21$ at 0.15 M HNO_3). Indeed, as shown in Figure 4.5, which depicts the elution behavior of the two ions on the 20%(w/w) HDEHP resin, their complete separation is easily accomplished. Curiously, and in contrast to the report of Payne *et al.*⁴⁸, results for the Ln resin (not shown) indicate that it too is capable of providing a satisfactory separation of the two ions, although the resolution achieved with the “lightly loaded” resin ($R = 7.7$), defined as per Equation 4.5, is superior to that obtained with the commercial material ($R = 2.1$).

$$R_s = 2 (t_{R2} - t_{R1}) / (w_{b1} + w_{b2}) \quad (4.5)$$

where R_s is the chromatographic peak resolution, t_R is the retention time, and w_b is the peak width at baseline.

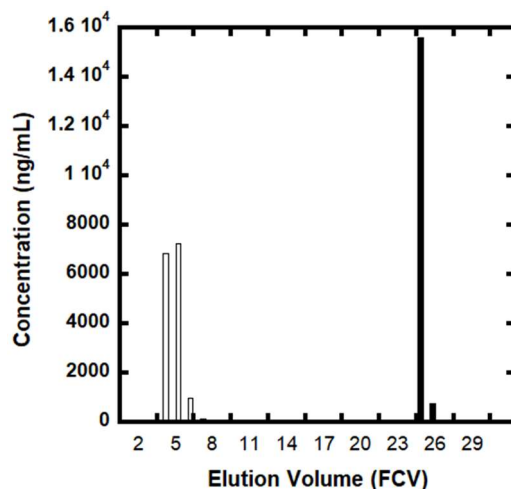


Figure 4.5: Separation of Nd(III) and Eu(III) on a column (0.90 mL bed volume) containing 20% (w/w) HDEHP-loaded Amberchrom CG-71m resin. (50-100 μm particle size; mobile phase = 0.13 M HNO_3). (o) Nd; (•) Eu.

The case of Eu(III) and Gd(III) represents a more challenging separation, and one of considerable practical significance. In addition to its growing importance as a low-energy gamma source (as ^{153}Gd) for single-photon emission computed tomography (SPECT) imaging,⁴⁹

gadolinium finds application in radiochemical analysis in the determination of the extent of burn-up of nuclear fuels (as ^{154}Gd - ^{157}Gd)⁴¹ and in nuclear forensics (as ^{157}Gd) to establish an attribution of radioactive materials.⁴³ These applications generally require the separation of gadolinium from other lanthanides, in the case of ^{153}Gd , for example, from the Eu_2O_3 from which it is produced. The difficulty in achieving satisfactory Eu(III)/Gd(III) separation using extraction chromatography employing HDEHP or related organophosphorus reagents has long been recognized.^{37,38,42,48-51} In a study employing a pre-packed (2-mL), gravity-flow Ln resin column, for example, Payne *et al.*⁴⁸ observed essentially complete overlap of the elution bands of the two ions, even when a nitric acid step gradient was employed. Such results have led other investigators to employ lengthy/large volume chromatographic columns,³⁸ or to electrochemically⁵² or photochemically⁵³ reduce the europium prior to introduction of the Eu/Gd mixture to the EXC column in an effort to improve the separation.

As was the case in our examination of Nd(III)/Eu(III) separation, our studies of Eu(III) and Gd(III) separation began with weight distribution ratio measurements for the two ions between a series of nitric acid concentrations and Amberchrom CG-71m containing 20%(w/w) HDEHP. The observed Eu/Gd separation factors ($\alpha_{\text{Eu/Gd}}$), defined as the ratio of the respective D_w values, suggested that their separation may be feasible (*e.g.*, $\alpha_{\text{Eu/Gd}} = 2.53$ at 0.1 M HNO_3), albeit incomplete. Indeed, as shown in Figure 4.6 (panel A), although baseline separation of Eu(III) and Gd(III) is not achieved ($R = 0.89$), the resolution of the two ions is significantly better than that obtained using the conventional Ln resin ($R = 0.53$ at 0.30 M HNO_3), shown in panel B. For the latter material, the lack of separation is consistent with batch uptake (D_w) measurements that showed essentially identical retention behavior ($\alpha_{\text{Eu/Gd}} = 0.97$ at 0.25 M nitric acid; $\alpha_{\text{Eu/Gd}} = 0.92$ at 0.30 M nitric acid) for the two ions over a range of concentrations.

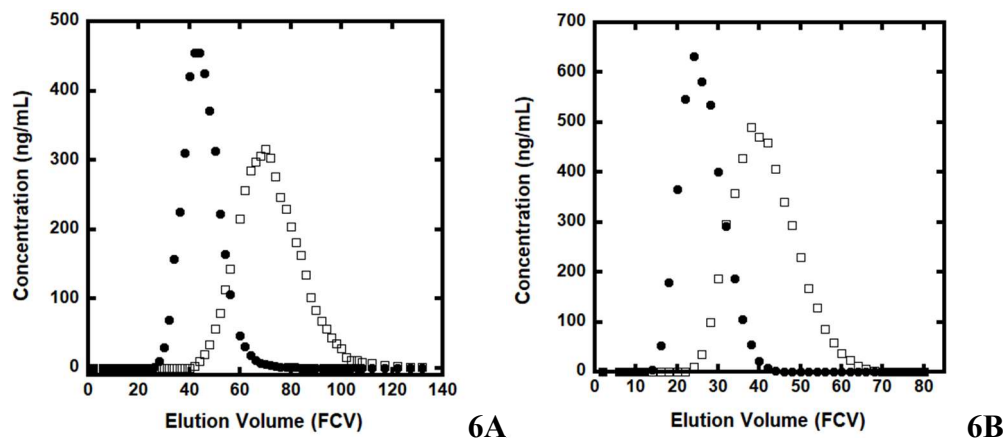


Figure 4.6.A-B: (A) Separation of Eu(III) and Gd(III) on a column (0.90 mL bed volume) containing 20% (w/w) HDEHP-loaded Amberchrom CG-71m resin. (50-100 μm particle size; mobile phase = 0.13 M HNO_3); (•)Eu; (o) Gd. (B) Separation of Eu(III) and Gd(III) on a column (0.90 mL bed volume) containing Ln resin (40% (w/w) HDEHP-loaded Amberchrom CG-71m resin; (50-100 μm particle size; mobile phase = 0.30 M HNO_3); (•)Eu (o) Gd.

In an effort to put the improvement arising from reduced support loading into perspective, the elution behavior of Eu(III) and Gd(III) was also examined on the smallest particle size Ln resin commercially available, comprising 20-50 μm particles of Amberchrom CG-71m resin fully-loaded (40% w/w) with HDEHP. Figure 4.7 shows the results obtained for elution of the two ions using 0.30 M HNO_3 as the mobile phase. Resolution (0.91) comparable to that observed for the larger particle size, “lightly loaded” resin was observed, despite a somewhat greater column efficiency ($N=54$). Stated another way, in this instance, reduced support loading has the same effect as decreasing the particle size of the support. We note, however, that the small particle size material requires the application of pressure to the column to maintain a satisfactory flow rate (*ca.* 1.5 $\text{mL}/\text{cm}^2 \cdot \text{min}$).

In effort obtain the greatest resolution between Eu and Gd, small particle resin was impregnated to 20% (w/w) HDEHP. Unfortunately, the resulting elution, shown in Figure 4.8,

was unexpected. The resolution obtained, 0.76, is not an improvement over the small particle Ln resin nor the large particle 20% (w/w) HDEHP. Ultimately, should the interested reader wish to obtain an improved separation, simply decreasing the support particle size would have the greatest effect.

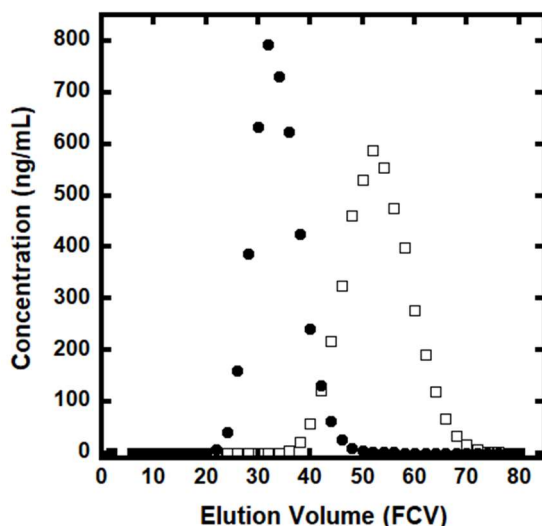


Figure 4.7: Separation of Eu(III) and Gd(III) on a column (0.90 mL bed volume) containing small particle size (20-50 μm) Ln resin (40% w/w HDEHP on Amberchrom CG-71m), mobile phase = 0.30 M HNO_3 . (•)Eu; (◻) Gd.

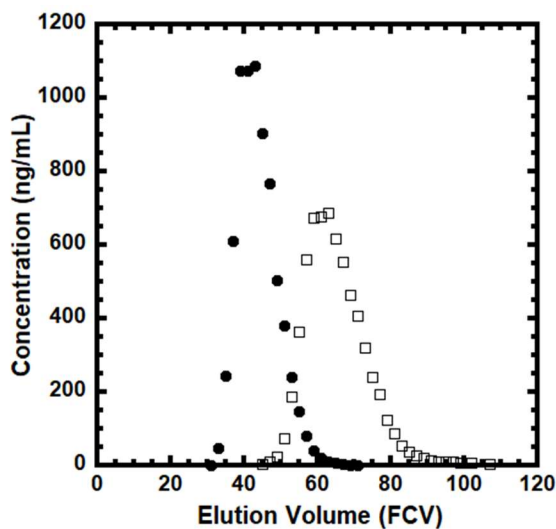


Figure 4.8: Separation of Eu(III) and Gd(III) on a column (0.90 mL bed volume) containing small particle size (20-50 μm) 20% w/w HDEHP on Amberchrom CG-71m, mobile phase = 0.127 M HNO_3 . (•)Eu (◻) Gd.

4.4 Conclusions

The results presented here not only illustrate the beneficial effects of reduced support loading on the quality of metal ion separations possible with EXC, but also demonstrate clearly the importance of understanding the pore structure of the support in developing new extraction chromatographic materials. Although our initial efforts have focused on the separation of trivalent lanthanides, the potential utility of “lightly loaded” sorbents is by no means confined to this separation. Indeed, a number of radionuclide separations of interest in nuclear medicine,⁵⁴ among other areas, could benefit from the availability of more efficient extraction chromatographic resins. Obviously, the reduced capacity resulting from decreased loading represents a potential drawback of these materials in certain applications. This capacity reduction may be of no consequence in many tracer-level separations, however. Of course, an ideal extraction chromatographic sorbent would combine high capacity and high efficiency, and work to develop such materials is now underway in this laboratory.

4.5 References

1. E.P. Horwitz, M.L. Dietz, D.E. Fisher. (1991). Separation and preconcentration of strontium from biological, environmental, and nuclear waste samples by extraction chromatography using a crown ether. *Anal. Chem.*, 63, 522-525.
2. E.P. Horwitz, M.L. Dietz, R. Chiarizia, H. Diamond, A.M. Essling, D. Graczyk. (1992). Separation and preconcentration of uranium from acidic media by extraction chromatography. *Anal. Chim. Acta.* 266, 25-37.
3. E.P. Horwitz, R. Chiarizia, M.L. Dietz, H. Diamond, D.M. Nelson. (1993). Separation and preconcentration of actinides from acidic media by extraction chromatography. *Anal. Chim. Acta.*, 281, 361-372.
4. E.P. Horwitz, M.L. Dietz, S. Rhoads, C. Felinto, N.H. Gale, J. Houghton. (1994). A lead-selective extraction chromatographic resin and its application to the isolation of lead from geological samples. *Anal. Chim. Acta.*, 292, 263-273.
5. E.P. Horwitz, M.L. Dietz, R. Chiarizia, H. Diamond, S.L. Maxwell III, M.R. Nelson. (1995). Separation and preconcentration of actinides by extraction chromatography using a supported

liquid anion exchanger: Application to the characterization of high-level nuclear waste solutions. *Anal. Chim. Acta.*, 310, 63-78.

6. E.P. Horwitz, R. Chiarizia, M.L. Dietz. (1997). DIPEX: A new extraction chromatographic material for the separation and preconcentration of actinides from aqueous solution. *React. Funct. Polym.*, 33, 25-36.
7. C.A. Hawkins, Md. A. Momen, M.L. Dietz. (2018). Application of ionic liquids in the preparation of extraction chromatographic materials for metal ion separations: Progress and prospects. *Sep. Sci. Technol.* 53 1820-1833.
8. K. Rama Swami, R. Kumaresan, K.A. Venkatesan, M.P. Antony. (2017). Synergic extraction of Am(III) and Eu(III) in *N,N*-dioctyl-2-hydroxyacetamide-*bis*(2-ethylhexyl) phosphoric acid solvent system. *J. Mol. Liquids.*, 232, 507–515.
9. H.O. Fourie, J.P. Ghijssels. (1969). Radiostrontium in biological material: A precipitation and extraction procedure eliminating the use of fuming nitric acid. *Health Phys.*, 17, 685–689.
10. R.D. Ibbett. (1967). The determination of strontium-90 in environmental materials by ion exchange and preferential chelation techniques. *Analyst*, 92, 417–422.
11. J.A. Drader, L. Zhu, P. Smith, K. McCann, S. Boyes, J.C. Braley. (2016). Assessment of monoamide extractants and solid supports as new extraction chromatographic materials. *Sep. Purif. Technol.*, 163, 352-356.
12. S. Bao, Y. Tang, Y. Zhang, L. Liang. (2016). Recovery and separation of metal ions from aqueous solutions by solvent-impregnated resins. *Chem. Eng. Technol.* 39 1377-1392.
13. N. Kabay, J.L. Cortina, A. Trochimczuk, M. Streat. (2010). Solvent impregnated resins (SIRs) – Methods of preparation and their applications. *React. Funct. Polym.*, 70, 484-496.
14. A. Zhang, C. Chen, Z. Chai, M. Kumagai. (2008). SPEC Process III. Synthesis of a macroporous silica-based crown ether-impregnated polymeric composite modified with 1-octanol and its adsorption capacity for Sr(II) ions and some typical co-existent metal ions. *Adsorpt. Sci. Technol.*, 26 705-720.
15. Y. Wei, M. Kumagai, Y. Takashima, G. Modolo, R. Odoj. (2000). Studies on the separation of minor actinides from high-level wastes by extraction chromatography using novel silica-based extraction resins. *Nucl. Technol.*, 132, 413-423.
16. M.L. Dietz, “Recent progress in the development of extraction chromatographic methods for radionuclide separation and pre-concentration”, In *Radiochemical methods in interdisciplinary research: Fundamentals in cutting-edge applications*. C.A. Laue and K.L. Nash (Eds.), ACS Symposium Series, Vol. 868, American Chemical Society, Washington, DC, 2003, p. 161-176.
17. D. Muraviev, I. Ghantous, M. Valiente. (1998). Stabilization of solvent impregnated resin capacities by different techniques. *React. Funct. Polym.*, 38, 259-268.

18. S.D. Alexandratos, K.P. Ripperger. (1998). Synthesis and characterization of high-stability solvent-impregnated resins. *Ind. Eng. Chem. Res.*, *37*, 4756-4760.
19. Md. A. Momen, M.L. Dietz. (2019). High-capacity extraction chromatographic materials based on polysulfone microcapsules for the separation and preconcentration of lanthanides from aqueous solution. *Talanta*, *197*, 612-621.
20. M. Kaminski, G. Sandi, M. Dietz, A. Park. (2020). Optimization of a tandem ion exchange—Extraction chromatographic scheme for the recovery of strontium from raw urine. *Sep. Sci. Technol.*, *55*, 176-185.
21. V.H. Grosse-Ruyken, J. Bosholm. (1964). Partition chromatography of rare earths with *bis*(2-ethylhexyl)phosphoric acid. I. Effect of working conditions on the separation performance of the column. *J. Prakt. Chem.*, *4*, 79-87.
22. R.J. Sochacka, S. Siekierski. (1964). Reversed-phase partition chromatography with di-(2-ethylhexyl) orthophosphoric acid as the stationary phase. Part I. Separation of rare earths. *J. Chromatogr.*, *16*, 376-384.
23. S. Siekierski, R.J. Sochacka. (1964). Reversed-phase partition chromatography with di-(2-ethylhexyl) orthophosphoric acid as the stationary phase. Part II. Factors affecting the height of the plate. *J. Chromatogr.*, *16*, 385-395.
24. E. Herrmann. (1968). Contribution to the separation of rare earths by extraction chromatography with di(2-ethylhexyl)phosphoric acid (HDEHP). I. Silica gel as a support material for the stationary phase. *J. Chromatogr.*, *38*, 498-507.
25. E.P. Horwitz, C.A.A. Bloomquist, D.J. Henderson. (1969). Extraction chromatography of californium, einsteinium, and fermium with di(2-ethylhexyl)orthophosphoric acid. *J. Inorg. Nucl. Chem.*, *31*, 1149-1166.
26. E.P. Horwitz, C.A.A. Bloomquist. (1972). Preparation, performance, and factors affecting band spreading of high efficiency extraction chromatographic columns for actinide separations. *J. Inorg. Nucl. Chem.*, *34*, 3851-3871.
27. R.E. Louis, G. Duyckaerts. (1984). Some parameters affecting the extraction chromatographic performance of TBP-impregnated macroporous XAD-4 columns for Am(III)-Eu(III) separations. *J. Radioanal. Chem.*, *81*, 305-315.
28. M.M. Abdel Badei, S.M. Khalifa, H.A. Dessouky, H.M. Aly, H.F. Aly. (1989). Extraction chromatographic performance of uranium using XAD-4 loaded with di-2-ethylhexylphosphoric acid and nitrate solution. *Isotopenpraxis*, *25*, 211-214.
29. J.A. Partridge, R.C. Jensen, R. C. (1969). Purification of di-(2-ethylhexyl)phosphoric acid by precipitation of copper (II) di-(2-ethylhexyl)phosphate. *J. Inorg. Nucl. Chem.*, *31*, 2587–2589.
30. E.P. Horwitz, M.L. Dietz. (1990). Concentration and separation of actinides from urine using a supported bifunctional organophosphorus extractant. *Anal. Chim. Acta*, *238*, 263–271.

31. E.P. Horwitz, R. Chiarizia, M.L. Dietz. (1992). A novel strontium-selective extraction chromatographic resin. *Solv. Extr. Ion. Exch.*, 10, 313–336.
32. McDowell, W. J. (1971). Equilibria in the system: di(2-ethylhexyl)phosphoric acid-benzene-water-alkali (hydroxide, nitrate). *Journal of Inorganic and Nuclear Chemistry*, 33, 1067–1079.
33. A. Arias, I. Saucedo, R. Navarro, V. Gallardo, M. Martinez, E. Guibal. (2011). Cadmium(II) recovery from hydrochloric acid solutions using Amberlite XAD-7 impregnated with a tetraalkyl phosphonium ionic liquid. *React. Funct. Polym.*, 71, 1059–1070.
34. J.W. Dolan. (2002). Resolving minor peaks. *LC •GC North America*, 20, 594-598.
35. J.W. Dolan. (2002). Peak tailing and resolution. *LC •GC Asia Pacific*, 5, 14-20.
36. T.B. Pierce, P.F. Peck. (1962). Use of di-(2-ethylhexyl) orthophosphoric acid for the separation of the elements lanthanum-gadolinium by reverse phase partition chromatography. *Nature*, 194, 84.
37. T.B. Pierce, P.F. Peck. (1962). Use of di-(2-ethylhexyl) orthophosphoric acid for the separation of the rare earths by reverse phase partition chromatography. *Nature*, 194, 597.
38. E.P. Horwitz, D.R. McAlister, M.L. Dietz. (2006). Extraction chromatography versus solvent extraction: How similar are they? *Sep. Sci. Technol.*, 41, 2163-2182.
39. D.R. McAlister, E.P. Horwitz. (2007). Characterization of extraction chromatographic materials containing bis(2-ethyl-1-hexyl)phosphoric acid, 2-ethyl-1-hexyl(2-ethyl-1-hexyl)phosphonic acid, and bis(2,4,4-trimethyl-1-pentyl)phosphinic acid. *Solv. Extr. Ion Exch.*, 25, 757-769.
40. K.L. Nash, G.R. Choppin. (1997). Separations chemistry for actinide elements: Recent developments and historical perspective. *Sep. Sci. Technol.*, 32, 255-274.
41. C. Klug, R. Sudowe. (2013). A novel extraction chromatography resin for trivalent actinides using 2,6-bis(5,6-diisobutyl-1,2,4-triazine-3-yl)pyridine. *Sep. Sci. Technol.*, 48, 2567-2575.
42. A. Vesterlund, H. Ramebäck. (2019). Avoiding polyatomic interferences in measurements of lanthanides in uranium material for nuclear forensic purposes. *J. Radioanal. Nucl. Chem.*, 321, 723-731.
43. A. Pitois, L. A. de Las Heras, M. Betti. (2008). Determination of fission products in nuclear samples by capillary electrophoresis-inductively coupled plasma mass spectrometry (CE-ICP-MS). *Int. J. Mass Spectrom.*, 270, 118-126.
44. A. Leoncini, J. Huskens, W. Verboom. (2017). Ligands for *f*-element extraction used in the nuclear fuel cycle. *Chem. Soc. Rev.*, 46, 7229-7273.
45. H.H. Dam, D.N. Reinhoudt, W. Verboom. (2007). Multicoordinate ligands for actinide/lanthanide separations. *Chem. Soc. Rev.*, 36, 367-377.

46. A. Bhattacharyya, P.K. Mohapatra. (2019). Separation of trivalent actinides and lanthanides using various 'N', 'S' and mixed 'N,O' donor ligands: A review. *Radiochim. Acta*, 107, 931-949.
47. E.R. Bertelsen, G. Deodhar, K.T. Kluherz, M. Davidson, M.L. Adams, B.G. Trewyn, J.C. Shafer. (2019). Microcolumn lanthanide separation using bis-(2-ethylhexyl)phosphoric acid functionalized ordered mesoporous carbon materials. *J. Chrom. A*, 1595, 248-256.
48. R.F. Payne, S.M. Schulte, M. Douglas, J.I. Friese, O.T. Farmer III, E.C. Finn. (2011). Investigation of gravity lanthanide separation chemistry. *J. Radioanal. Nucl. Chem.*, 287, 863-867.
49. A.M. Johnsen, C.Z. Soderquist, B.K. McNamara, D.R. Fisher. (2013). A non-aqueous reduction process for purifying ^{153}Gd produced in natural europium targets. *Appl. Radiat. Isotopes*, 82, 158-165.
50. Q. Wang, K. Tsunoda, H. Akaiwa. (1997). Mutual separation of rare earth elements by extraction chromatography using bis(1,1,3,3-tetramethylbutyl)phosphinic acid as a stationary phase. *Anal. Sci.*, 13, 153-156.
51. K. Kondo, M. Oguri, M. Matsumoto. (2013). Novel separation of samarium, europium, and gadolinium using a column packed with microcapsules containing 2-ethylhexylphosphonic acid mono-2-ethylhexyl ester. *Chem. Eng. Trans.*, 32, 919-924.
52. L. Jelinek, Y. Wei, T. Arai, M. Kumagai. (2007). Selective Eu(III) electro-reduction and subsequent separation of Eu(II) from rare earths(III) via HDEHP impregnated resin. *Solv. Extr. Ion Exch.*, 25, 503-513.
53. S.-C. Li, S.-C. Kim, C.-S. Kang, C.-J. Kim, C.-J. Kang. (2018). Separation of samarium, europium, and gadolinium in high purity using photochemical reduction-extraction chromatography. *Hydrometallurgy*, 178, 181-187.
54. M.G. Ferrier, V. Radchenko, D.S. Wilbur. (2019). Radiochemical aspects of alpha-emitting radionuclides for medical applications. *Radiochim. Acta*, 107, 1065-1085.

CHAPTER 5:

INCREASING COLUMN EFFICIENCY IN EXTRACTION CHROMATOGRAPHY MATERIALS THROUGH STAGNANT PORE PLUGGING

5.1 Introduction

Numerous extraction chromatographic materials have been developed for a wide range of applications, particularly in the field of radiochemical separations.¹⁻¹⁰ One of the most difficult challenges is separating metal ions of similar chemical and physical makeup. No region of the periodic table better illustrates this than the *f*-elements. Known for their similar ionic radii and oxidation state, these metal ions remain a challenge to separate not only in extraction chromatographic applications, but in liquid-liquid and ion-exchange separations as well.¹¹⁻¹⁴

Several commercial extraction chromatographic resins (manufactured by EiChrom Technologies, LLC (Lisle, IL)), consist of an inert support (*e.g.* Amberchrom CG-71m) impregnated with a suitable extractant,¹⁵ which are designed to be selective for these families of metal ions. The DGA resin, for example, is used to extract both lanthanides and actinides while the Ln and Ac resins are selective to lanthanides and actinides, respectively. To ensure adequate metal ion uptake capacity, the pores of the support are generally filled nearly to capacity with extractant (40% (%w/w) loading).¹⁶⁻¹⁸ Unfortunately, this near-capacity filling produces long metal ion diffusion paths within the resin, reducing column efficiency. The modest column efficiency of the material is reflected in their inadequate performance in certain important applications. For example, Gharibyan *et al.* attempted to separate Am³⁺ from Cm³⁺ using seven different EiChrom resins, but observed nearly identical elution behavior for the two ions on all resins.¹⁹ Similarly, Bertelsen *et al.* attempted to separate Eu³⁺ from Nd³⁺ using EiChrom Ln resin but observed almost complete overlap between the two during elution studies.²⁰

Column efficiency, expressed below as the height equivalent to a theoretical plate (HETP), is governed by several factors, expressed mathematically in the van Deemter Equation:

$$\text{HETP} = A + B/u + (C_m + C_s)u \quad (5.1)$$

where A, B, C_s, C_m, and u represent the eddy diffusion of the analyte between particles, its axial diffusion within the column, its mass transfer rate between the mobile and stationary phases, and the mobile phase velocity, respectively.²¹

Commercial supports possess a complex system of micro- (<2 nm), meso- (2-50 nm), and macropores (>50 nm),²² resulting in an essentially infinite number of paths for analyte diffusion and thus, sources of inefficiency. As shown in Chapter 4 (Figure 4.2), the micropores are mostly found within the larger meso- and macropores. During the filling of the empty support with extractant, the micropores are filled first, with the meso- and macropores acting as transport pores.²³ Given the location of the micropores, metal ions trapped within would almost certainly cause band broadening during elution. Blocking these pores within the support should therefore decrease this source of band broadening, provided that the blocking reagent (*i.e.* filler) is carefully chosen. In attempting to fill the mesoporous materials MCM-41 and SBA-15 with C₆mim⁺Tf₂N⁻, C₆mim⁺CF₃SO₃⁻, and C₆mim⁺OAc⁻, for example, Heinze *et al.* noted the formation of droplets of the hydrophobic C₆mim⁺Tf₂N⁻ in the presence of the hydrophilic support surface due to the preference of the IL cation for interaction with the IL anion rather than the silica support surface. In contrast, hydrophilic ILs tended to form parallel monolayers on the silica surface.²⁴ Clearly then, a reagent for pore blocking should not react with the support, but it should not be completely incompatible with it either. In addition, given the volume of aqueous solution passed through during column during use (*e.g.* free-column volume (FCV) determination, elution profile testing, etc.), the filler should be water-immiscible.

Once a suitable filler has been chosen, the loading level at which the micropores are completely filled (or nearly so) must be determined. As discussed in Chapter 4, Arias *et al.* measured the surface area of Amberlite XAD-7 loaded with varying amounts of Cyphos 101®. The changes in slope of the surface area vs. loading plot were attributed to the loading levels at which the pores of size <40 Å, 40-200 Å, and >200 Å were filled.²⁵ This information, coupled with our own observations (also described in Chapter 4) provides a clear map of the bead interior, from which the appropriate loading with filler can be determined.

In this chapter, we build on the results presented in Chapter 4. In particular, we examine the effect of an inert, pore-blocking reagent, selected to maximize its compatibility with the support and minimize its water solubility, on the properties of an extraction chromatographic resin loaded to various levels with *bis*(2-ethylhexyl)phosphoric acid (HDEHP). The utility of the resultant EXC materials in the separation of trivalent lanthanides is then evaluated.

5.2 Experimental

5.2.1 Materials

All water was obtained from a Milli-Q2 system and exhibited a specific resistance of at least 18 MΩ-cm. HDEHP, 1-dodecanol, 1-bromododecane, 1-bromohexadecane, 1-methylimidazole, lithium tetrafluoroborate (LiBF₄), silver nitrate, cetyl alcohol, eicosane, dimethylammonium dimethylcarbamate (DIMCARB), formic acid (HCOOH), *N,N*-dimethylethanolamine (DMEA) and polytetrahydrofuran (PTHF) 250 were obtained from Sigma-Aldrich (St. Louis). Lithium *bis*[(trifluoromethyl)sulfonyl]imide (Li⁺Tf₂N⁻) was purchased from TCI America (Portland, OR). 1-ethyl-3-methylimidazolium *bis*(trifluoromethanesulfonyl)imide (C₂mim⁺Tf₂N⁻) was purchased from Covalent Associates Inc.

(Woburn, MA). Methanol (ACS Grade), hexanes (ACS Grade), and nitric acid (Optima) were purchased from Fisher Scientific (Hampton, NH). Ethanol (200 proof) was purchased from KOPTEC (King of Prussia, PA). Trihexyltetradecylphosphonium *bis*(trifluoromethanesulfonyl)imide ($P_{66614}^{+}Tf_2N^{-}$) and its chloride ($P_{66614}^{+}Cl^{-}$), and tetrafluoroborate ($P_{66614}^{+}BF_4^{-}$) analogues were a generous gift from Cytec Industries (Woodland Park, NJ). The *N,N*-dimethylethanolamine formate was synthesized according to published procedures.²⁶ Briefly, equimolar amounts of DMEA and HCOOH were mixed for one hour in an ice bath. The $C_{12}mim^{+}Tf_2N^{-}$, $C_{12}mim^{+}BF_4^{-}$, and $C_{16}mim^{+}Tf_2N^{-}$ were synthesized *via* a two-step procedure involving quaternization of the methylimidazole with 1-bromododecane or 1-bromohexadecane to yield the halide form of the IL ($C_nmim^{+}Br^{-}$), followed by anion metathesis to provide the desired (*e.g.*, Tf_2N^{-}) product.^{27,28} The resulting IL was water washed until no precipitate (AgBr) was observed upon mixing the water wash with silver nitrate. Its identity was confirmed by ¹H-NMR. Ln resin and Pre-filter (20-50 μ m) material were purchased from the Eichrom (Lisle, IL). (Note that the Pre-filter resin is simply a small particle analogue of Amberchrom CG-71m). Amberchrom CG-71m was purchased from Sigma and was purified as described previously. Briefly, the Amberchrom CG-71m or Pre-filter resin was contacted with deionized water for 30 minutes with occasional swirling and then removed. The resin was then contacted with methanol, which was allowed to flow through the resin under gravity. The process was repeated twice more until the methanol wash was clear and colorless and the water wash was pH ≤ 7 . The ^{152/154}Eu and ¹³⁷Cs radiotracers were purchased from Eickert and Ziegler (Berlin, Germany). Europium (III) nitrate pentahydrate, neodymium (III) nitrate hexahydrate and gadolinium (III) nitrate hexahydrate were trace metal grade (99.9% pure) and purchased

from Sigma-Aldrich. Elution profiles were obtained on BioRad Econo-Column chromatography columns (Hercules, CA) with dimensions of 0.5 x 5 cm or 0.5 x 10 cm.

5.2.2 Instrumentation

The radiotracers were assayed using a Perkin-Elmer Model 2480 Automatic Gamma counter. Inactive metal ions were assayed using a Shimadzu Model 2030 Inductively-Coupled Plasma-Mass Spectrometer (ICP-MS) 2030. Surface area determinations were conducted using a Micromeritics ASAP 2020 Plus. $^1\text{H-NMR}$ spectra were obtained with a Bruker DPX-300 NMR spectrometer equipped with a broad-band optimized BBO probe operating a frequency of 300.13 MHz and referenced against TMS. All NMR spectra were recorded with Bruker Topspin (version 3.5 pl7) software. All NMR experiments were performed at 25°C. The phosphorus profile of the materials was determined using a Hitachi Model S4800 field emission scanning electron microscope (SEM) with an energy dispersive x-ray spectrometer (EDX). SEM-EDX experiments were performed on the [DMEA][HCOO] resins loaded with 10% (%w/w) HDEHP. To mount the sorbents in the SEM column, a cylindrical graphite pole was used. One end of the pole was formed into the shape of a trapezium (Figure 5.1), on which two-ton adhesive from Devcon (Danvers, MA) was applied and allowed to dry for ~30 minutes. The resin was then sprinkled on top of the trapezium and allowed to settle overnight. The following day, the resin-adhesive surface was cut in half to expose the bead interior, thereby permitting examination of the cross-section of the bead under SEM. The exposed interior was then carbon-coated to ensure surface conductivity.



Figure 5.1: Example graphite, trapezium-shaped pole.

5.2.3 Methods

5.2.3.1 SPP Resin Preparation

Beads of pure Amberchrom CG-71m or Pre-filter resin were slurried with methanol and then mixed with the desired amount of filler as a solution in methanol. The mixtures were then shaken for 24 hours, after which the methanol was removed using rotary evaporation at 55 °C under vacuum (dry impregnation) to yield the filler-loaded sorbent. $C_{12}mim^+Tf_2N^-$, $P_{666,14}^+Tf_2N^-$, $P_{666,14}^+BF_4^-$, $C_{12}mim^+BF_4^-$, eicosane, DIMCARB, and [DMEA][HCOO] were loaded to the full available volume of the resin. In addition, a series of other resins were prepared in which the support was filled to various levels. For example, support was filled with $C_{16}mim^+Tf_2N^-$ to a volume fraction of 0.80. Similarly, the support was filled with either PTHF 250 or cetyl alcohol to a fraction of 0.30 of the total volume. Lastly, 1-dodecanol was used to fill the support to a volume fraction of 0.15. For surface area determinations, HDEHP, PTHF 250, $P_{666,14}^+Cl^-$, and $C_2mim^+Tf_2N^-$ were loaded to various loading levels.

5.2.3.2 Addition of HDEHP to impregnated resins

Beads of Amberchrom CG-71m beads or Pre-filter material (filled to 0.15 volume fraction with 1-dodecanol) were slowly added to a small volume of HDEHP-methanol solution. The methanol was then quickly dried by rotary evaporation at 55 °C with vacuum. Pre-filter material was also loaded to 10% (%w/w) with HDEHP only, also using rotary evaporation at 55 °C with vacuum. Amberchrom CG-71m was used to prepare the remaining resins.

5.2.3.3 Determination of Weight Distribution Ratios

Solid-liquid (weight) distribution ratios (D_w) for Eu^{3+} were measured radiometrically using $^{152/154}\text{Eu}^{3+}$ radiotracer. For Nd^{3+} and Gd^{3+} , inactive neodymium (III) nitrate hexahydrate and gadolinium (III) nitrate hexahydrate solutions were quantified using ICP-MS. Specifically, the uptake of each radiotracer or inactive metal ion from a series of nitric acid solutions by the resins was measured by contacting a known volume (mL) of $^{152/154}\text{Eu}$ -spiked or Gd^{3+} - or Nd^{3+} -spiked acid solutions of appropriate concentration with a known quantity of resin (20-25 mg). The ratio of the aqueous phase volume (mL) to the weight of the chromatographic material (in grams) typically ranged from 40-50. This ratio generally produces an easily measured decrease in the aqueous phase activity or concentration upon contact with the resin. A two-hour contact time was used for equilibration. Following equilibration, an aliquot of aqueous phase was withdrawn from each culture tube and the activity counted or concentration measured.

From the counts or metal ion concentration present in the aqueous phase both before and after contact with the resins, the weight distribution ratios (D_w) of $^{152/154}\text{Eu}^{3+}$, Nd^{3+} , and Gd^{3+} were calculated by using Eqn. 5.2:

$$D_w = [(A_0 - A_f) / A_f] (V/w) \quad (5.2)$$

where A_0 and A_f are the aqueous phase activity (cpm) or concentration before and after equilibration, respectively, w is the mass (g) of the resin, and V is the volume of the aqueous phase (mL).

5.2.3.4 Capacity of the resins

In this work, a solution of cold europium (III) nitrate hexahydrate in dilute nitric acid containing five times the stoichiometric amount of extractant present was prepared and spiked with $^{152/154}\text{Eu}^{3+}$ radiotracer. Each resin was weighed (20-25 mg) into separate test tubes and contacted with 1 mL of this radiotracer solution. After mixing, samples were equilibrated for 24 hours, far longer than the time required for equilibrium. The acid concentration chosen was such that a distribution ratio of 300-400 (corresponding to >99% extraction) was obtained. After equilibration, the aqueous phase was withdrawn and filtered through a fritted plastic column. Assuming the fraction of inactive europium corresponds to the fraction of $^{152/154}\text{Eu}^{3+}$ sorbed, then the capacity of the sorbent (mg Eu/ g of sorbent) can be calculated. Data was obtained for the 10-30% (w/w) HDEHP resins and the commercial resin (40% (w/w) HDEHP).

5.2.3.5 Column preparation and characterization

To pack a column, a small quantity of the resin was slurried in 18 M Ω -cm MilliPore water and transferred to the column. Packing was carried out under flow of gravity. When the resin bed reached the desired height, a small plug of glass wool was added so that the bed would not be disturbed upon sample introduction. Prior to sample introduction, the column was preconditioned with 10 free column volumes (FCVs) of the desired nitric acid solution. Unless otherwise noted, all column runs utilizing 50-100 μm particles carried out as part of studies of the effects of support loading with pore-blocked resins were performed without applied pressure,

corresponding to a flow rate of 1.39 ± 0.08 mL/min·cm². No systematic changes in gravity flow rates were noted upon changes in the level of support loading. All small particle size (20-50 μm) runs were carried out at a flow rate of 1.50 ± 0.05 mL/cm²·min with applied pressure.

The bed density, resin density, stationary phase volume (v_s , the volume of liquid extractant contained in the pores of the support), and mobile phase volume (v_m , the free column volume) were determined using the following methods outlined in Chapter 4. Specifically, the bed density was determined for bed volumes of 0.9 mL and 1.9 mL for the 1- and 2-mL columns, respectively. The resin density was calculated by adding a small quantity of resin to solutions of nitric acid of known density. The resin density matched that of the nitric acid solution when it remained suspended after mixing. The stationary phase volume was calculated from the resin mass, the extractant loading (%w/w), and the extractant density. The mobile phase volume was determined by first equilibrating the column with a concentrated (~1 M) nitric acid solution of known density. A small volume (~5 μL) of ¹³⁷Cs⁺ was then added to the top of the bed. As HDEHP extracts a negligible amount of this monovalent cation,³⁰ it elutes through the column unretained. Individual drops of acid were collected and counted. From the average drop volume and the number of the drop in which cesium nitrate is first detected, and the total elution volume, which corresponds to the mobile phase volume, was determined. All runs were carried out at ambient temperature ($23 \pm 2^\circ\text{C}$).

5.2.3.6 Elution curves of ^{152/154}Eu³⁺ for resin characterization

The elution profiles of ^{152/154}Eu³⁺ on packed beds of resin comprising Amberchrom CG-71m filled to 0.15 volume fraction filled with 1-dodecanol and loaded to 5, 10, 15, 20, and 30% (w/w) HDEHP were determined using BioRad Econo-Columns (0.5 x 5 cm or 0.5 x 10 cm) using dilute HNO₃ as the eluent. Column characteristics (Table 5.1) were determined prior to elution

experiments using the procedures outlined in 5.2.3.4. For the 5, 10, 15, 20, and 30% resins and the commercial Ln (40% w/w) resin, 0.0257 M, 0.045 M, 0.086 M, 0.097 M, 0.17 M HNO₃ and 0.30 M HNO₃ were used as the eluents, respectively. Eluent volumes of two FCVs were collected, with 100 μL of each subsequently sampled for gamma counting. The theoretical plate count (N) and height (H), tailing factor (T_f), peak asymmetry (A_s), and resolution (when a second ion is present) were calculated from the resultant elution plots according to Equations 5.3, 5.4, 5.5, 5.6, and 5.7 respectively.

$$N = 5.54 * \left(\frac{V_R}{W_{0.5h}} \right)^2 \quad (5.3)$$

$$H = \frac{L}{N} \quad (5.4)$$

$$T_f = \frac{a}{2b} \quad (5.5)$$

$$A_s = \frac{c}{d} \quad (5.6)$$

$$R_s = 2 (V_{R2} - V_{R1}) / (w_{b1} + w_{b2}) \quad (5.7)$$

where V_R is the number of FCVs at which the metal ion concentration reaches a maximum, $w_{0.5h}$ is the peak width at half-height, L is the column length, a is the full peak width and b is the front half-width at 5% of the peak height, c is the width of the front half of the peak and d is the width of the back half of the peak at 10% of the peak height, and R_s is the chromatographic peak resolution, V_R is the retention time, and w_b is the peak width at baseline.

Table 5.1 Characteristics of prepared and commercial Ln resins and packed columns

Bulk Materials 1-dodecanol used	5% HDEHP-loaded SPP resin	10% HDEHP-loaded SPP resin	10% HDEHP-loaded SPP resin	15% HDEHP-loaded SPP resin	20% HDEHP-loaded SPP resin	30% HDEHP-loaded SPP resin	Ln resin (40% HDEHP)
Stationary Phase	HDEHP	HDEHP	HDEHP	HDEHP	HDEHP	HDEHP	HDEHP
Support	Amberchrom CG-71m	Amberchrom CG-71m	EiChrom Pre-filter	Amberchrom CG-71m	Amberchrom CG-71m	Amberchrom CG-71m	Amberchrom CG-71m
Particle Diameter	75 μm	75 μm	35 μm	75 μm	75 μm	75 μm	75 μm
Extractant Loading	5%	10%	10%	15%	20%	30%	40%
Density of extractant-loaded beads	1.17	1.13	1.21	1.12	1.12	1.11	1.14
Packed columns							
V_s , mL/mL of bed	0.01324	0.02829	0.06383	0.04519	0.05059	0.09815	0.15
Bed Density (g/mL)	0.2840	0.3033	0.3422	0.3230	0.2712	0.3898	0.36
V_m , mL/mL of bed (also FCV)	0.672	0.690	1.14	0.694	0.686	0.663	0.69
V_s/V_m	0.020	0.041	0.056	0.065	0.074	0.148	0.217
Capacity, mg Eu/mL of bed	N/A	3.50	N/A	5.10	6.25	14.35	11.04

5.2.3.7 Elution curves of cold Eu^{3+} , Nd^{3+} , and Gd^{3+}

After column conditioning with designated eluents as described in 5.2.3.4, $\sim 10 \mu\text{L}$ each of solutions of Eu^{3+} (2.5 mM), Nd^{3+} (2.3 mM), and Gd^{3+} (2.5 mM) were introduced at the top of the column, depending on the separation, and eluted using the appropriate acid. The eluent was collected in 1-2 FCV fractions and assayed using the ICP-MS. All runs were carried out at ambient temperature ($23 \pm 2^\circ\text{C}$).

5.3 Results and Discussion

In initial experiments, so-called “outside-in stripping” (first described by Momen³¹) was carried out in an effort to prepare a support whose porous region is confined largely to the near-surface areas of the support beads. In the work of Momen, polypropylene glycol (PPG) 400 was used as the filler, and completely-filled PPG 400 beads were stripped with hexanes. Because the

support is hydrophilic while hexane is hydrophobic, it would be expected that hexane would not be able to penetrate the interior of the support.³² Thus, the PPG 400 filler should be stripped only from the outermost regions of the filled support. Indeed, this was observed. The near-surface space once occupied by the PPG 400 was then filled with HDEHP to a loading level of ~20% (w/w). Concerns over interaction between PPG 400 and HDEHP was assuaged by SEM-EDX analysis, which showed that phosphorus (*i.e.* the extractant) was present only in the near-surface regions of the impregnated support (Figure 5.2).³¹ Thus, even though PPG 400 and HDEHP are completely miscible, they are not interacting within the support. Also, as hoped, minimal loss of filler due to its water-miscibility was observed, as apparently the filler is not exposed to the aqueous elution solvent. Finally, and also as hoped, the resulting extraction efficiency substantially increased (N = 43) compared to that of EiChrom Ln resin (N = 25).

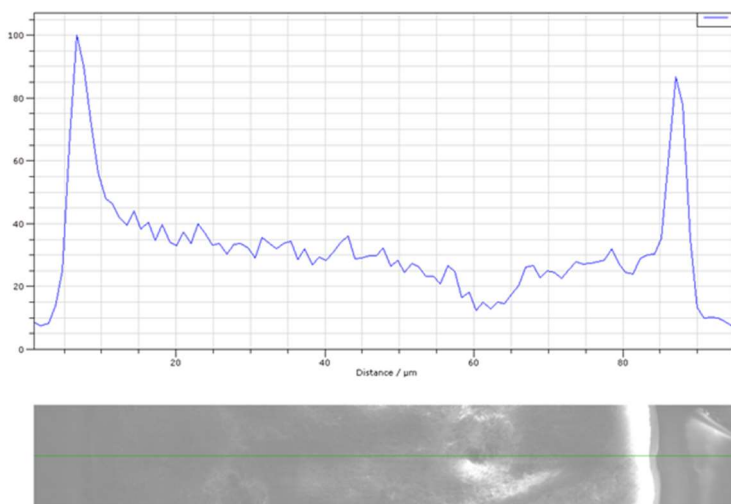


Figure 5.2: Phosphorus profile obtained using SEM-EDX for a PPG 400-loaded, 20% (w/w) HDEHP resin.

On the downside, initial studies suggested that the process for stripping the PPG 40 filler is only poorly reproducible. That is, removal of the filler in a consistent manner is not straightforward. For this reason, other fillers, stripping solvents, and stripping protocols were

examined. As a first step in these studies, the suitability of ionic liquids as fillers was examined. In principle, their extraordinary tunability could make them useful in this application. In particular, $C_n\text{mimTf}_2\text{N}$ ILs are water-insoluble and their viscosity equals or exceeds that of PPG 400, thus minimizing potential interaction with HDEHP.^{33,34} Unfortunately, these ILs are hexane-immiscible, and thus require a more polar solvent to strip. With this in mind, various ethanol-hexane mixtures were employed to strip a resin containing $C_n\text{mim}^+\text{Tf}_2\text{N}^-$ ILs as the filler. Figure 5.3 shows the results obtained for two trials in which beads loaded with $C_{12}\text{mim}^+\text{Tf}_2\text{N}^-$ were stripped with a 12% (v/v) ethanol in hexane solution. As can be seen, the amount of filler stripped increased as a function of contact time for one trial (as expected), but inexplicably decreased during a second trial with an identically prepared set of beads. To determine if this irreproducible behavior is simply a characteristic of $C_{12}\text{mim}^+\text{Tf}_2\text{N}^-$, several other ILs - $P_{66614}^+\text{Tf}_2\text{N}^-$, $P_{66614}^+\text{BF}_4^-$, and $C_{12}\text{mim}^+\text{BF}_4^-$ - were next evaluated using the same bead preparation and stripping procedure. Unfortunately, the resins prepared using either $P_{66614}^+\text{Tf}_2\text{N}^-$ or $P_{66614}^+\text{BF}_4^-$ as the filler floated, making them impractical. Along these same lines, $C_{12}\text{mim}^+\text{BF}_4^-$ -loaded resin was found to be physically unstable, as the IL readily leached from it upon passage of aqueous phase.

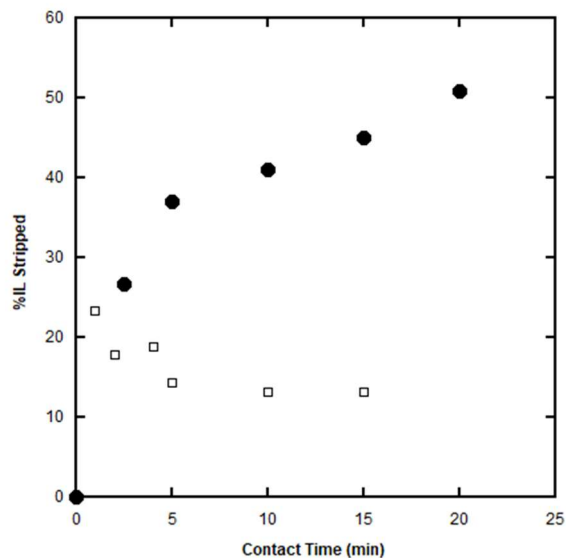


Figure 5.3: Stripping of ionic liquid from a C₁₂mimTf₂N-impregnated resin as a function of contact time with an ethanol (12 %v/v) solution in hexane.

These results led us to revisit a hexane-miscible filler. This time, however, a filler was sought that would solidify in the pores of the support, thereby minimizing any possible interaction with the extractant. Eicosane (C₂₀H₄₂), a waxy material at room temperature, was therefore evaluated as a filler. Unfortunately, eicosane deposited largely on the exterior of the beads rather than in the pores. Apparently, it is simply too hydrophobic to be taken into the interior of such a hydrophilic resin.

Distillable ionic liquids (DILs) were next considered as fillers. In contrast to conventional fillers, which require a strip solution for their removal, beads impregnated with DILs can be stripped using only heat and reduced pressure, such as can be achieved with a rotary evaporator. Of course, this approach will work only if the filler does not evaporate with the impregnation solvent. Unfortunately, even with an easily evaporated impregnation solvent, methylene chloride (boiling point = 39.6 °C at ambient pressure), the first distillable IL used, dimethylammonium dimethyl carbamate (DIMCARB; boiling point = 60 °C at ambient pressure)

co-evaporated, and therefore could not be used further. The second distillable IL used, *N,N*-dimethylethanolammonium formate, had greater thermal stability^{35,36} than DIMCARB, and did not co-evaporate with the CH₂Cl₂ during support impregnation. Unfortunately, following the addition of HDEHP, SEM-EDX analysis showed that phosphorus is distributed throughout the bead, rather than being confined to the near-surface regions (Figure 5.4). Because this and our other attempts at the “outside-in” approach to support preparation did not yield the desired results, alternate methods of resin preparation were pursued.

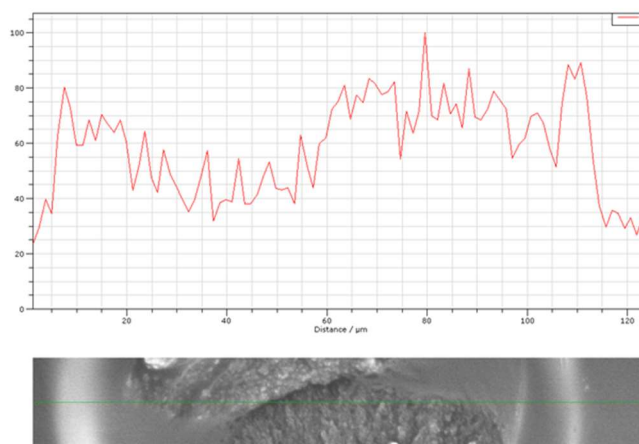


Figure 5.4: Phosphorus profile obtained using SEM-EDX [DHEA][HCOO] resin impregnated with 10% (%w/w) HDEHP

As discussed in some detail in Chapter 4 and elsewhere,²⁵ the pore structure of commercial solid supports such as Amberchrom CG-71m is complex. Despite this, surface area measurements carried out at various levels of impregnation enable one to determine where the various types of pores present become filled. As shown in Figure 5.5, which depicts the effect of PTHF 250 impregnation on the surface area of Amberchrom CG-71m, two points at which the slope changes are readily evident. These correspond to a loading level at which the smallest pores are essentially filled (0.18), while the second (0.30) corresponds to the filling of the

intermediate pores. As an alternative to the “outside-in” method of achieving a readily accessible layer of extractant, at this point an “inside-out” approach, in which extractant would be deposited atop a quantity of filler placed in the least accessible, deep interior pores was investigated.

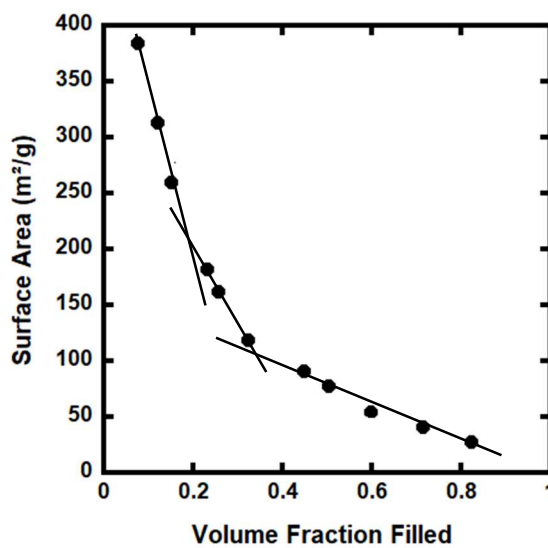


Figure 5.5: Surface Area (m²/g) of PTHF 250-impregnated resins

Work by Momen³¹ has established that PPG 400 was not lost during column elution when employed as a filler. Therefore, a structurally similar, low molecular weight polymer polytetrahydrofuran 250 (PTHF 250) was investigated in this application. In our initial experiment, the empty support was filled to a loading level of 0.30. Unexpectedly, significant loss of this PTHF 250 was observed when it was topped with HDEHP and the resultant resin subjected to water rinsing. In fact, using either a gravimetric method or ¹H-NMR indicates that *ca.* 89% of the filler initially present was lost during column preconditioning. Clearly then, it cannot be assumed that the water-immiscible HDEHP completely covers the filler in this method of support preparation. Therefore, a more water-immiscible filler was required.

Water-immiscible ionic liquids (ILs), specifically short-chain, imidazolium-based ILs (as they have ≤ 5 mM HDEHP solubility³⁷) were therefore evaluated. $C_2mim^+Tf_2N^-$ was thought to be a proper choice, but upon resin preparation and column preconditioning, a significant amount of a water-immiscible liquid, determined by 1H NMR to be the IL, was observed to have leached from the column. It is important to note that although this IL is often regarded as water-immiscible,³⁸ only a few milligrams are present on the column while over 100 mL of aqueous solution are added during the column preparation, preconditioning, and elution process. Clearly then, this IL is simply too water-soluble under the experimental conditions to be used as the filler.

Up to this point, it was known that water-immiscibility and support compatibility were the two most important factors in choosing a filler, but the importance of another factor soon became evident. From Figure 5.6, it can be seen that for a given level of support loading, $P_{666,14}^+Cl^-$ yields a higher measured surface area than either PTHF 250 or $C_2mim^+Tf_2N^-$. As shown in Table 5.2, the viscosity of $P_{666,14}^+Cl^-$ is significantly higher than that of the other two fillers. Apparently, this high viscosity limits access of the filler into the smallest pores of the support. The next filler tested, cetyl alcohol, is water-immiscible, and should be compatible with the support given its hydroxyl functional group. Although it is a solid at room temperature, if heated to 55° C, it is a liquid with a viscosity of only 9.3 cP,³⁹ less than that of either PTHF 250 or $C_2mim^+Tf_2N^-$ at room temperature. Unfortunately, this particular filler loaded to a volume fraction level of 0.30 had a surface area not in agreement (Figure 5.6) with that of either $C_2mim^+Tf_2N^-$ or PTHF 250. Accordingly, it was not used going forward.

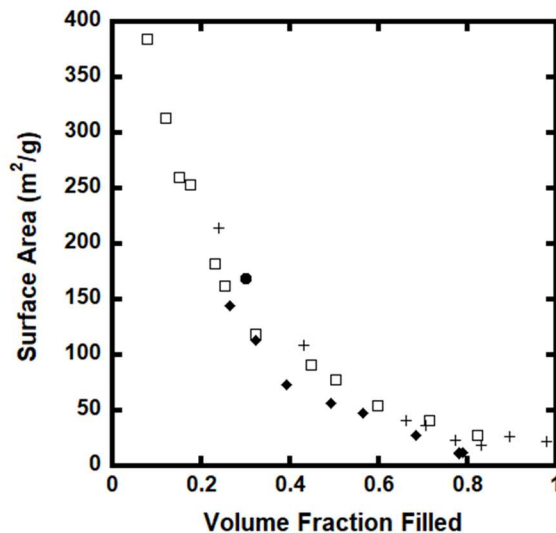


Figure 5.6: Surface Area (m²/g) of PTHF 250- (□), C₂mim⁺Tf₂N⁻ (◻), P_{666,14}⁺Cl⁻ (+), and Cetyl Alcohol (•)-impregnated resins.

Table 5.2: Viscosity of Select Fillers at 25 °C

Filler	Viscosity at 25 °C (cP)
PTHF 250	158
C ₂ mim ⁺ Tf ₂ N ⁻	33
P _{666,14} ⁺ Cl ⁻	1824

Figure 5.5 also appears to show that regardless of filler viscosity or polarity, filling the support to near capacity (~80% of the available volume) yields much the same surface area. With this in mind, C₁₆mim⁺Tf₂N⁻ was evaluated next, as such a long-chain IL will be much less water soluble than any of the other ILs used. As hoped, loading the support to a volume fraction of 0.80 with the IL, then flushing a column (1 mL) packed with the sorbent with water (40 mL or 40 bed volumes) resulted in no detectable C₁₆mim⁺Tf₂N⁻ leaching from the support. Unfortunately, as shown by Figure 5.7, 10% (%w/w) HDEHP loading of a C₁₆mim⁺Tf₂N⁻-filled

support did not yield a greater column efficiency ($N = 8$) compared to the commercial Ln resin ($N = 24$).

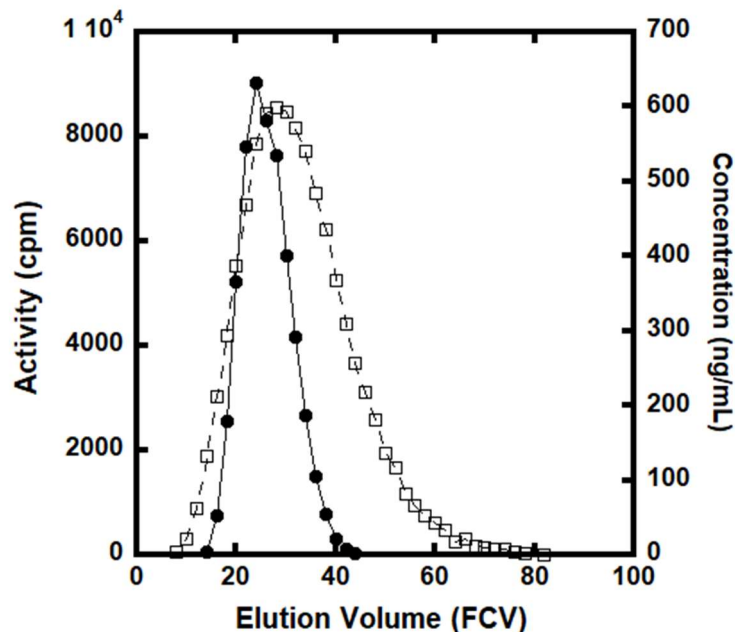


Figure 5.7: $C_{16}mim^+Tf_2N^-$ -impregnated, 10% (%w/w) HDEHP (□, cpm) (Eluent: 0.608 M HNO_3 , Flow Rate = 1.38 ± 0.02 mL/min·cm², $T = 23 \pm 2^\circ C$, 0.9 mL bed volume) and commercial Ln (•, concentration (ng/mL)) resins (Eluent: 0.30 M HNO_3 $T = 23 \pm 2^\circ C$, 0.9 mL bed volume) $^{152/4}Eu^{3+}$ Elution Profile.

In an effort to explain these unexpectedly poor results, published data on the size of various $C_nmim^+Tf_2N^-$ ILs were extrapolated to estimate the diameter of $C_{16}mim^+Tf_2N^-$ (0.801 nm) and $C_2mim^+Tf_2N^-$ (0.629 nm).⁴⁰ Published surface area data on Amberlite XAD-7, the large particle analog of Amberchrom CG-71m, shows the presence of pores with diameters less than that of $C_{16}mim^+Tf_2N^-$.⁴¹ Accordingly, it would be expected that its use as a filler would leave small pores unfilled. Indeed, as can be seen from Figure 5.8, which compares the pore distribution of $C_2mim^+Tf_2N^-$ (panel B) and $C_{16}mim^+Tf_2N^-$ -filled (panel A) resins (filled to a volume fraction of 0.80), pores of less than 0.801 nm are present in the $C_{16}mim^+Tf_2N^-$ -loaded resin. In contrast, for $C_2mim^+Tf_2N^-$, no pores below 10 nm in diameter are present, proving that

the smallest pores are completely filled with the smaller IL. Thus, despite its other favorable properties, $C_{16}mim^+Tf_2N^-$ is simply too large to fill the small pores that are present in the support. It therefore cannot be considered further.

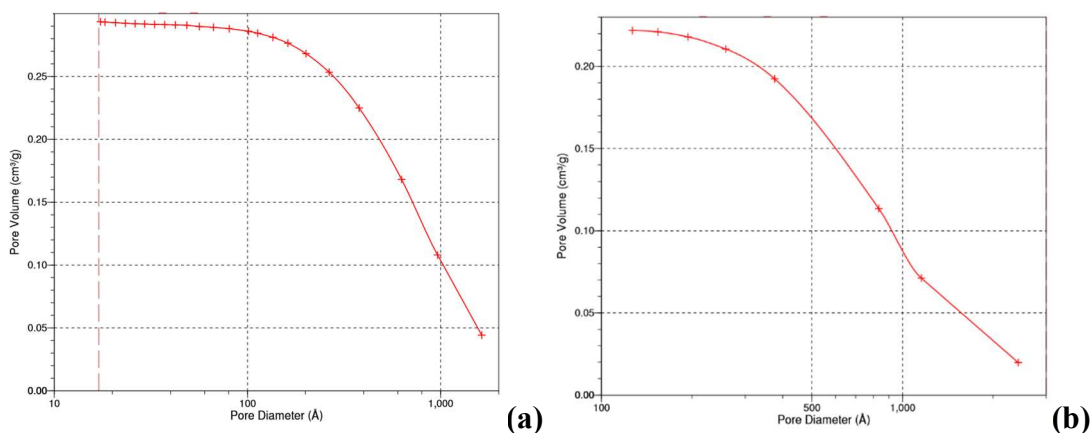


Figure 5.8: Pore distribution of $C_{16}mim^+Tf_2N^-$ (a) and $C_2mim^+Tf_2N^-$ (b)-impregnated supports. 80% of the available resin volume is filled for both resins.

Up to this point, none of the fillers had been employed at a loading level of less than 0.30. To gain further insight into the nature of the support interior, thus providing information to guide additional studies of fillers, the column efficiencies of 10, 15, 20 and 30% (w/w) HDEHP resins, discussed in Chapter 4, were considered. As shown by the theoretical plate counts (N) in Table 4.1, nothing is gained by operating at loading levels $\leq 15\%$ (%w/w) HDEHP. However, the 20% (%w/w) HDEHP resin shows an increase in theoretical plate count. Surface area analysis (Figure 5.9) of the same resin indicates that the majority of the HDEHP is consumed in complete filling of the micropores of the support. What remains is probably present as a thin layer on the walls of the intermediate pores as evidenced by the increase in column efficiency. For resin loaded with 30% (w/w) HDEHP, a similar explanation is appropriate. That is, based on surface area data, at this level of loading, nearly all of the intermediate pores of the resin have been filled, leaving the remaining HDEHP on the surface of the large pores. However, while a

layer of HDEHP on the walls of the intermediate pores produces a gain in column efficiency, an analogous layer present on the walls of the macropores, does not provide a comparable efficiency gain.

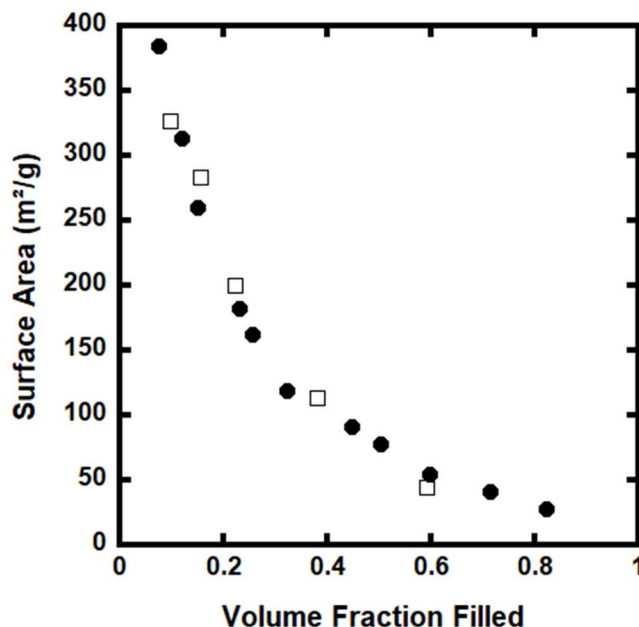


Figure 5.9: The effect of support loading (%w/w) with HDEHP (□) or PTHF 250 (•) on the surface area of Amberchrom CG-71m resin.

The question thus remains as to how much of the filler and HDEHP to use. Again, on the basis of surface area data, the 15% (w/w) support loading with HDEHP appears to nearly completely fill the smallest pores (Figure 5.9). Moreover, the column efficiency of this same resin, as indicated by the plate counts (N) shown in Table 4.1 indicates that at this loading level a thin layer of extractant is not present in the mesopores, as is the case for the 20% (w/w)-loaded HDEHP resin. Taken together, these observations indicate that the empty support should be loaded with filler to the same volume filled by the 15% (w/w) HDEHP resin, and that HDEHP should be placed atop the filler at a yet to be determined thickness.

From the results described thus far, it is clear that a suitable filler must be inert, water-immiscible yet compatible with a hydrophilic support,³² and relatively non-viscous. These requirements led us to revisit the use of aliphatic alcohols, this time those with a carbon chain shorter than that of cetyl alcohol (C₁₆). Our initial efforts focused on 1-dodecanol, which ultimately proved to be satisfactory. In particular, the surface area of a 1-dodecanol-impregnated support (299.65 m²/g) was found to be in good agreement with that observed for a support impregnated with HDEHP (282.91 m²/g) when both resins were loaded to the same volume fraction. Furthermore, upon flushing the resin with water (40 mL or 40 bed volumes), no 1-dodecanol was detected in the column effluent by ¹H-NMR analysis. Empty solid supports were then filled with 1-dodecanol to the same volume fraction as that occupied by the 15% (w/w) HDEHP, and atop this filler was loaded extractant (HDEHP) to levels ranging from 5 to 30% (w/w).

The characteristics used to assess the performance of these resins are shown in Table 5.4. These values are derived from the plots shown in Figure 5.10, panels A-E, which depict the elution behavior of Eu on packed columns of the materials. That the highest plate count is observed for the resin containing 10% (w/w) HDEHP is reasonable, given that the 10% (w/w) HDEHP SPP (*i.e.* 1-dodecanol loaded) resin occupies a volume fraction (~0.26) of the support similar to that observed for the 20% HDEHP resin (~0.22). Just as important is that the results suggest that no interactions between the 1-dodecanol filler and the HDEHP extractant are taking place. That is, if HDEHP did interact with the filler, the column efficiency, peak tailing, and peak asymmetry values would have been unsatisfactory due to the retention of metals ions in the deep, inaccessible pores of the support.

Table 5.4: Theoretical plate height (H) and count (N), tailing factor (T_f), and peak asymmetry (A_s), and capacity for HDEHP-stagnantly-pore plugged resins.

Resin ((%w/w) SPP HDEHP)	T _f	A _s	H	N	Capacity (mg Eu/mL bed)	Moles HDEHP consumed/ Moles HDEHP present*100
10	1.18	1.27	0.145	33	3.50	66.8
15	1.15	1.19	0.164	29	5.10	67.0
20	1.18	1.29	0.251	19	6.25	73.3
30	1.07	1.15	0.281	17	14.35	78.1
40	-	-	-	-	-	80.4

Experimental conditions: V_{column} = 0.90 mL; L_{column} = 4.77 cm; Flow rate: 1.39 ± 0.08 mL/cm²·min.

In considering results for resins loaded to other levels, it can be seen that for the 5% (w/w) HDEHP SPP resin (Figure 5.10A), ^{152/4}Eu³⁺ elutes from the column almost immediately, but that complete elution is nonetheless protracted, as was the case for the 5% (w/w) pure HDEHP resin. Thus, no calculation of the performance metrics was attempted. As can also be seen, the 10% (w/w) HDEHP SPP resin is the most efficient and, thus, apparently an appropriately thin extractant layer in the intermediate pores.

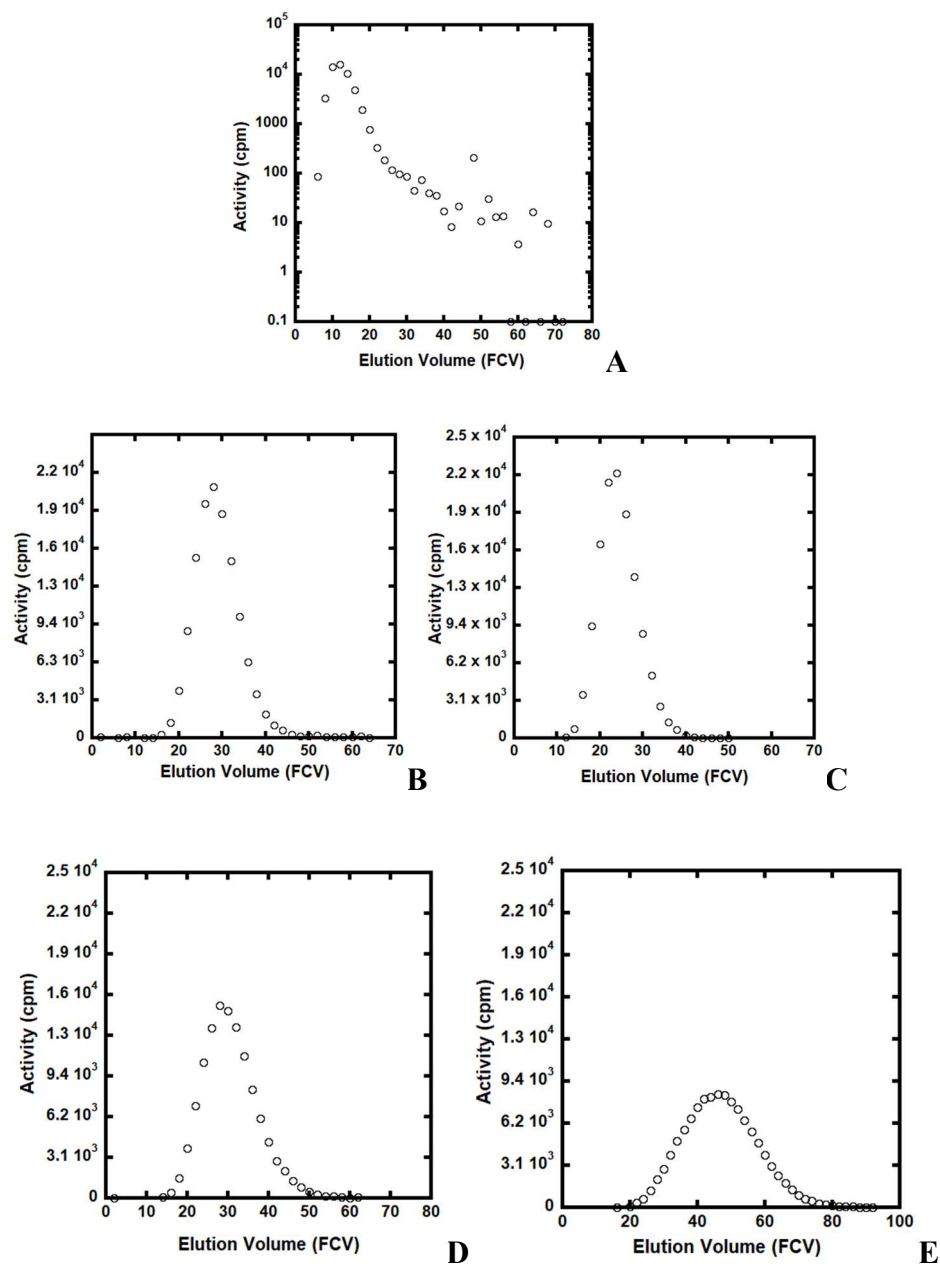


Figure 5.10A-E: 5%-30% (w/w) HDEHP stagnantly-pore plugged (SPP) resins, 0.9 mL be volume (Temperature: $23 \pm 2^\circ\text{C}$, eluents: 0.026, 0.045, 0.086, 0.097, and 0.17 M HNO_3 , respectively)

The decrease in column efficiency with loading, noted here (Table 5.4), has been previously observed for other EXC sorbents. For example, Sochacka *et al.* noted an increase in plate height with increasing HDEHP loading with a diatomaceous earth support.⁴² Horwitz *et*

*al.*⁴³ observed the same effect with HDEHP-loaded Celite. As the Celite was loaded with HDEHP, the authors noted, the smaller pores filled first, allowing a thin layer of extractant to coat the larger pores. Loading past intermediate levels, however, only increased the diffusion distance of the metal ion in the support, resulting in decreased column efficiency.⁴³ The trend in column efficiency shown in Table 5.4 is consistent with the explanation posed by Horwitz *et al.* That is, the 1-dodecanol occupies the smallest and least accessible pores in the support, thereby allowing the HDEHP to be present at different layer thicknesses in the larger pores.

Besides improved column efficiency, plugging of small pores by addition of the 1-dodecanol to the various resins leads to a near-constant value of the tailing (1.1-1.2) and peak asymmetry (1.15-1.30) factors, regardless of the support filling level. The support micropores, therefore, must be the source of peak tailing in this support, an observation which to the knowledge of the authors, has not been previously reported.

Unexpectedly, the observed improvements in column efficiency and peak tailing were also accompanied by higher metal ion uptake. As can be seen in Table 5.4, the capacity of the 10-20% (w/w) HDEHP SPP resins is about double that of their pure HDEHP analogues. More interesting is that the capacity of the 30% (w/w) HDEHP SPP resin actually exceeds that of the commercial Ln resin which is loaded to a higher level. Also notable from Table 5.4 are data for fraction of available extractant consumed for the SPP resins. As shown, the SPP resins allow for ~70-80% of the available extractant to be used. In contrast, the HDEHP-only resin can exhibit as little as ~30% capacity utilization, as illustrated by the 10% (w/w) HDEHP resin. In published literature, HDEHP is frequently described as existing as a dimer in solution.⁴⁴ If this were the case here, however, for the prepared SPP resins, the capacity would be more than stoichiometrically possible. The only possible explanation is that the HDEHP is present in

monomeric form. Apparently then, micropore filling allows for improvements not only in tailing but in resin capacity as well.

5.4 Applications in Intra-lanthanide Metal Ion Separations

5.4.1 $\text{Eu}^{3+}/\text{Nd}^{3+}$ Separation

The data shown in Table 5.4 show the potential of the SPP resins. Should the desired separation be possible with the commercial Ln resin, however, then the use of SPP resins becomes unnecessary. Given the reported difficulty in separating trivalent europium from neodymium,⁴⁸ the separation of these two metal ions was the first attempted. It is clear from the D_w values for Eu and Nd and the corresponding separation factors (SFs), that a separation of the two metal ions should be possible with either the 10% (%w/w) HDEHP SPP resin or conventional Ln resin. While distribution ratio data allow one to predict where a metal ion will elute on a given column, it does not prove that complete separation will occur. Thus, the two metal ions were applied to both 10% (%w/w) HDEHP SPP and Ln resin columns and their elution behavior determined. As shown in Figures 5.11 and 5.12, complete resolution is achieved with both the 10% HDEHP SPP and the Ln resin. The ability of the latter to resolve the two metal ions was certainly unexpected given the published results.^{20, 48} Wishing to demonstrate that a sorbent employing blocked stagnant pores can provide separation ability superior to that of the Ln resin, a more challenging separation, that of Eu^{3+} and Gd^{3+} , was pursued.

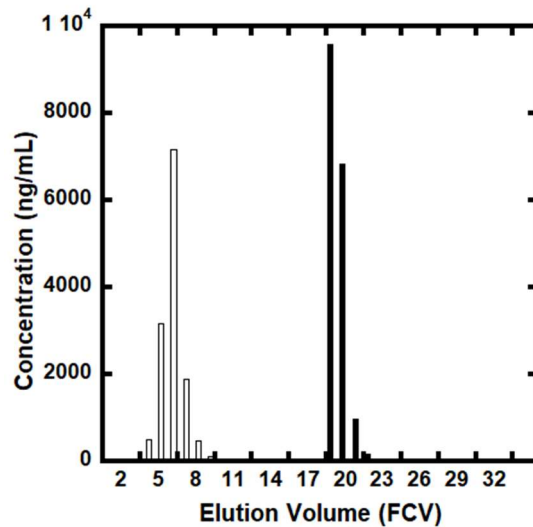


Figure 5.11: 10% (%w/w) SPP HDEHP resin separation of Eu^{3+} (Filled)/ Nd^{3+} (Open), 0.9 mL bed volume (Temperature: $23 \pm 2^\circ\text{C}$, eluents: 0.045 M HNO_3 followed by 1 M HNO_3 at FCV = 17)

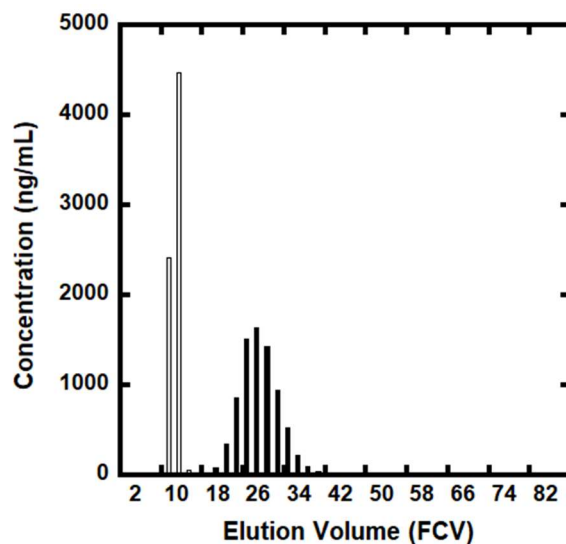


Figure 5.12: Ln resin separation of Eu^{3+} (Filled)/ Nd^{3+} (Open), 0.9 mL bed volume (Temperature: $23 \pm 2^\circ\text{C}$, eluents: 0.3 M HNO_3)

5.4.2 $\text{Eu}^{3+}/\text{Gd}^{3+}$ Separation

Metal ions directly adjacent to one another in the periodic table are among the most difficult to separate. The separation of americium and curium is a well-known example of such a problem,⁴⁵⁻⁴⁷ which is especially evident with commercial resins.¹⁹ Therefore, the separation of europium and gadolinium was attempted, as these metal ions are directly above americium and curium, respectively, in the periodic table and been cited as difficult to separate in numerous published works.⁴⁸⁻⁵⁰ As before, a comparison of D_{Eu} , D_{Gd} , and SF data of both the 10% HDEHP SPP and Ln resins was done first. The Ln resin was found to extract Eu^{3+} and Gd^{3+} equally well at both 0.25 M ($D_{\text{w,Eu}} = 163$; $D_{\text{w,Gd}} = 158$) and 0.30 M HNO_3 ($D_{\text{w,Eu}} = 90$; $D_{\text{w,Gd}} = 83$). While the SFs improve at 0.15 M ($D_{\text{w,Eu}} = 610$; $D_{\text{w,Gd}} = 1144$) and 0.20 M HNO_3 ($D_{\text{w,Eu}} = 195$; $D_{\text{w,Gd}} = 352$), both metal ions are strongly retained, making their separation difficult. At 0.40 M HNO_3 ($D_{\text{w,Eu}} = 20$; $D_{\text{w,Gd}} = 37$), conversely, the metals ions are not held strongly enough, and both would be eluted from the column almost unretained.

Contrary to the Ln resin, a separation between the two metal ions seems possible for the 10% (%w/w) HDEHP SPP resin. Between 0.025 M HNO_3 ($D_{\text{w,Eu}} = 823$; $D_{\text{w,Gd}} = 1280$) and 0.05 M HNO_3 ($D_{\text{w,Eu}} = 76$; $D_{\text{w,Gd}} = 117$), the metals ions are not too strongly retained for baseline resolution to occur. Furthermore, the SFs (1.56 and 1.54 for 0.025 M and 0.05 M HNO_3 , respectively) at the same acidities indicate a separation should occur. The remaining acidities (0.075-0.15 M HNO_3) show the column would not retain the metal ions strongly enough ($D_{\text{w}} < 40$), and each would be eluted almost unretained.

Elution profiles for the two resins are shown in Figures 5.13 and 5.14. Unexpectedly and unfortunately, resolution values of 0.42 and 0.53 are observed for the 10% (%w/w) HDEHP SPP and Ln resins, respectively. The poor resolution by the SPP column indicates that simply

applying a thin layer of extractant to a porous resin is not enough to completely separate the two metal ions. Thankfully, other changes can be made to solve the problem.

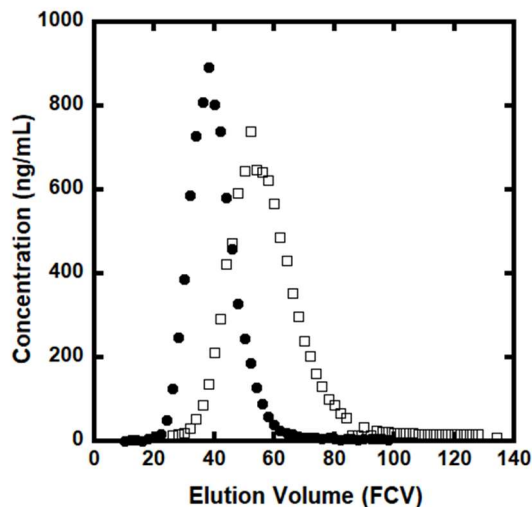


Figure 5.13: 10% (%w/w) SPP HDEHP separation of Eu³⁺ (•)/Gd³⁺ (□), 0.9 mL bed volume (Temperature: 23 ± 2°C, eluent: 0.045 M HNO₃)

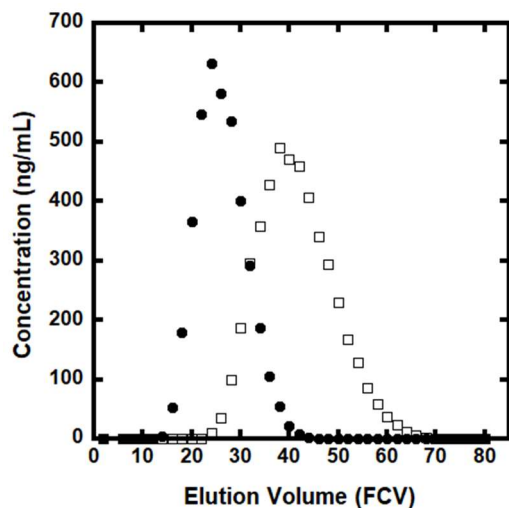


Figure 5.14: Ln resin separation of Eu³⁺ (•)/Gd³⁺ (□), 0.9 mL bed volume (Temperature: 23 ± 2°C, eluent: 0.3 M HNO₃)

According to the van Deemter Equation (Eq. 5.1), decreasing the resin particle size should decrease the theoretical plate height by lowering the A and C terms, as the column bed should be more uniformly packed and the metal ion will spend less time diffusing through the

mobile phase and more time interacting with the stationary phase.²¹ Horwitz *et al.*⁵¹ discussed improvements in strontium ion separations by simply decreasing the particle size of the support material. In eluting ⁸⁵Sr using a resin impregnated with 1.0 M 4, 4'(5')-bis(*t*-butylcyclohexano)-18-crown-6 in 1-octanol solution, the 100-125 μm resin displayed a theoretical plate height of 0.53 cm, while that of the 50-100 μm resin was 0.11 cm.⁵⁰ Besides lowering the resin particle size, simply lengthening the column will increase the number of theoretical plates.

Identical 10% (w/w) HDEHP SPP beads were then prepared as previously described but the pre-filter material (20-50 μm particle size) was used instead of the Amberchrom CG-71m (50-100 μm particle size). In addition, the column length was increased from 5 to 10 cm. Similarly, a small particle analogue of the commercial resin was prepared by impregnating the pre-filter material with 40% (w/w) HDEHP. The Eu³⁺/Gd³⁺ elution profiles for the two resins are shown in Figure 5.15 and 5.16. By decreasing the particle size of the 10% (w/w) HDEHP SPP resin and lengthening the column, the resolution was improved to 0.79 (vs. 0.42 for a 0.9 mL bed of 50-100 μm particle size resin). Decreasing the particle size and lengthening the column also gave an improved Eu³⁺/Gd³⁺ separation for the Ln resin, as the resolution improved from 0.53 to 1.09. As the small-particle 10% (w/w) HDEHP SPP resin had a thinner layer of extractant compared that of the small-particle Ln resin, it should have given a more resolved chromatogram. Previous work by these authors, however, has shown that by simply decreasing the particle size of the Ln resin, comparable improvement in resolution (0.92) is observed compared to a decreased loading level (0.89 of the 20% (w/w) HDEHP). Under these conditions then, column efficiency must be more strongly controlled by column height and particle size than stationary phase thickness.

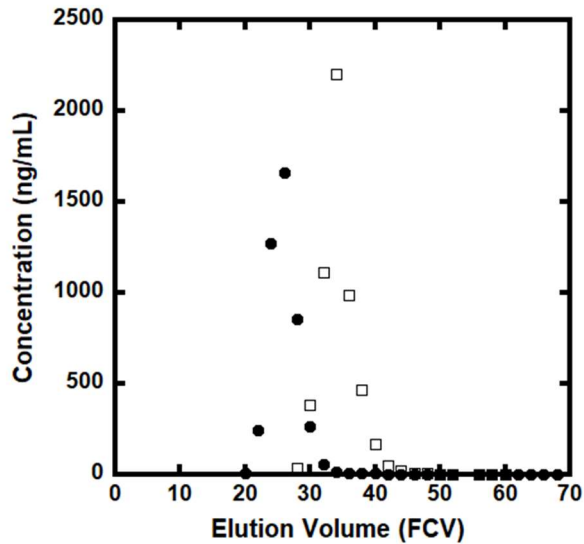


Figure 5.15: Small particle 10% (%w/w) SPP HDEHP separation of Eu³⁺ (•)/Gd³⁺ (□), 1.8 mL bed (Temperature: 23 ± 2°C, eluent: 0.045 M HNO₃)

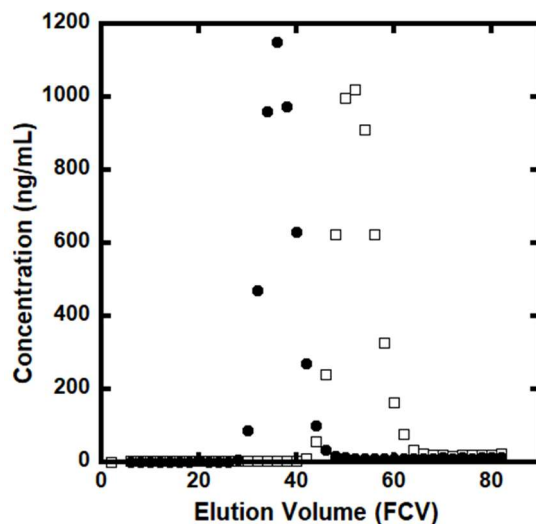


Figure 5.16: Small particle Ln resin separation of Eu³⁺ (•)/Gd³⁺ (□), 1.8 mL bed (Temperature: 23 ± 2°C, eluents: 0.3 M HNO₃)

5.5 Conclusion

The results of this study demonstrate the advantages of a stagnantly-pore plugged (SPP) supports, as it provides improvements in column efficiency, peak tailing, and column capacity. While other methods used in metal ion separations involve more complicated resin preparation,

these materials are easily prepared with only a balance and rotary evaporator, available in almost all chemistry laboratories. An ideal filler, as has been shown, must be water-immiscible, support compatible, and inert to the support and extractant, properties that solvents other than 1-dodecanol undoubtedly have.

Surprisingly, the separation ability of the prepared resins for $\text{Eu}^{3+}/\text{Gd}^{3+}$ was not significantly greater than that of the commercially available Ln resin. Apparently, column length and particle size have a much greater influence on the separation ability of a sorbent than the thickness of the stationary phase. Therefore, the SPP supports would be of greatest value in applications where the additional theoretical plates provided by a thinner stationary phase layer would be most useful. Such an application was recently described by Kaminski *et al.* and involved the rapid determination $^{90}\text{Sr}^{2+}$ in human urine. By using two commercial resin columns in tandem, one a cation exchange resin and the other a Sr-selective EXC material, the throughput of human urine samples was increased by a factor of at least four over existing methods. Nonetheless, it was still not fast enough to satisfy the Centers for Disease Control goal of processing 10,000 samples per day in the event of a nuclear attack. The authors commented on potentially increasing the sample flow rate to increase sample throughput. This would come at a cost to the column efficiency, however, already at a meager $N = 1.3$ plates at the highest flow rate.⁵² The extra plates provided by the SPP resins would no doubt prove useful in this application. Work to address this issue is currently underway in this laboratory.

5.6 References

1. Eschrich, H. (1967). Separation of Neptunium (IV), neptunium (V), neptunium (VI) by extraction chromatography. *Fresenius' Zeitschrift Fur Analytische Chemie*, 226, 100–114.
2. McClaine, B. L. A., Noble, P., & Bullwinkel, E. P. (1958). The development and properties of an adsorbent for uranium. *The Journal of Physical Chemistry*, 62, 299-303.

3. E.P. Horwitz, K.A. Orlandini, C. A. A. Bloomquist. (1966). The separation of americium and curium by extraction chromatography using molecular weight quaternary ammonium nitrate. *Inorganic and Nuclear Chemistry Letters*, 2, 87–91.
4. Cerrai, E., Esla, C., Triulzi, C. (1962). Separation of rare earths by column chromatography with cellulose powder treated with di(2-ethylhexyl)orthophosphoric acid-Part 2. *Energia*, 9, 377–384.
5. Horwitz, E.P.; Chiarizia, R.; Diamond, H. (1992). Separation and preconcentration of uranium from acidic media by extraction chromatography. *Analytica Chimica Acta*, 266, 25–37.
6. Melnik, M.I.; Karelin, E.A.; Filimonov, V. T. (1995). Production of high-purity Gd-153. 2. Removal of samarium, terbium, and microamounts of europium from gadolinium by extraction chromatography. *Radiochemistry*, 37, 169–172.
7. Wang, Q.; Tsunoda, K.; Akaiwa, H. (1997). Mutual separation of rare earth elements by extraction chromatography using bis(1,1,3,3-tetramethylbutyl)phosphinic acid as a stationary phase. *Analytical Sciences*, 13, 153–156.
8. Ansari, S. A., & Mohapatra, P. K. (2014). Evaluation of an extraction chromatographic resin containing CMPO and ionic liquid for actinide ion uptake from acidic feeds: Part II. Batch actinide sorption, radiolytic degradation and column studies. *Radiochimica Acta*, 102, 589–597.
9. Bhattacharyya, A., Mohapatra, P. K., Gadly, T., Ghosh, S. K., Raut, D. R., & Manchanda, V. K. (2011). Extraction chromatographic study on the separation of Am³⁺ and Eu³⁺ using ethyl-BTP as the extractant. *Journal of Radioanalytical and Nuclear Chemistry*, 288, 571–577.
10. Gujar, R. B., Ansari, S. A., & Mohapatra, P. K. (2015). Spectacular enhancements in actinide ion uptake using novel extraction chromatography resins containing TODGA and ionic liquid. *Separation and Purification Technology*, 141, 229–234.
11. Mincher, M.E.; Quach, D.L.; Liao, Y.J.; Mincher, B.J.; Wai, C. M. (2012). The partitioning of americium and the lanthanides using tetrabutyl diglycolamide (TBDGA) in octanol and in ionic liquid solution. *Solvent Extraction and Ion Exchange*, 30, 735–747.
12. Banda, R., Jeon, H., & Lee, M. (2012). Solvent extraction separation of Pr and Nd from chloride solution containing Ia using Cyanex 272 and its mixture with other extractants. *Separation and Purification Technology*, 98, 481–487.
13. Diamond, R.M.; Street Jr., K.; Seaborg, G. T. (1954). An ion-exchange study of possible hybridized 5f bonding in the actinides. *Journal of the American Chemical Society*, 76, 1461–1469.
14. Stefula, V., Sebesta, F. (1990). Composite ion exchanger with ammonium molybdophosphate and its properties. *Journal of Radioanalytical and Nuclear Chemistry*, 14, 15–21.
15. Dietz, M. L. (2003). *Recent progress in the development of extraction chromatographic methods for radionuclide separation and preconcentration*. (K. L. Nash & C. A. Laue, Eds.), *Radioanalytical methods in interdisciplinary research: fundamentals in cutting edge applications*. Washington D.C.: American Chemical Society.

16. Horwitz, E. P., McAlister, D. R., Bond, A. H., & Barrans, J. E. (2005). Novel extraction of chromatographic resins based on tetraalkyldiglycolamides: Characterization and potential applications. *Solvent Extraction and Ion Exchange*, 23, 319–344.
17. McAlister, D. R., & Horwitz, P. E. (2007). Characterization of extraction of chromatographic materials containing bis(2-ethyl-1-hexyl)phosphoric acid, 2-ethyl-1-hexyl (2-ethyl-1-hexyl) phosphonic acid, and bis(2,4,4-trimethyl-1-pentyl)phosphinic acid. *Solvent Extraction and Ion Exchange*, 25, 757–769.
18. Horwitz, E. P., Chiarizia, R., & Dietz, M. L. (1997). DIPEX: A new extraction chromatographic material for the separation and preconcentration of actinides from aqueous solution. *Reactive and Functional Polymers*, 33, 25–36.
19. Gharibyan, N., Dailey, A., McLain, D. R., Bond, E. M., Moody, W. A., Happel, S., & Sudowe, R. (2014). Extraction behavior of americium and curium on selected extraction chromatography resins from pure acidic matrices. *Solvent Extraction and Ion Exchange*, 32, 391–407.
20. Bertelsen, E. R., Deodhar, G., Kluherz, K. T., Davidson, M., Adams, M. L., Trewyn, B. G., & Shafer, J. C. (2019). Microcolumn lanthanide separation using bis(2-ethylhexyl) phosphoric acid functionalized ordered mesoporous carbon materials. *Journal of Chromatography A*, 1595, 248–256.
21. Ornaf, R.M., Dong, M. W. (2005). Key concepts of HPLC in pharmaceutical analysis. In M. . Ahuja, S. Dong (Ed.), *Handbook of Pharmaceutical Analysis by HPLC* (pp. 19–45). London: Elsevier.
22. Zdravkov, B. D., Čermák, J. J., Šefara, M., & Janků, J. (2007). Pore classification in the characterization of porous materials: A perspective. *Central European Journal of Chemistry*, 5, 385–395.
23. Long, C., Li, A., Wu, H., & Zhang, Q. (2009). Adsorption of naphthalene onto macroporous and hyper-crosslinked polymeric adsorbent: Effect of pore structure of adsorbents on thermodynamic and kinetic properties. *Colloids and Surfaces A: Physicochemical and Engineering Aspects*, 333, 150–155.
24. Heinze, M. T., Zill, J. C., Matysik, J., Einicke, W. D., Gläser, R., & Stark, A. (2014). Solid-ionic liquid interfaces: Pore filling revisited. *Physical Chemistry Chemical Physics*, 16, 24359–24372.
25. Arias, A., Saucedo, I., Navarro, R., Gallardo, V., Martinez, M., & Guibal, E. (2011). Cadmium(II) recovery from hydrochloric acid solutions using Amberlite XAD-7 impregnated with a tetraalkyl phosphonium ionic liquid. *Reactive and Functional Polymers*, 71, 1059–1070.
26. Idris, A., Vijayaraghavan, R., Patti, A. F., & Macfarlane, D. R. (2014). Distillable protic ionic liquids for keratin dissolution and recovery. *ACS Sustainable Chemistry and Engineering*, 2, 1888–1894.
27. Deetlefs, M., Seddon, K.R. (2003). Improved preparation of ionic liquids using microwave irradiation. *Green Chem.*, 5, 181–186.
28. Fredlake, C.P., Crosthwaite, J.M., Hert, D.G., Aki, S.N.V.K., Brennecke, J.F. (2004) Thermophysical properties of imidazolium-based ionic liquids. *J. Chem. Eng. Data*, 49, 954-964.

29. E. Philip Horwitz, Mark L. Dietz, Donald M. Nelson, Jerome J. LaRosa, W. D. F. (1990). Concentration and separation of actinides from urine using a supported bifunctional organophosphorus extractant. *Analytica Chimica Acta*, 238, 263–271.
30. McDowell, W. J. (1971). Equilibria in the system: di(2-ethylhexyl)phosphoric acid-benzene-water-alkali (hydroxide, nitrate). *Journal of Inorganic and Nuclear Chemistry*, 33, 1067–1079.
31. Momen, A. (2015). Improved extraction chromatographic materials for the separation and preconcentration of metal ions. University of Wisconsin-Milwaukee, Milwaukee, WI.
32. Parrish, J. R. (1977). Macroporous resins as supports for a chelating liquid ion exchanger in extraction chromatography. *Analytical Chemistry*, 49, 1189–1192.
33. Tariq, M., Carvalho, P. J., Coutinho, J. A. P., Marrucho, I. M., Lopes, J. N. C., & Rebelo, L. P. N. (2011). Viscosity of (C2-C14) 1-alkyl-3-methylimidazolium bis(trifluoromethylsulfonyl)amide ionic liquids in an extended temperature range. *Fluid Phase Equilibria*, 301, 22–32.
34. Polypropylene Glycol. (2020). *Sigma-Aldrich*. Darmstadt, Germany: Sigma-Aldrich.
35. Kreher, U. P., Rosamilia, A. E., Raston, C. L., Scott, J. L., & Strauss, C. R. (2004). Self-associated, “distillable” ionic media. *Molecules*, 9, 387–393.
36. Idris, A., Vijayaraghavan, R., Patti, A. F., & Macfarlane, D. R. (2014). Distillable protic ionic liquids for keratin dissolution and recovery. *ACS Sustainable Chemistry and Engineering*, 2, 1888–1894.
37. Smith, C. D., Foersterling, F. H., Dietz, M. L. (2020). Solvent structural effects on the solubility of bis(2-ethylhexyl) phosphoric acid (HDEHP) in room- temperature ionic liquids (HDEHP) in room-temperature ionic liquids. *Separation Science and Technology*, 55, 1–11.
38. 1-ethyl-3-methylimidazolium bis(trifluoromethanesulfonyl)imide. (2019). Toulouse, France: Solvionic SA.
39. Matsuo, S., & Makita, T. (1989). Viscosities of six 1-alkanols at temperatures in the range 298–348 K and pressures up to 200 MPa. *International Journal of Thermophysics*, 10, 833–843.
40. Tokuda, H., Hayamizu, K., Ishii, K., Susan, M. A. B. H., & Watanabe, M. (2005). Physicochemical properties and structures of room temperature ionic liquids. 2. variation of alkyl chain length in imidazolium cation. *Journal of Physical Chemistry B*, 109, 6103–6110.
41. Yang, W., Li, A., Cai, J., Meng, G., & Zhang, Q. (2006). Adsorption of surfactants onto acrylic ester resins with different pore size distribution. *Science in China, Series B: Chemistry*, 49, 445–453.
42. Sochacka, R.J.; Siekierski, S. (1964). Reversed-phase partition chromatography with di-(2-ethylhexyl)orthophosphoric acid as the stationary phase. *Journal of Chromatography*, 16, 376–384.
43. Horwitz, E.P.; Bloomquist, C.A.A; Henderson, D. J. (1969). The extraction chromatography of californium, einsteinium, and fermium with di(2-ethylhexyl)orthophosphoric acid. *Journal of Inorganic and Nuclear Chemistry*, 31, 1149–1166.

44. Cocalia, V. A., Jensen, M. P., Holbrey, J. D., Spear, S. K., Stepinski, D. C., & Rogers, R. D. (2005). Identical extraction behavior and coordination of trivalent or hexavalent f-element cations using ionic liquid and molecular solvents. *Dalton Transactions*, *11*, 1966–1971.
45. Kurosaki, H., & Clark, S. B. (2011). Chromatographic separation of Am and Cm. *Radiochimica Acta*, *99*, 65–69.
46. Suzuki, T., Otake, K., Sato, M., Ikeda, A., Aida, M., Fujii, Y., Ozawa, M. (2007). Separation of americium and curium by use of tertiary pyridine resin in nitric acid/methanol mixed solvent system. *Journal of Radioanalytical and Nuclear Chemistry*, *272*, 257–262.
47. Kraak, W., Van Der Heijden, W. A. (1966). Anion exchange separation between americium and curium and between several lanthanide elements. *Journal of Inorganic and Nuclear Chemistry*, *28*, 221–234.
48. Payne, R. F., Schulte, S. M., Douglas, M., Friese, J. I., Farmer, O. T., & Finn, E. C. (2011). Investigation of gravity lanthanide separation chemistry. *Journal of Radioanalytical and Nuclear Chemistry*, *287*, 863–867.
49. Kondo, K., Oguri, M., & Matsumoto, M. (2013). Novel separation of samarium, europium and gadolinium using a column packed with microcapsules containing 2-ethylhexylphosphonic acid mono-2-ethylhexyl ester. *Chemical Engineering Transactions*, *32*, 919–924.
50. Li, S. C., Kim, S. C., Kang, C. S., Kim, C. J., & Kang, C. J. (2018). Separation of samarium, europium and gadolinium in high purity using photochemical reduction-extraction chromatography. *Hydrometallurgy*, *178*, 181–187.
51. Horwitz, E.P.; Chiarizia, R.; Dietz, M. L. (1992). A novel strontium-selective extraction chromatographic resin. *Solvent Extraction and Ion Exchange*, *10*, 313–336.
52. Kaminski, M., Sandi, G., Dietz, M., & Park, A. (2020). Optimization of a tandem ion exchange—extraction chromatographic scheme for the recovery of strontium from raw urine. *Separation Science and Technology (Philadelphia)*, *55*, 176–185.

CHAPTER 6

COMPARISON OF *BIS*(2-ETHYLHEXYL) PHOSPHORIC ACID (HDEHP) TO DEHP-BASED FUNCTIONALIZED IONIC LIQUIDS IN *f*-ELEMENT EXTRACTION

6.1 Introduction

Isolating individual and groups of metals of the *f*-element group can be thought as the “last frontier” of metal separations. Commonly found in the trivalent oxidation state and with similar ionic radii,¹ lanthanide and actinide series elements represent a major separation challenge. Early attempts at their separations dating back to the 1950s² focused on single-extractant systems. Unfortunately, acceptable selectivity between these two families in these single-extractant systems was not achieved.³⁻⁵

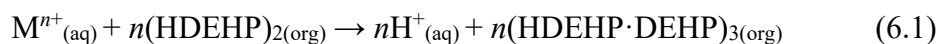
As it became clear that single-extractant systems would not yield adequate lanthanide-actinide separation, adding a complexant to the aqueous phase to establish competition as the basis for selectivity was studied, and the TALSPEAK (Trivalent Actinide Lanthanide Separation with Phosphorus reagent Extraction from Aqueous Komplexes) Process was born. Using a *bis*(2-ethylhexyl)phosphoric acid (HDEHP)-diisopropylbenzene (DIPB) organic phase and a pH 3.5 sodium lactate-sodium diethylenetriamine-*N,N,N',N'',N''*-pentaacetic acid (DTPA) buffer as the aqueous phase, separation factors of ~100 were achieved between trivalent europium and americium.⁶

With separation achieved, intense investigation into the process ensued, and as a result, its weaknesses became evident. For example, the extraction kinetics were slow, resulting in lengthy equilibration times.⁷ Also metal ion distribution ratios were modest (~10), so multistage cycling was required to obtain acceptable Eu^{3+} extraction into the organic phase.⁶ TALSPEAK

also requires strict pH control, a result of the fact that metal ion extraction exhibits a third-power dependence on pH.⁷ Clearly then, system modification was necessary.

Ionic liquids (ILs) are a relatively new class of solvents known for their thermal stability,⁸ tunability,⁹ low volatility,¹⁰ high ionicity,¹¹ and ability to dissolve a wide range of solutes, including wool,¹² bananas,¹³ and proteins,¹⁴ to name a few. Of the fields best-suited for these solvents, metal ion extraction has been among the most studied.¹⁵⁻²⁰ Anticipating water-immiscible ILs would exhibit enhanced metal-ion extraction due to the “like-dissolves-like” principle,²¹ liquid-liquid extraction experiments with a multitude of extractant-IL systems have been performed.²²⁻²⁴ As expected, ILs can provide substantially improved (up to 50x) efficiency for the extraction of metal ions from aqueous solution under appropriate conditions.²⁵

As the number of publications in the field increased, two problems became evident. First, metal ion extraction into ILs is governed by multiple processes, one type of which (*i.e.*, ion exchange) is detrimental to the long-term stability of the solvent. That is, in some extraction systems, the cation of the IL is exchanged for the metal-extractant complex in stoichiometric proportion, degrading the solvent.²⁶ In an ideal extraction employing a solution of HDEHP in an IL, a stoichiometric number of HDEHP dimers will exchange n protons with the M^{n+} ion, as shown in Equation 6.1 below, allowing the metal ion-extractant complex to partition into the organic phase.²⁷ A second, completely unexpected, problem encountered was the limited solubility of metal ion extractants. HDEHP, the extractant of choice in the TALSPEAK process, exhibits limited (<0.1 M) solubility in short-chain ($n = 2-6$) $C_n\text{mim}^+\text{Tf}_2\text{N}^-$ ILs.²⁸



So-called functionalized ionic liquids (FILs) were developed by making the anionic form of the extractant a part of the IL, in part, to address the shortcomings discussed above.²⁹ Unfortunately, the viscous nature^{30,31} of FILs makes a liquid-liquid experiment difficult or completely impractical. Rather, they must be impregnated as a thin layer onto extraction chromatographic supports for studies on these solvents in pure form.

For the FILs to be considered useful, they will need to exhibit greater extraction efficiency, selectivity and/or stability than the corresponding extractants in either pure form or diluted with a conventional solvent or a conventional (*i.e.*, non-functionalized) ionic liquid. Sun *et al.*³⁷ assessed the extractability of almost the entire lanthanide series using HDEHP dissolved in DIPB and several $C_n\text{mim}^+\text{X}^-$ ILs ($n = 4, 6, 8, 10$; $\text{X}^- = \text{Tf}_2\text{N}^-$, BETI). Unexpected to the authors was the increased distribution ratios of the light and heavy lanthanides relative to the middle lanthanides (*e.g.* Eu^{3+}). The uptake of the middle lanthanide ions was similar for HDEHP in $C_{10}\text{mim}^+\text{Tf}_2\text{N}^-$ and DIPB. The authors also observed the presence of an ion exchange process with the short-chain ionic liquids (*e.g.* $C_4\text{mim}^+\text{Tf}_2\text{N}^-$),³⁷ contrary to published work by Cocalia *et al.*, who noted the absence of the ion-exchange mechanism when using HDEHP dissolved in either *n*-dodecane or $C_{10}\text{mim}\text{Tf}_2\text{N}$ to extract Am^{3+} and Eu^{3+} .³⁸ While HDEHP dissolved in the short-chain $C_4\text{mim}^+\text{Tf}_2\text{N}^-$ did extract more efficiently than HDEHP dissolved in DIPB, the same trend was not observed for $C_{10}\text{mim}\text{Tf}_2\text{N}$. While ion exchange is limited with long-chained IL cations (*e.g.* $C_{10}\text{mim}^+$), it apparently comes at a cost to metal ion extractability.

The hydrophobicity of the DEHP⁻ anion would be expected to limit ion exchange, but published data indicate otherwise. For example, Rout *et al.* synthesized imidazolium-, pyridinium-, and quaternary ammonium-based FILs with DEHP as the anion and used a solution of the FIL in $C_6\text{mim}\text{Tf}_2\text{N}$ to extract Nd(III) from nitric acid media. Ion exchange was observed

in both the imidazolium- and pyridinium-based systems, but not in the quaternary ammonium system. Disappointingly, only limited comment was made, leaving the results largely unexplained.³² Clearly, however if these solvents do exhibit ion exchange, their reuse over multiple extraction cycles would be difficult or impossible.

Selectivity is also used in assessing solvent performance, which is especially important considering the near overlap of Eu^{3+} and Am^{3+} acid dependencies. For example, Rout *et al.*⁴³ observed separation factors of 1-2 across the entire acid range used when extracting these two metal ions using 0.05 M HDEHP in $\text{C}_8\text{mimTf}_2\text{N}$. Similar separation factors (1-2) for the same pair of ions were observed by Swami *et. al.*²⁷ using 0.25 M HDEHP in *n*-dodecane. If the FIL does not exhibit increased metal ion extraction efficiency versus HDEHP, perhaps it will outperform HDEHP in terms of $\text{Eu}^{3+}/\text{Am}^{3+}$ extraction selectivity.

In this chapter, we describe our efforts to evaluate the utility of FILs in the separation of trivalent *f*-elements. $\text{C}_{10}\text{mimDEHP}$ or HDEHP, either in pure form or diluted in *n*-dodecane or $\text{C}_{10}\text{mimTf}_2\text{N}$. The extraction of $^{241}\text{Am}^{3+}$ and $^{152/4}\text{Eu}^{3+}$ will then be measured to assess the kinetics, extraction efficiency, and selectivity of both neat and dilute HDEHP and $\text{C}_{10}\text{mimDEHP}$ towards the two metal ions. In addition, nitrate and extractant dependencies will be carried out to determine if ion-exchange is occurring and therefore the resin stability. Finally, resin capacity and metal ion stripping will be examined.

6.2 Experimental

6.2.1 Materials

All chemicals were of reagent grade and unless otherwise noted, were used as received. Lithium *bis*[(trifluoromethyl)sulfonyl]imide (LiTf_2N) was purchased from TCI America (Portland, OR). 1-decyl-3-methyl-imidazolium chloride ($\text{C}_{10}\text{mimCl}$), silver nitrate and sodium ethoxide were purchased from ACROS Organics (Pittsburgh, PA). Two hundred proof ethanol was purchased from KOPTEC (King of Prussia, PA). HDEHP, methanol, *n*-dodecane (*n*-dd), 1-methylimidazole, 1-bromodecane, 1-dodecanol, sodium nitrate, sodium hydroxide, methylene chloride and Optima™ nitric acid were obtained from Sigma-Aldrich (St. Louis, MO). Aqueous nitric acid solutions were prepared using water from a Milli-Q2 system (specific resistance $\geq 18 \text{ M}\Omega\text{-cm}$) and standardized using sodium hydroxide solutions with a phenolphthalein indicator (Ricca, Arlington, TX). $\text{C}_{10}\text{mimTf}_2\text{N}$ was synthesized *via* a two-step procedure involving quaternization of the methylimidazole with 1-bromodecane to yield the halide form of the IL,³⁴ followed by anion metathesis to provide the desired (*e.g.*, Tf_2N^-) product.³⁵ The IL was then dried for 24 hours *in vacuo* at 80°C and stored in a desiccator until use. $\text{C}_{10}\text{mimDEHP}$ was synthesized by first mixing a $\text{C}_{10}\text{mimCl}$ -ethanol solution with an equimolar amount of sodium ethoxide. The mixture was stirred for 24 hours and the supernatant was decanted and mixed with an equal volume of water for 30 minutes.³⁶ An equimolar solution of HDEHP in ethanol was added and mixed for an additional 4 hours. Methylene chloride was added while decanting the aqueous layer. The organic phase was then washed with water until no precipitate was observed upon mixing the water wash with silver nitrate solution. The methylene chloride was then removed using rotary evaporation. The identity of all ILs was confirmed using ^1H NMR. $^{152/154}\text{Eu}$ and ^{241}Am were purchased from Eickart and Ziegler. Amberchrom CG-71m was

purchased from Rohm and Haas (Philadelphia, PA) and was purified according to published methods. Briefly, the impure resin was contacted with water for 30 minutes with occasional swirling, then removed. Methanol was contacted with the same resin and allowed to percolate through the resin under gravity flow. The entire process was repeated twice more until the water wash was $\text{pH} \leq 7$ and the methanol wash was clear and colorless.

6.2.2 Methods

6.2.2.1 Filler-Impregnated Resin Preparation

A weighed quantity of purified Amberchrom CG-71m beads was slurried with methanol, then mixed with a 1-dodecanol-methanol solution containing sufficient 1-dodecanol to fill 15% of the available volume of the beads. The mixture was then equilibrated (w/ shaking) for 24 hours and the 1-dodecanol-loaded beads recovered by rotary evaporation ($T = 55\text{ }^\circ\text{C}$) under reduced pressure.

6.2.2.2 Stagnantly-Pore Plugged (SPP) Resin Preparation

After impregnation of the resin beads with the 1-dodecanol filler, HDEHP, a 1 M solution of HDEHP in *n*-dodecane, a 1 M solution of HDEHP in $\text{C}_{10}\text{mimTf}_2\text{N}$, $\text{C}_{10}\text{mimDEHP}$, a 1 M solution of $\text{C}_{10}\text{mimDEHP}$ in *n*-dodecane, and a 1 M solution of $\text{C}_{10}\text{mimDEHP}$ in $\text{C}_{10}\text{mimTf}_2\text{N}$, all in methanol were slowly added to weighed quantities of 1-dodecanol-impregnated (stagnantly-pore plugged) resin. The methanol was then immediately removed with rotary evaporation ($T = 55\text{ }^\circ\text{C}$ with reduced pressure), leaving sorbents whose least accessible pores are blocked by 1-dodecanol and whose remaining pores are partially occupied by the extractant of interest or its solution.

6.2.2.3 Determination of Weight Distribution Ratios

Solid-liquid (weight) distribution ratios (D_w) were measured radiometrically using $^{152/154}\text{Eu}$ and ^{241}Am radiotracers. Specifically, the uptake of each radiotracer from a series of nitric acid solutions by the resins was measured by contacting a known volume (mL) of $^{152/154}\text{Eu}$ - or ^{241}Am -spiked acid solutions of appropriate concentration with a known quantity of resin. The ratio of the aqueous phase volume (mL) to the weight of the chromatographic material (in grams) typically ranged from 40-50. This ratio produces an easily measured decrease in the aqueous phase activity or concentration by contact with the resin. A two-hour contact time was used for equilibration. Following equilibration, an aliquot of aqueous phase was withdrawn from each culture tube and the activity counted.

From the counts or concentration of the aqueous phase both before and after contact with the resins, the weight distribution ratio (D_w) of $^{152/154}\text{Eu}$ or ^{241}Am was calculated by the following:

$$D_w = [(A_0 - A_f) / A_f] (V/w) \quad (6.2)$$

where A_0 and A_f are the aqueous phase activity (cpm) or concentration before and after equilibration, respectively, w is the mass (g) of the resin, and V is the volume of the aqueous phase (mL).

Separation factors were calculated by the following equation:

$$\text{Separation Factor (SF)} = D_{\text{Eu}} / D_{\text{Am}} \quad (6.3)$$

6.2.2.4 Metal Ion Uptake Kinetics

Into a series of culture tubes, 20-25 mg portions of resin were weighed. Each resin was contacted with 1 mL of dilute nitric acid solution spiked with the appropriate radiotracer. At specific time intervals, the aqueous phase was withdrawn from one of the test tubes, filtered through a plastic frit and its activity counted.

6.2.3 Equipment

A Bruker DPX 300 MHz NMR spectrometer equipped with a broad-band optimized BBO probe operating at a frequency of 300.13 MHz and referenced against tetramethylsilane at 25°C was used for all NMR measurements. The radiotracers were assayed using a Perkin-Elmer Model 2480 Automatic Gamma counter equipped with WIZARD² software.

6.3 Results and Discussion

Any attempt to change the chemistry of the TALSPEAK system must begin with a comparison of the distribution ratios of the lanthanide ions extracted to that of americium (Am^{3+}), a model actinide ion. If the changes do not provide increased separation factors relative to the conventional system, then they will not be adopted. McAlister *et al.* measured the resin capacity factor, k' , where $k' = 0.57D_{w,M^{n+}}$, of several organophosphorus extractant-impregnated commercial resins in the extraction of a series of lanthanides, actinides, and selected divalent metal ions. For Eu^{3+} and Am^{3+} , two ions that can serve as the basis for assessing the effectiveness of new systems for lanthanide-actinide separations, the commercial Ln resin was unable to provide adequate separation at either 0.01 M or 1 M HNO_3 , but did at 0.1 M HNO_3 , where $\text{SF}_{\text{Eu}/\text{Am}} \sim 5$. These results will be useful in evaluating the performance of the FIL.³³

Prior work with solutions of DEHP-based ILs has shown that they can provide increased metal ion uptake efficiency *vs.* analogous solutions of HDEHP. For example, Sun *et al.* prepared three quaternary ammonium and phosphonium, DEHP-based FILs, and examined their performance, dissolved in C₆mimTf₂N, relative to that of the HDEHP solution in the extraction of lanthanides from a “TALSPEAK-like” aqueous phase. As noted above, increased distribution ratios were observed for the light and heavy lanthanide ions relative to those of the middle lanthanide ions. The FILs exhibited middle lanthanide ion (*e.g.* Eu³⁺) extraction similar to that seen for the HDEHP solution, however.³⁹ Curiously, these authors did not measure the extraction of Am³⁺. There is thus no way to evaluate the utility of any of these systems as prospective improvement to conventional TALSPEAK.

Previous work by these authors and others has shown that the solubility of HDEHP in common IL families is often too low to be useful.^{28,37,39} On the basis of results obtained in this laboratory (Chapter 3), we have been able to avoid the issue of HDEHP insolubility. That is, HDEHP is completely miscible with conventional solvents (*e.g.* *n*-dodecane) and with long-chain, C_{*n*}mim⁺ ILs (*n*≥10). In fact, 1 M solutions of both HDEHP and C₁₀mimDEHP can be prepared readily in either C₁₀mimTf₂N or *n*-dodecane, and all of these solutions can serve as the stationary phase in an extraction chromatographic material. On the basis of the results discussed in Chapters 4 and 5, the best chromatographic performance can be expected for materials incorporating a thin layer of extractant in the intermediate size pores. The need for a thin stationary phase layer is even more important here given the high viscosity of FILs.^{40,41} In fact, loading the support beyond the volume occupied in the 10% (%w/w) HDEHP SPP resin may lead to lengthy equilibration times. Therefore, the volume occupied by the HDEHP in this resin will be used for all of the sorbents prepared here.

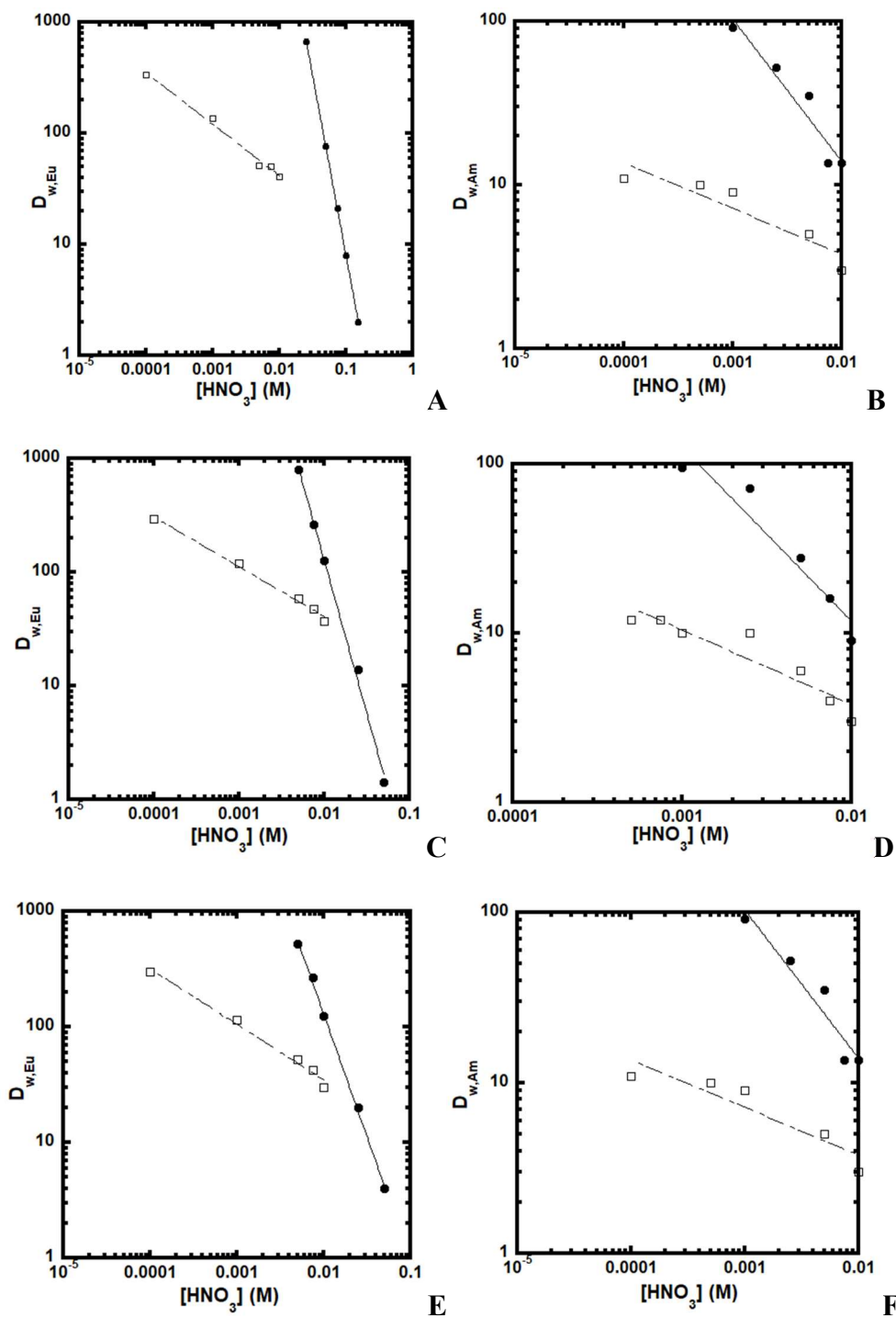


Figure 6.1A-F: Effect of nitric acid concentration on metal ion uptake in (A) undiluted HDEHP and C_{10} mimDEHP w/ Eu^{3+} (B) undiluted HDEHP and C_{10} mimDEHP w/ Am^{3+} (C) 1 M HDEHP and C_{10} mimDEHP in *n*-dodecane w/ Eu^{3+} (D) 1 M HDEHP and C_{10} mimDEHP in *n*-dodecane w/ Am^{3+} (E) 1 M HDEHP and C_{10} mimDEHP in C_{10} mimTf₂N w/ Eu^{3+} (F) 1 M HDEHP and C_{10} mimDEHP in C_{10} mimTf₂N w/ Am^{3+} . HDEHP (•); C_{10} mimDEHP (□); $T = 23 \pm 2^\circ C$. All extractants are supported on Amberchrom CG-71m resin whose deep pores have been blocked by 1-dodecanol (see text)

In our initial extraction studies, $D_{w,Eu}$ and $D_{w,Am}$ were measured for both neat HDEHP and $C_{10}mimDEHP$ and their solutions in either *n*-dodecane or $C_{10}mim^+Tf_2N^-$ impregnated into a SPP (1-dodecanol-loaded) resin. As shown in Figure 6.1A-F, all resins impregnated with HDEHP exhibit increased Eu^{3+} and Am^{3+} uptake efficiency (*i.e.* higher D_w values) relative to $C_{10}mimDEHP$. Consistent with published work as well was the similar Eu^{3+} uptake of HDEHP in both diluents.³⁷ The similar Eu^{3+} ion uptake of $C_{10}mimDEHP$ dissolved in $C_{10}mimTf_2N$ and *n*-dodecane is consistent with that shown by Sun *et al.*³⁹ The flattish dependence of $D_{w,Am}$ on the $C_{10}mimDEHP$ -based resins on acid concentration is consistent with the fact that the extractant lacks a proton to exchange with the metal ion. Unexpectedly, however, the uptake of Eu^{3+} on the same resins does show a dependence on the aqueous acidity. Although the reason for this observation is unknown at present, it is clearly potentially useful in achieving extraction selectivity for Eu over Am.

Of course, once a metal ion has been extracted (and ideally separated from other ions), it must be recovered (*i.e.*, back-extracted) from the organic phase, which is often accomplished by exploiting “acid swings” (*i.e.*, changes in aqueous acidity). Obviously, this approach will be difficult (or even impossible) for systems with acid dependencies of $D_{w,M}$ exhibiting near zero slopes (such as are seen in Figure 6.1A-F) or with high distribution ratios over a wide acidity range. Others have noted the insensitivity of D_w to aqueous acidity and the associated difficulty in stripping extracted metal ions when ILs incorporating an extractant are employed. Mohapatra *et al.*, for example, noted the difficulty in stripping Am^{3+} from a diglycolamide extractant tethered to a C_4mim^+ cation, a so-called “task-specific ionic liquid (TSIL)”, and observed a trend in the acid dependency similar to that seen here. This made necessary the use of 0.05 M ethylenediaminetetraacetic acid (EDTA) or DTPA in 1 M guanidine carbonate solutions to strip

the Am³⁺ from the TSIL.⁴⁴ While adding a complexing agent may be effective in metal ion stripping, the use of nitric acid is preferred, as it would keep the overall process simple. Sun *et al.* achieved almost 100% recovery of extracted Eu³⁺ after stripping from Aliquat 336⁺DEHP⁻ with 0.01 M HNO₃.⁴⁵ Similar recovery was also achieved while recovering lanthanide metal ions from a trioctylmethyl ammonium *bis*(2-ethylhexyl)phosphate FIL using 6 M HNO₃.³⁹ Unfortunately, contacting a DEHP-based FIL with a nitric acid solution at pH ≤ 2 can protonate the DEHP⁻ anion.⁴⁶ HDEHP would be made but so would a nitrate ionic liquid. This newly made IL could be significantly water-soluble, risking loss to the aqueous phase. Based on the acid dependencies observed here with both dilute and undiluted HDEHP, stripping these resins with HNO₃ should be simpler than with C₁₀mimDEHP.

Apparent from Figure 6.2A-F, a re-plot of that data from Figure 6.1A-F, is the selectivity (SF_{Eu/Am}) provided by both the pure and dilute HDEHP resins. This selectivity is certainly not expected given published results for analogous liquid-liquid systems,²⁷ but it is consistent with that observed in extraction chromatographic systems.³³ Upon dilution, the 1 M HDEHP in *n*-dodecane resin reached SF_{Eu/Am} = 28 at 0.005 M HNO₃ while dilution in C₁₀mimTf₂N reached SF_{Eu/Am} = 19 at 0.0075 M HNO₃. The highest separation achieved by the undiluted HDEHP-based resin was SF_{Eu/Am} = 13 at 0.025 M HNO₃. With no separation factor below nine for HDEHP, dilution does seem to buy enhanced selectivity.

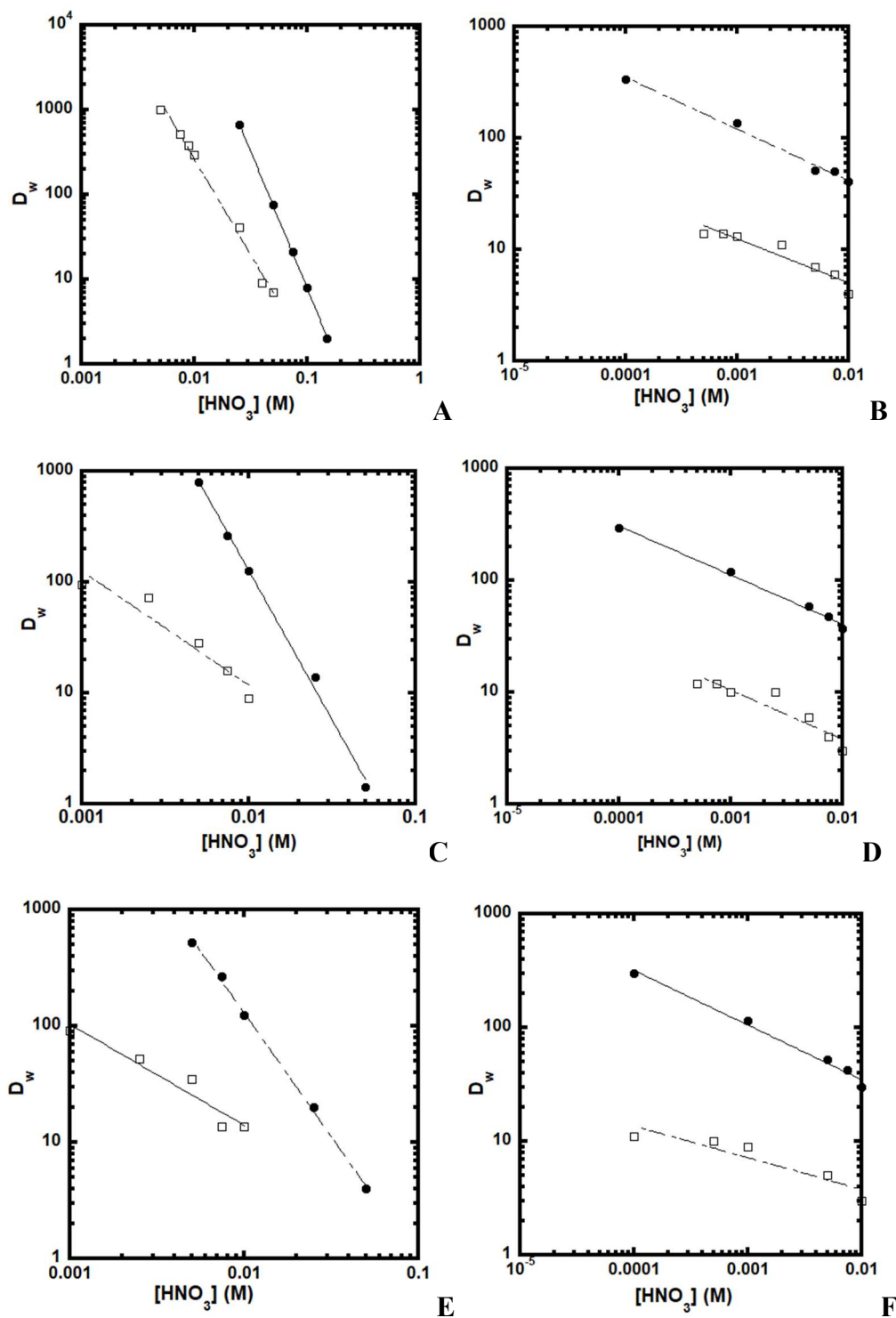


Figure 6.2A-F: Effect of nitric acid concentration on Eu^{3+} (\bullet) and Am^{3+} (\square) uptake in undiluted HDEHP (A), undiluted $\text{C}_{10}\text{mimDEHP}$ (B), 1 M HDEHP in n-dd (C), 1 M $\text{C}_{10}\text{mimDEHP}$ in n-dd (D), 1 M HDEHP in $\text{C}_{10}\text{mimTf}_2\text{N}$ (E) and 1 M $\text{C}_{10}\text{mimDEHP}$ in $\text{C}_{10}\text{mimTf}_2\text{N}$ (F); $T = 23 \pm 2^\circ\text{C}$.

The C₁₀mimDEHP, in both pure and dilute form, exhibits comparable selectivity to the pure and dilute HDEHP resins, with no separation factor less than seven for all resins and a high of 27 for the 1 M C₁₀mimDEHP in C₁₀mimTf₂N at 0.0001 M HNO₃. The undiluted C₁₀mimDEHP exhibits a maximum separation of 10 at 0.01 M and 0.001 M HNO₃ while that of 1 M C₁₀mimDEHP in *n*-dodecane reaches as high as 12 at 0.01 M HNO₃. Similar to the HDEHP SPP resins, the dilution of C₁₀mimDEHP does seem to exhibit increased resin selectivity.

Although extraction via ion exchange should be minimal for C₁₀mim⁺ given its hydrophobicity,⁴² and the Eu³⁺ and Am³⁺ acid dependencies for C₁₀mimDEHP show a near-zero slope, nitrate and extractant dependencies were measured for the C₁₀mimDEHP resins. The only other possible extraction mechanism, ion exchange, is unlikely, given the hydrophobicity of the C₁₀mim⁺ cation and the similar Am³⁺ extraction mechanism of HDEHP diluted in both *n*-dodecane and C₁₀mimTf₂N.³⁸ Like the flattish acid dependency, the effect of nitrate concentration on metal ion uptake, shown in Figure 6.3A-F, is negligible, indicating the absence of nitrate in the extraction mechanism.

As both the nitrate and acid dependencies exhibit near zero slopes, the only possible extraction mechanism for the C₁₀mimDEHP is through ion exchange of the C₁₀mim⁺ cation. The extractant dependencies shown in Figure 6.4, indicate three C₁₀mimDEHP molecules are used, allowing for an ion exchange process to occur with Eu³⁺ and Am³⁺.

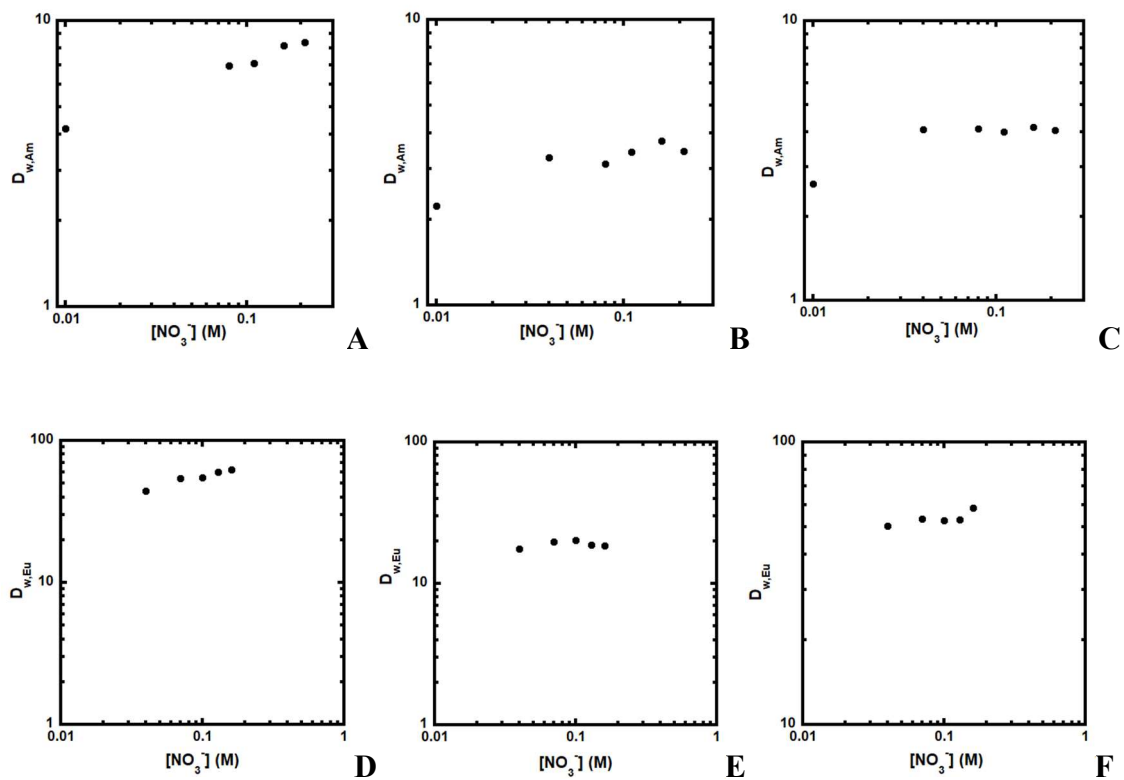


Figure 6.3A-F: Nitrate dependence on Am^{3+} uptake for undilute $C_{10mim}DEHP$ (A), 1 M $C_{10mim}DEHP$ in n -dd (B) and 1 M $C_{10mim}DEHP$ in $C_{10mim}Tf_2N$ (C) and Eu^{3+} uptake for undilute $C_{10mim}DEHP$ (D), 1 M $C_{10mim}DEHP$ in n -dd (E) and 1 M $C_{10mim}DEHP$ in $C_{10mim}Tf_2N$ (F).

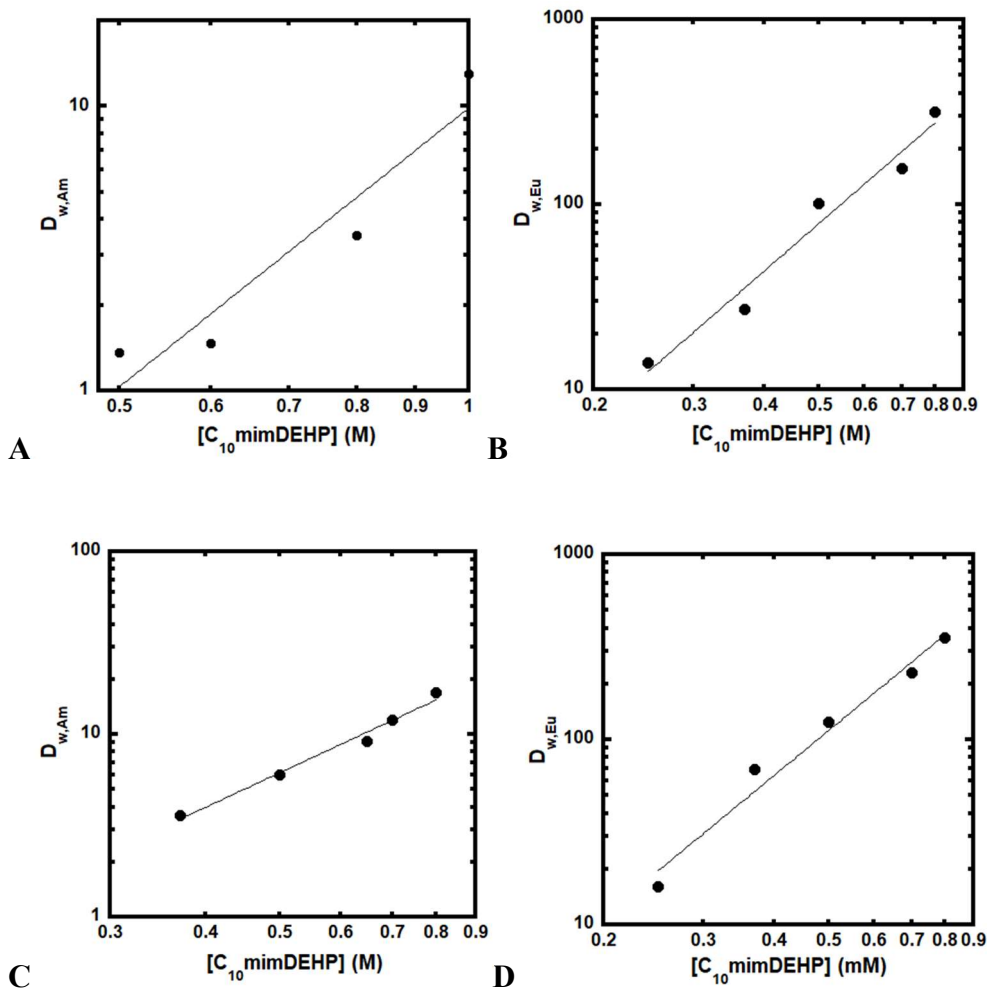


Figure 6.4A-D: Extractant dependence on Am^{3+} and Eu^{3+} uptake for 1 M $C_{10}mimDEHP$ in n -dd (A,B) and 1 M $C_{10}mimDEHP$ in $C_{10}mimTf_2N$ (C,D).

Previous reports discuss HDEHP diluted in short-chained, C_nmim^+ ILs ($n = 4,6$), as the organic phase, which are much more hydrophilic than that used here, $C_{10}mim^+$, allowing for enhanced lanthanide ion uptake relative to DIPB but at a cost of losing the IL cation to the aqueous due to the ion exchange extraction mechanism.³⁷ Given that HDEHP dissolved in $C_{10}mimTf_2N$ exhibits similar D_{Eu} values compared to HDEHP dissolved in n -dodecane and DIPB, this may explain the enhanced metal ion uptake for the HDEHP systems compared to that of the $C_{10}mimDEHP$ discussed here. As $C_{10}mim^+$ nearly suppresses all cation exchange,⁴² thus exhibiting comparable extraction behavior to conventional diluents, and the $C_{10}mimDEHP$

possesses no proton to exchange with the trivalent metal ions, the distribution ratios exhibited by the undiluted and dilute C₁₀mimDEHP should be decreased compared to the undiluted and dilute HDEHP as the trivalent metal ions can more easily exchange with H⁺ than the hydrophobic, C₁₀mim⁺.

To verify the extraction mechanism was ion exchange, the aqueous phase was spiked with the C₁₀mim⁺ cation. As shown in Figure 6.5, the distribution ratios drop immediately from 0 to 10 mM C₁₀mim⁺ proving that ion exchange of C₁₀mim⁺ for Eu³⁺ or Am³⁺ is the extraction mechanism. These results were certainly unexpected given the hydrophobicity of the C₁₀mim⁺ cation and that published previously showing the similar extraction mechanism (*i.e.* the absence of ion exchange) of 1 M HDEHP in n-dodecane and C₁₀mimTf₂N.³⁸ While HDEHP loses H⁺ to the aqueous phase, obviously, during extraction, this is readily replaced by contacting the organic phase with dilute HNO₃. A similar process could be used to replenish the C₁₀mim⁺ lost during extraction by contacting the resin with dilute C₁₀mim⁺NO₃⁻ solution. Unfortunately, this would be an expensive endeavor, giving the HDEHP resins yet another advantage over their C₁₀mimDEHP counterparts.

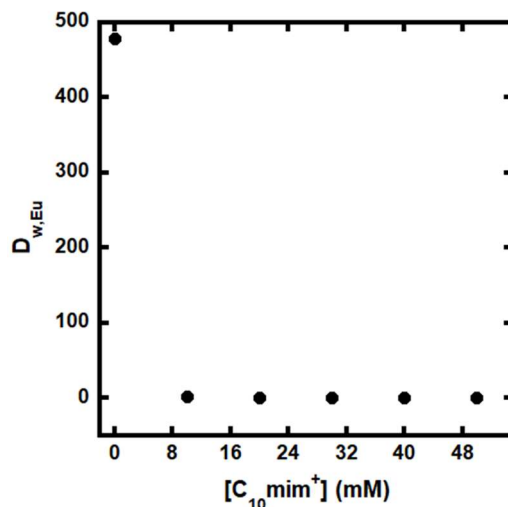


Figure 6.5: Effect of spiking aqueous phase with C₁₀mim⁺ cation on Eu³⁺ uptake for undiluted C₁₀mimDEHP SPP resin

The results of the last metric to assess C₁₀mimDEHP performance relative to HDEHP, kinetics, are shown in Figure 6.6 and Table 6.1. Equilibrium for both resins is essentially achieved in approximately 30 minutes well before the contact time of two hours used in all experiments. The undiluted HDEHP resin does achieve equilibrium more quickly than the undiluted C₁₀mimDEHP resin. This is responsible given the viscous nature of FILs in published works.^{30,31} Should the application warrant the use of a FIL, however, equilibrium can be achieved in a short time with the loading used here. Increased loading of the FIL into the SPP support would no doubt increase the time required to achieve equilibrium.

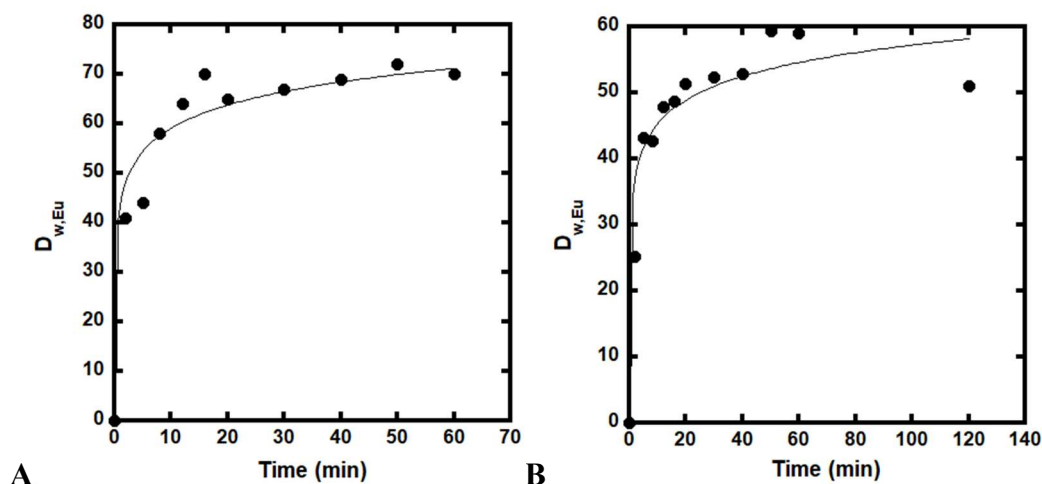


Figure 6.6A-B: Kinetics of the uptake of europium ion from 0.05 M and 0.005 M HNO₃ by 10% (w/w) HDEHP SPP and 9.69% (w/w) C₁₀mimDEHP SPP resins, respectively.

Table 6.1: Kinetics of the uptake of europium ion from 0.05 M and 0.005 M HNO₃ by 10% (w/w) HDEHP SPP and 9.69% (w/w) C₁₀mimDEHP SPP resins, respectively

Resin	%Equilibrium at 2 minutes	%Equilibrium at 20 minutes	Time to achieve 90% equilibrium
10% HDEHP SPP	70.7	93.3	14.1
9.69% C ₁₀ mimDEHP SPP	66.9	89.1	21.8

6.4 Conclusions

The results presented here provide a direct comparison of an undiluted extractant to its FIL analogue in terms of metal ion extractability, Eu³⁺/Am³⁺ selectivity, physical stability, and ease of stripping. Of the sorbents characterized here, that containing 10% (w/w) undiluted HDEHP provided better metal ion extraction efficiency and Eu³⁺/Am³⁺ selectivity equal to or better than that observed for undiluted C₁₀mimDEHP or its solutions in *n*-dodecane or C₁₀mim⁺Tf₂N⁻. While some DEHP-based FILs have been reported to exhibit higher metal ion extraction efficiency than dilute HDEHP,³⁹ loss of IL cation to the aqueous still occurs even with long-chained (*e.g.* C₁₀mim⁺) cations.

Lengthening the cation alkyl chain may further suppress ion exchange but could come with undesirable side effects. Wankowski *et al.* noted the presence of micelle formation in pyridinium-based ILs with $n = 12, 14$ which, unexpectedly, led to the loss of the IL cation to the aqueous phase. As this process favored ion exchange, the resulting acid dependencies of these same ILs were almost superimposable with short-chained ILs (*e.g.* $n = 7$).⁴⁷ As observed here, the C₁₀mimDEHP exhibited increased metal uptake in dilute nitric acid solutions but at a cost to ion exchange. Furthermore, the loss of DEHP⁻ is also possible should more concentrated acids be used ($\text{pH} \leq 2$).⁴⁶ Clearly then, interested readers must be mindful of all exchange processes in pursuing their own applications.

Previous work by this author noted the limited solubility of HDEHP in ILs, especially those with short alkyl chains (*i.e.* C₂mim⁺, C₄mim⁺).²⁸ In mixing equal volumes of C₁₀mimDEHP and C₂mimTf₂N, though, complete miscibility was observed. As several FILs exhibited increased metal ion uptake with the light and heavy lanthanides relative to HDEHP, should the loss of the IL cation be acceptable, the use of a FIL may be appropriate in this instance. If one is interested in studying the middle lanthanide ions and is limited by IL stability, however, simply using HDEHP impregnated onto the SPP extraction chromatographic support will suffice.

6.5 References

1. Alvarez, S. (2013). A cartography of the van der Waals territories. *Dalton Transactions*, 42, 8617–8636.
2. Warf, J. C. (1949). Extraction of cerium(IV) nitrate by butyl phosphate. *Journal of the American Chemical Society*, 71, 3257–3258.

3. Peppard, D.F.; Mason, G.W.; Driscoll, W.J.; McCarty, S. (1959). Application of phosphoric acid esters to the isolation of certain trans-plutonides by liquid-liquid extraction. *Journal of Inorganic and Nuclear Chemistry*, *12*, 141–148.
4. Isaac, N.M., Fields, P.R., Gruen, D. M. (1961). Solvent extraction of actinides and lanthanides from molten salts. *Journal of Inorganic and Nuclear Chemistry*, *21*, 152–168.
5. Peppard, D.F., Moline, S.W., Mason, G. W. (1957). Isolation of berkelium by solvent extraction of the tetravalent species. *Journal of Inorganic and Nuclear Chemistry*, *4*, 344–348.
6. Weaver, B., & Kappelmann, F. A. (1964). *TALSPEAK: A new method of separating americium and curium from the lanthanides by extraction from an aqueous solution of an aminopolyacetic acid complex with a monoacidic organophosphate or phosphonate* (Vol. 32). ORNL-3559.
7. Nash, K. L. (2015). The chemistry of TALSPEAK: A review of the science. *Solvent Extraction and Ion Exchange*, *33*, 1-55.
8. Baranyai, K. J., Deacon, G. B., MacFarlane, D. R., Pringle, J. M., & Scott, J. L. (2004). Thermal degradation of ionic liquids at elevated temperatures. *Australian Journal of Chemistry*, *57*, 145–147.
9. Freire, M. G., Neves, C. M. S. S., Carvalho, P. J., Gardas, R. L., Fernandes, A. M., Marrucho, I. M., Coutinho, J. A. P. (2007). Mutual solubilities of water and hydrophobic ionic liquids. *Journal of Physical Chemistry B*, *111*, 13082–13089.
10. Sengupta, A., Mohapatra, P. K., Iqbal, M., Verboom, W., Huskens, J., & Godbole, S. V. (2012). Extraction of Am(III) using novel solvent systems containing a tripodal diglycolamide ligand in room temperature ionic liquids: A “green” approach for radioactive waste processing. *RSC Advances*, *2*, 7492–7500.
11. Shimojo, K., & Goto, M. (2004). Solvent extraction and stripping of silver ions in room-temperature ionic liquids containing calixarenes. *Analytical Chemistry*, *76*, 5039–5044.
12. Idris, A., Vijayaraghavan, R., Rana, U. A., Patti, A. F., & MacFarlane, D. R. (2014). Dissolution and regeneration of wool keratin in ionic liquids. *Green Chemistry*, *16*, 2857–2864.
13. Fort, D. A., Swatloski, R. P., Moyna, P., Rogers, R. D., & Moyna, G. (2006). Use of ionic liquids in the study of fruit ripening by high-resolution ¹³C NMR spectroscopy: “Green” solvents meet green bananas. *Chemical Communications*, *7*, 714–716.
14. Schröder, C. (2017). Proteins in ionic liquids: current status of experiments and simulations. *Topics in Current Chemistry*, *375*, 1-26.

15. Yoon, S. J., Lee, J. G., Tajima, H., Yamasaki, A., Kiyono, F., Nakazato, T., & Tao, H. (2010). Extraction of lanthanide ions from aqueous solution by *bis*(2-ethylhexyl)phosphoric acid with room-temperature ionic liquids. *Journal of Industrial and Engineering Chemistry*, *16*, 350–354.
16. Bhattacharyya, A., Ansari, S. A., Gadly, T., Ghosh, S. K., Mohapatra, M., & Mohapatra, P. K. (2015). A remarkable enhancement in Am³⁺/Eu³⁺ selectivity by an ionic liquid-based solvent containing bis-1,2,4-triazinyl pyridine derivatives: DFT validation of experimental results. *Dalton Transactions*, *44*, 6193–6201.
17. Dietz, M. L., & Dzielawa, J. A. (2001). Ion-exchange as a mode of cation transfer into room-temperature ionic liquids containing crown ethers: implications for the “greenness” of ionic liquids as diluents in liquid-liquid extraction. *Chemical Communications*, *20*, 2124–2125.
18. Rout, A., Souza, E. R., & Binnemans, K. (2014). Solvent extraction of europium(III) to a fluorine-free ionic liquid phase with a diglycolamic acid extractant. *RSC Advances*, *4*, 11899–11906.
19. Zhou, H., Ao, Y., Yuan, J., Peng, J., Li, J., & Zhai, M. (2014). Extraction mechanism and γ -radiation effect on the removal of Eu³⁺ by a novel BTPPhen/[C_nmim][NTf₂] system in the presence of nitric acid. *RSC Advances*, *4*, 45612–45618.
20. Bell, J. R., Luo, H., & Dai, S. (2012). Solvent extraction separation of La³⁺ and Ba²⁺ using imidazolium ionic liquids and TODGA extractant. *Separation Science and Technology (Philadelphia)*, *47*, 2002–2006.
21. Sun, X., Ji, Y., Hu, F., He, B., Chen, J., & Li, D. (2010). The inner synergistic effect of bifunctional ionic liquid extractant for solvent extraction. *Talanta*, *81*, 1877–1883.
22. Rout, A., Venkatesan, K. A., Srinivasan, T. G., & Vasudeva Rao, P. R. (2011). Room temperature ionic liquid diluent for the extraction of Eu(III) using TRUEX extractants. *Journal of Radioanalytical and Nuclear Chemistry*, *290*, 215–219.
23. Sengupta, A., Mohapatra, P. K., Kadam, R. M., Manna, D., Ghanty, T. K., Iqbal, M., Verboom, W. (2014). Diglycolamide-functionalized task specific ionic liquids for nuclear waste remediation: Extraction, luminescence, theoretical and EPR investigations. *RSC Advances*, *4*, 46613–46623.
24. Luo, H. Dai, S. Bonnesen, P.V. Buchanan III, A. C., Holbrey, J.D., Bridges, N.J., Rogers, R.D. (2004). Extraction of cesium ions from aqueous solutions using calix[4]arene-bis(tert-octylbenzo-crown-6) in ionic liquids. *Analytical Chemistry*, *76*, 3078–3083.
25. Panja, S., Mohapatra, P.K., Tripathi, S.C., Gandhi, P.M., Janardan, P. (2012). A highly efficient solvent system containing TODGA in room temperature ionic liquids for actinide extraction. *Separation and Purification Technology*, *96*, 289–295.

26. Rao, V., Venkatesan, P.R., Rout, A., Srinivasan, T. G., Nagarajan, K. (2012). Potential applications of room temperature ionic liquids for fission products and actinide separation. *Separation Science and Technology*, 47, 204–222.
27. Rama Swami, K., Kumaresan, R., Venkatesan, K. A., & Antony, M. P. (2017). Synergic extraction of Am(III) and Eu(III) in N,N-dioctyl-2-hydroxyacetamide-bis(2-ethylhexyl)phosphoric acid solvent system. *Journal of Molecular Liquids*, 232, 507–515.
28. Smith, C. D., Foersterling, F. H., & Dietz, M.L. (2020). Solvent structural effects on the solubility of bis(2-ethylhexyl) phosphoric acid (HDEHP) in room-temperature ionic liquids (RTILs). *Separation Science and Technology*, 55, 1–11.
29. Dietz, M. L., Hawkins C. A. (2020). Task-specific ionic liquids for metal ion extraction: progress, challenges, and prospects. Bruce A. Moyer (Ed.), In *Ion Exchange and Solvent Extraction* (Vol. 23, pp. 83–113). Boca Raton, FL: CRC Press.
30. Sengupta, A., Murali, M. S., Mohapatra, P. K., Iqbal, M., Huskens, J., & Verboom, W. (2015). An insight into the complexation of UO_2^{2+} functionalized task specific ionic liquid : Kinetic, cyclic voltammetric, extraction and spectroscopic investigations. *Polyhedron*, 102, 549–555.
31. Wang, G., Hou, W., Xiao, F., Geng, J., Wu, Y., & Zhang, Z. (2011). Low-viscosity triethylbutylammonium acetate as a task-specific ionic liquid for reversible CO_2 Absorption. *J. Chem. Eng. Data*, 56, 1125–1133.
32. Rout, A., Kotlarska, J., Dehaen, W., & Binnemans, K. (2013). Liquid-liquid extraction of neodymium(III) by dialkylphosphate ionic liquids from acidic medium: The importance of the ionic liquid cation. *Physical Chemistry Chemical Physics*, 15, 16533–16541.
33. McAlister, D. R., & Horwitz, P. E. (2007). Characterization of extraction of chromatographic materials containing bis(2-ethyl-1-hexyl)phosphoric acid, 2-ethyl-1-hexyl(2-ethyl-1-hexyl) phosphonic acid, and bis(2,4,4-trimethyl-1-pentyl)phosphinic acid. *Solvent Extraction and Ion Exchange*, 25, 757–769.
34. Deetlefs, M., & Seddon, K. R. (2003). Improved preparations of ionic liquids using microwave irradiation. *Green Chemistry*, 5, 181–186.
35. Luo, H., Huang, J.-F., & Dai, S. (2008). Studies on thermal properties of selected aprotic and protic ionic liquids. *Separation Science and Technology*, 43, 2473–2488.
36. Sun, X., Ji, Y., Liu, Y., Chen, J., & Li, D. (2010). An engineering-purpose preparation strategy for ammonium-type ionic liquid with high purity. *AIChE Journal*, 56, 989–996.
37. Sun, X., Bell, J. R., Luo, H., & Dai, S. (2011). Extraction separation of rare-earth ions via competitive ligand complexations between aqueous and ionic-liquid phases. *Dalton Transactions*, 40, 8019–8023.

38. Cocalia, V. A., Jensen, M. P., Holbrey, J. D., Spear, S. K., Stepinski, D. C., & Rogers, R. D. (2005). Identical extraction behavior and coordination of trivalent or hexavalent f-element cations using ionic liquid and molecular solvents. *Dalton Transactions*, *11*, 1966–1971.
39. Sun, X., Luo, H., & Dai, S. (2012). Solvent extraction of rare-earth ions based on functionalized ionic liquids. *Talanta*, *90*, 132–137.
40. Gutowski, K. E., & Maginn, E. J. (2009). Amine-functionalized task-specific ionic liquids : A mechanistic explanation for the dramatic increase in viscosity upon complexation with CO₂ from molecular simulation. *Journal of the American Chemical Society*, *130*, 14690–14704.
41. Kasahara, S., Kamio, E., Otani, A., & Matsuyama, H. (2014). Fundamental investigation of the factors controlling the CO₂ permeability of facilitated transport membranes containing amine- functionalized task-specific ionic liquids. *Industrial & Engineering Chemistry Research*, *53*, 2422–2431.
42. Hawkins, C. (2012). Fundamental and applied studies of metal ion extraction by crown ethers into imidazolium-based room temperature ionic liquids. University of Wisconsin-Milwaukee, Milwaukee, WI.
43. Rout, A., Karmakar, S., Venkatesan, K. A., Srinivasan, T. G., & Vasudeva Rao, P. R. (2011). Room temperature ionic liquid diluent for the mutual separation of europium(III) from americium(III). *Separation and Purification Technology*, *81*, 109–115.
44. Mohapatra, P. K., Sengupta, A., Iqbal, M., Huskens, J., & Verboom, W. (2013). Highly efficient diglycolamide-based task-specific ionic liquids: Synthesis, unusual extraction behavior, irradiation, and fluorescence studies. *Chemistry - A European Journal*, *19*, 3230–3238.
45. Sun, X., Ji, Y., Hu, F., He, B., Chen, J., & Li, D. (2010). The inner synergistic effect of bifunctional ionic liquid extractant for solvent extraction. *Talanta*, *81*, 1877–1883.
46. Djane, N.K., Ndungu, K., Malcus, F., Johansson, G. Mathiasson, L. (1997). Supported liquid membrane enrichment using an organophosphorus extractant for analytical trace metal determinations in river waters. *Fresenius J Anal Chem*, *358*, 822–827.
47. Wankowski, J. L., Kaul, M. J., & Dietz, M. L. (2017). Micelle formation as a factor influencing the mode(s) of metal ion partitioning into: *N*-alkylpyridinium-based ionic liquids (ILs): Implications for the design of IL-based extraction systems. *Green Chemistry*, *19*, 5674–5682.

Chapter 7:

CONCLUSIONS AND RECOMMENDATIONS

7.1 Conclusions

In this work, the solubility of a well-known lanthanide extractant and the basis of the TALSPEAK Process, HDEHP, was measured in a series of ILs using a novel, thermogravimetric method. In particular, the method was employed to determine the effect on solubility of the IL cation and anion. While knowledge of extractant solubility is essential in designing a liquid-liquid extraction system, few studies have been published on this topic. Even so, certain families of extractants, such as non-aromatic crown ethers lack a suitable detection tag. Phosphorus-based extractants such as HDEHP may be quantified via ICP-MS or ^{31}P NMR but either require large amounts of sample or are inconvenient, respectively. As ILs and non-aromatic metal-ion extractants possess starkly contrasting thermal stabilities, degrading the extractant while leaving the IL intact made possible the quantification of three different extractants using thermogravimetric analysis.

Understanding the solvent characteristics necessary to maximize the solubility of HDEHP in ILs was essential in order to prepare a HDEHP solution to compare to a DEHP-based IL in pure form and in solution. Because extractions of lanthanide and actinide metal ions using HDEHP dissolved in ILs would be eventually carried out, the solubility of HDEHP in several families of ILs was measured. With the results indicating an effect of both IL cation and anion on solubility, the impact of each was studied. The alkyl chain length of the IL cation, solvent molar volume, and IL anion hydrogen bond basicity were used to explain trends in solubility, with molar volume having the greatest impact. With factors governing HDEHP solubility

known, the experimental concentrations for studying metal ion extraction in FILs using both liquid-liquid extractions and extraction chromatographic systems were determined.

As FILs are highly viscous solvents², they are most conveniently evaluated following impregnation into a solid support for extraction. A thin layer of FIL impregnated into a solid support is required to avoid lengthy equilibration times. With this goal in mind, a clear map of the interior of the solid support was constructed using surface area and column efficiency measurements to obtain a support filled as planned. First, the surface area of an inert, hydrophilic support Amberchrom CG-71m impregnated with a hydrophilic filler, PTHF 250, was measured. By plotting surface area as a function of support loading, the loading levels corresponding to filled micro- and mesopores were determined. The same support was then loaded with HDEHP to assess column efficiency, with the idea that the most efficient material would correspond to the thinnest extractant layer in the mesopores. In filling the support with HDEHP to loading levels bracketing the points corresponding to filled micro- and mesopores and then measuring column efficiency, the loading that produced a thin layer of extractant was determined. The results showed that the number of theoretical plates exhibited a maximum at intermediate levels (20% (w/w) HDEHP) of extractant loading. These results proved useful not only in designing the studies employing FILs for extraction, but also in separating adjacent lanthanides. In particular, the separation of trivalent europium and neodymium, as well as of trivalent europium and gadolinium was achieved simply by varying the extractant loading of the support. Previous works in intra-lanthanide separations required expensive mesoporous materials³, laser reduction⁴ of Eu^{3+} to Eu^{2+} , or extractant incorporation into the solid support matrix to separate Eu^{3+} from adjacent lanthanide ions⁵. These elaborate procedures often did not produce adequate resolution³, produced hydroxyl radicals⁴, or required multiple columns for

separation.⁵ The 20% (%w/w) HDEHP resin merely required a laboratory balance and rotary evaporator for resin preparation and dilute nitric acid for elution. During column elution of $\text{Eu}^{3+}/\text{Gd}^{3+}$, the same resin exhibited improved resolution compared to the commercial Ln resin due to its increased theoretical plate count.

By filling the smallest pores of the support to near capacity with a water-insoluble, inert filler and then adding an extractant atop this filler, substantial improvements in column efficiency and peak shape were also observed. Several fillers were evaluated to determine which characteristics are most important. Again, column efficiencies were measured with HDEHP atop filler to determine the appropriate layer thickness. Ultimately, 1-dodecanol was chosen as the best filler due to its viscosity at room temperature, support compatibility, and hydrophobicity. The reduced peak asymmetry was found to facilitate both the separation of europium and neodymium and that of europium and gadolinium. Contrary to the resin impregnated with pure HDEHP, 10% (%w/w) HDEHP SPP was the most efficient loading. Besides the improved column efficiency relative to the commercial resin, the near constant peak asymmetry (1.1-1.2) for all loadings was another welcomed surprise. With the peak asymmetry for the supports filled with pure HDEHP spanning a greater range (1.14-1.67), metal ion diffusion into the unfilled micropores proved to be the source of peak asymmetry.

Once the bead interior had been completely mapped, FILs were examined to assess their utility in metal ion separations versus their conventional analogues. Once the support micropores were filled with an inert filler, a thin layer of FIL was added atop. Of the sorbents characterized, undiluted HDEHP provided better metal ion extraction efficiency and $\text{Eu}^{3+}/\text{Am}^{3+}$ selectivity equal to or better than that observed for undiluted $\text{C}_{10}\text{mimDEHP}$ or its solutions in *n*-dodecane or $\text{C}_{10}\text{mim}^+\text{Tf}_2\text{N}^-$. Furthermore, the loss of the FIL cation to the aqueous phase still

occurs even with long-chain (*e.g.* C₁₀mim⁺) cations calling into question their physical stability. The highly viscous nature of the FIL also caused slower metal ion uptake kinetics relative to HDEHP. The lone advantage of DEHP-based FILs relative to neat or dilute HDEHP is their ability to efficiently extract the light and heavy lanthanides.

7.2 Recommendations

The following are a series of recommendations for improving extraction chromatographic materials as well as recommended studies to address the poor solubility of metal ion extractants in ILs. This is by no means a comprehensive list, but it will open the door to a new family of extraction chromatographic materials.

7.2.1 Assessing extractant solubility in ILs

While ILs are known to dissolve a wide variety of substances, the poor solubility of several metal ion extractants has been well documented.^{6,7} Fortunately, the families of extractants, BTPs and calixarenes, for which thermogravimetric analysis was not applicable possess aromatic rings making UV-Vis analysis possible. Furthermore, no solubility study of these extractants in ILs has been undertaken. Such a study will undoubtedly prove useful for BTPs given their selectivity in lanthanide-actinide separations. It would also be worthwhile to learn if the same factors governing HDEHP solubility in ILs, especially molar volume, control that of BTPs and calixarenes.

7.2.2 Effect of extractant loading on solid supports with high surface area

By varying the loading of extractant on a solid support, a new option will be available to separate the *f*-elements that merely requires commercially available materials without further modification. A similar study would be useful with a support of higher surface area and/ or a

different pore structure. Mesoporous materials, such as SBA-15 ($\geq 550 \text{ m}^2/\text{g}$)⁸, MCM-41 ($> 800 \text{ m}^2/\text{g}$)⁹ or KIT-6 ($600\text{-}800 \text{ m}^2/\text{g}$)¹⁰, are hydrophilic, uniform porosity supports with greater surface area than Amberchrom CG-71m ($500 \text{ m}^2/\text{g}$). Due to the uniform porosity these supports, varying the extractant load may not yield the same effect on column efficiency as Amberchrom CG-71m, but the higher surface area will permit greater extractant loading while maintaining a thin layer on the support.

7.2.3 Filling a solid support with a thermally-polymerizable monomer

1-dodecanol proved a useful filler due to its viscosity at room temperature, compatibility with the support, and, apparently, minimal interaction with the extractant, HDEHP. While 1-dodecanol was not detected during column preparation and use, it still possesses a finite water solubility¹¹ raising concerns over its long-term column stability. Impregnating the support with a thermally-polymerizable monomer, such as styrene, would address that issue. Styrene possesses a lower octanol-water partitioning coefficient ($\log P_{ow} = 2.95$)¹² than 1-dodecanol ($\log P_{ow} = 5.13$)¹¹ meaning it should be just as, if not more, compatible with the support than 1-dodecanol. As styrene can polymerize into polystyrene thermally,¹³ no polymer initiator is needed thereby simplifying the process.

7.2.4 Applying a thin layer of extractant in controlled-porosity supports

The development of controlled porosity supports produced a near two-fold improvement in efficiency over the commercial support. As HDEHP is a common extractant in metal ion extraction, preparing the same support with another commercially available extractant, such as N,N,N',N'-Tetraoctyl Diglycolamide (TODGA) would be worth pursuing. Horwitz et al. mentioned the lack of selectivity among heavier lanthanides of a TODGA-impregnated resin.¹⁴

Gharibyan noted the poor separation between americium and curium with several commercial resins, including EiChrom's Ln resin (HDEHP-based) and DGA Normal (TODGA-based) resins.¹⁵ Because americium and curium are actinides, nitrogen-based extractants are more applicable to these metals, whereas phosphorus-based extractants, such as HDEHP, are preferred by the lanthanides. A controlled porosity support with a thin layer of TODGA for Am/Cm separation is worth consideration.

7.3 References

- 1.) Peppard, D.F.; Mason, G.W.; Driscoll, W.J.; McCarty, S. (1959). Application of Phosphoric Acid Esters to the Isolation of Certain trans-Plutonides by Liquid-Liquid Extraction. *Journal of Inorganic and Nuclear Chemistry*, 12, 141–148.
- 2.) Mohapatra, P. K., Kandwal, P., Iqbal, M., Huskens, J., Murali, M. S., & Verboom, W. (2013). A novel CMPO-functionalized task specific ionic liquid: synthesis, extraction and spectroscopic investigations of actinide and lanthanide complexes. *Dalton Transactions*, 42, 4343–4347.
- 3.) Bertelsen, E. R., Deodhar, G., Kluherz, K. T., Davidson, M., Adams, M. L., Trewyn, B. G., & Shafer, J. C. (2019). Microcolumn lanthanide separation using *bis*(2-ethylhexyl) phosphoric acid functionalized ordered mesoporous carbon materials. *Journal of Chromatography A*, 1595, 248–256.
- 4.) Li, S. C., Kim, S. C., Kang, C. S., Kim, C. J., & Kang, C. J. (2018). Separation of samarium, europium and gadolinium in high purity using photochemical reduction-extraction chromatography. *Hydrometallurgy*, 178, 181–187.
- 5.) Kondo, K., Oguri, M., & Matsumoto, M. (2013). Novel separation of samarium, europium and gadolinium using a column packed with microcapsules containing 2-ethylhexylphosphonic acid mono-2-ethylhexyl ester. *Chemical Engineering Transactions*, 32, 919–924.
- 6.) Shimojo, K., & Goto, M. (2004). First application of calixarenes as extractants in room-temperature ionic liquids. *Chemistry Letters*, 33, 320–321.
- 7.) Bhattacharyya, A., Ansari, S. A., Gadly, T., Ghosh, S. K., Mohapatra, M., & Mohapatra, P. K. (2015). A remarkable enhancement in Am³⁺/Eu³⁺ selectivity by an ionic liquid-based solvent containing bis-1,2,4-triazinyl pyridine derivatives: DFT validation of experimental results. *Dalton Transactions*, 44, 6193–6201.
- 8.) ACS Materials. (2019). Technical data sheet: ACS material mesoporous silica molecular sieve SBA-15. Pasadena, CA: ACS Material.

- 9.) ACS materials. (2018). ACS material MCM-41: Type A and type B. Pasadena, CA:ACS Material.
- 10.) ACS Materials. (2017). Technical data sheet: ACS material mesoporous silica molecular sieve KIT-6. Pasadena, CA: ACS Material.
- 11.) Millipore Sigma (2018). *Safety data sheet: 1-dodecanol*. Darmstadt, Germany: Millipore Sigma.
- 12.) Millipore Sigma (2017). Safety data sheet: Styrene. *SDS Styrene*. Darmstadt, Germany: Millipore Sigma.
- 13.) Lloyd, L. E. (1952). *Styrene: Its Polymers, Copolymers and Derivatives*. (R. F. Boundy, R.H.; Boyer, Ed.). Baltimore, MA: Reinhold Publishing Corporation.
- 14.) Horwitz, E. P., McAlister, D. R., Bond, A. H., & Barrans, J. E. (2005). Novel extraction of chromatographic resins based on tetraalkyldiglycolamides: Characterization and potential applications. *Solvent Extraction and Ion Exchange*, 23, 319–344.
- 15.) Gharibyan, N., Dailey, A., McLain, D. R., Bond, E. M., Moody, W. A., Happel, S., & Sudowe, R. (2014). Extraction behavior of americium and curium on selected extraction chromatography resins from pure acidic matrices. *Solvent Extraction and Ion Exchange*, 32, 391–407.

CURRICULUM VITAE

CHARLES D. SMITH

Education:

Ph.D. Chemistry, University of Wisconsin-Milwaukee May 2020

Dissertation: Fundamental Studies of Trivalent *f*-Element Separations Using Ionic Liquids and Extraction Chromatography: Toward An Improved TALSPEAK Process

B.S. Chemistry, University of Minnesota-Duluth May 2008

Experience:

University of Wisconsin-Milwaukee, Milwaukee, WI January 2015-May 2020

Graduate Research Assistant

- Developed methods using ultraviolet-visible (UV-Vis), Thermogravimetric Analysis (TGA), Fourier Transform-Infrared (FT-IR), and Inductively-Coupled Plasma Mass Spectrometry (ICP-MS) instrumentation
- Published in *Solvent Extraction and Ion Exchange* and *Separation Science and Technology*
- Presented research at the 2018 Separation Science and Technology for Energy Applications Symposium and the 2019 Radiobioassay and Radiochemical Measurements Conference
- Supervised undergraduate researchers using gas chromatograph (GC), FT-IR, Karl Fisher Autotitrator and UV-Vis instrumentation during experimental development
- Maintained a detailed lab notebook
- Performed liquid-liquid extractions and extraction chromatographic separations on radioactive lanthanides while practicing radiation safety techniques
- Developed patentable extraction chromatographic materials for lanthanide-actinide and intra-lanthanide separations
- Studied the surface area and pore volume of microporous supports using Micromeritics 2020 Accelerated Surface Area and Porosimetry System (ASAP)
- Synthesized and identified ionic liquids for thermal analysis, liquid-liquid analysis, and task-specific purposes
- Delegated laboratory responsibilities between three graduate students to support research laboratory instrumentation, inventory, and safety
- Addressed laboratory conduct through in-person verbal communication, media, and group discussion

University of Wisconsin-Milwaukee, Milwaukee, WI September 2014-December 2019

Graduate Teaching Assistant

- Directly supervised over 100 undergraduate students in entry-level and upper-division laboratory courses
- Graded lab reports, quizzes and exams ensuring consistency and fairness
- Repaired UV-Vis spectrophotometer, cyclic voltammeter (CV), and flame atomic absorption (FAA) spectrometer in order to stay on laboratory schedule
- Disciplined students appropriately due to lateness, poor preparation, and lack of professionalism
- Organized department research symposium communicating with judges and participants and delegated to other members of the symposium organizing team
- Wrote instrument standard operating procedures (SOPs) for FAA, CV, and GC instruments
- Worked with other graduate students to improve research laboratory workspaces, independently of principal investigator
- Worked with university radiation safety officer to update radiation lab safety practices
- Addressed student concerns with one-on-one conversations and e-mail to facilitate a learning environment

Paddock Laboratories , Perrigo Company, Minneapolis, MN March 2009-July 2014

QC Chemist I

- Performed assay testing on liquids, powders, and tablets with the use of Agilent 1100 and Waters Alliance 2695 HPLC's equipped with UV, PDA, and Refractive Index detectors
- Performed alcohol content and residual solvent testing on raw materials and finished products using Agilent Series 6890 and 7890A Gas Chromatographs (GC) using Agilent Headspace G1888 when needed
- Ran identification tests with the use of an Avatar 360 FT-IR (ATR Diamond Crystal and KBR pellets), Hewlett Packard 8453 UV-Vis, and in accordance with current USP guidelines
- Determined water content using a Mettler Toledo DL38 Karl Fischer Titrator
- Performed dissolution testing on extended release tablets using a Hanson Dissolution Apparatus
- Performed particle size analysis using a Lecotrac LT-100 Particle Size Analyzer
- Determined osmolality of injectable drugs using a Micro Osmette Osmometer
- Tested for Heavy Metals, Ammonia Content, pH, Viscosity, Color, Description, etc.
- Reviewed analyst testing in laboratory notebooks considering all applicable methods, current USP guidelines, and Paddock/ Perrigo SOP's
- Performed solution, mobile phase and sample preparation in accordance with Paddock/ Perrigo methods
- Coordinated testing on products assigned to in order to ensure deadlines were met
- Performed in-process testing in order to meet production needs

Publications

Smith, C.D., Foersterling, F.H., Dietz, M.L. (2020) Solvent structural effects on the solubility of bis(2-ethylhexyl)phosphoric acid in room-temperature ionic liquids. *Separation Science and Technology*.

Smith, C.D., Downs, R.P., Carrick, J.D., Dietz, M.L. (2018). Determination of extractant solubility in ionic liquids by thermogravimetric analysis. *Solvent Extraction and Ion Exchange*.

Presentations

Smith, C.D. *, Dietz, M.L. *Improving the performance of extraction chromatographic materials. II. Controlled extractant impregnation*”, 64th Radiobioassay and Radiochemical Measurements Conference, Sante Fe, NM., Oct. 28th-31st, 2019.

Smith, C.D. *, Dietz, M.L., “Solvent Structural Effects on the Solubility of Metal Ion Extractants in Room-Temperature Ionic Liquids (RTILs)”, 20th Symposium of Separation Science and Technology, Gatlinburg, TN., Oct. 21st-24th, 2018.

Teaching Experience

Laboratory

General Chemistry (CHEM 102/104/105)

Elementary Quantitative Analysis (CHEM 221)

Advanced Chemistry Laboratory (CHEM 584)

Discussion

General Chemistry (CHEM 100/102/104/105)

Professional Development

UW-Milwaukee Department of Chemistry and Biochemistry Graduate Student Council

Symposium Chair-2018 Chemistry and Biochemistry Department Research Symposium

Skills

Basic experience with high pressure liquid chromatography (HPLC), gas chromatography (GC), ultraviolet-visible spectrophotometry (UV-Vis), thermogravimetric analysis (TGA) and Fourier-transform infrared spectrophotometry (FT-IR)

User

Nuclear magnetic resonance (NMR) spectrometer, differential scanning calorimeter (DSC), gamma counter, cyclic voltammeter (CV), fluorimeter, flame atomic absorption spectrophotometer (FAA), Micromeritics 2020 ASAP surface area analyzer, scanning electron microscopy (SEM)